PB-220 456

CONTROLLED EVALUATION OF THE REACTIVE ENVIRONMENTAL SIMULATION MODEL (REM)

VOL. 1

PACIFIC ENVIRONMENTAL SERVICES, INC.

PREPARED FOR
ENVIRONMENTAL PROTECTION AGENCY

FEBRUARY 1973

Distributed By:
NTIS
National Technical Information Service
U. S. DEPARTMENT OF COMMERCE

EPA-R4-73-013a

CONTROLLED EVALUATION OF THE REACTIVE ENVIRONMENTAL SIMULATION MODEL (REM)

Volume I

Final Report

PB 220 456

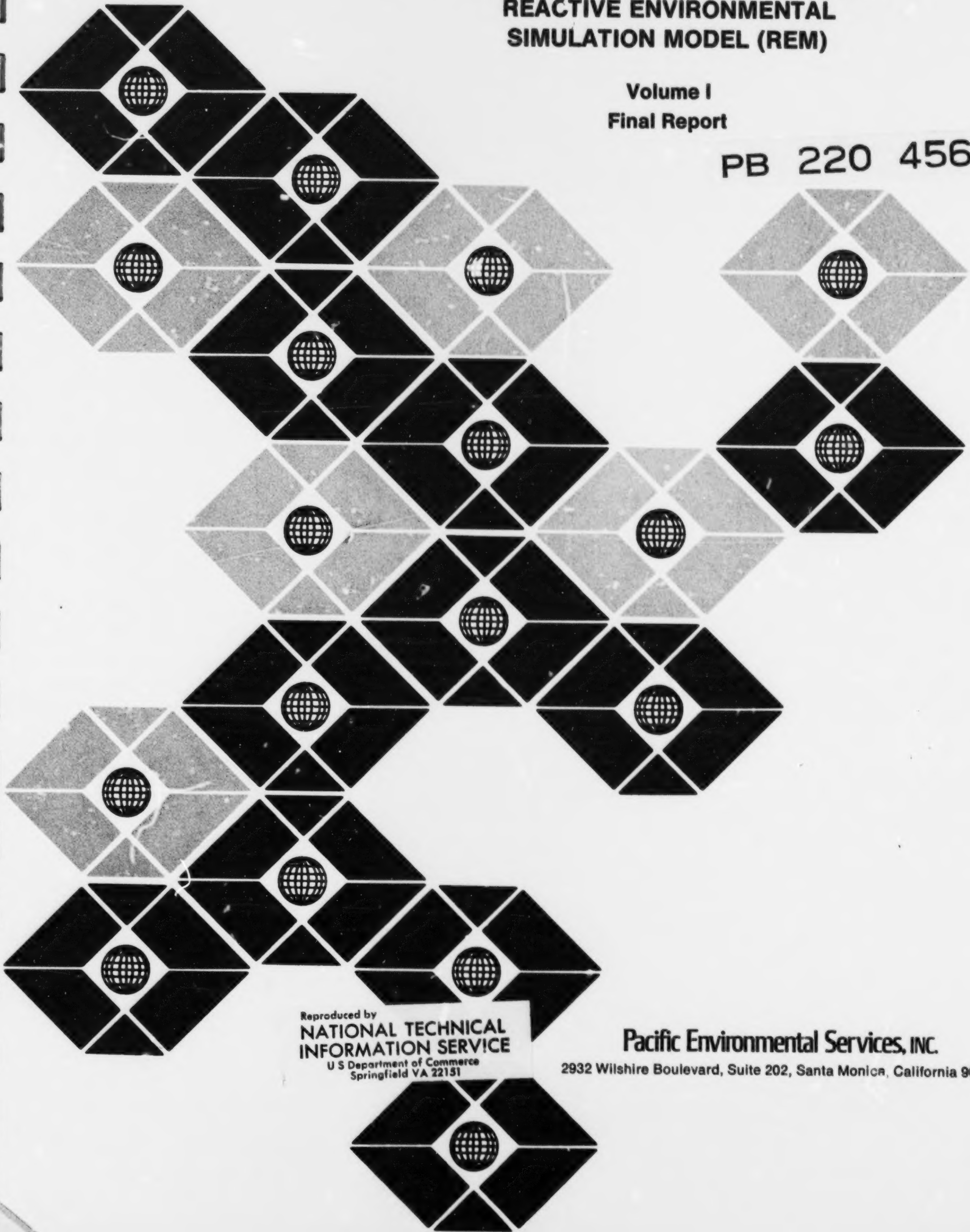

Reproduced by
NATIONAL TECHNICAL
INFORMATION SERVICE
U S Department of Commerce
Springfield VA 22151

Pacific Environmental Services, INC.
2932 Wilshire Boulevard, Suite 202, Santa Monica, California 90403

BIBLIOGRAPHIC DATA SHEET

1. Report No. EPA-R4-73-013a

2.

3. Recipient's Accession No. PB-228 456

4. Title and Subtitle
Controlled Evaluation of the Reactive Environmental Simulation Model (REM) Volume I: Final Report

5. Report Date February 1973

6.

7. Author(s) L.G. Wayne, A. Kokin, and M.I. Weisburd

8. Performing Organization Rept. No.

9. Performing Organization Name and Address
Pacific Environmental Services, Inc.
2932 Wilshire Boulevard (Suite 202)
Santa Monica, California 90403

10. Project/Task/Work Unit No.

11. Contract/Grant No. 68-02-0345

12. Sponsoring Organization Name and Address
ENVIRONMENTAL PROTECTION AGENCY
Office of Research and Monitoring
Washington, D. C. 20460

13. Type of Report & Period Covered Final

14.

15. Supplementary Notes

16. Abstracts The development and validation of an operational version of the Reactive Environmental Simulation Model (REM) were completed. REM was specifically designed to handle large chemical mechanisms to assess the impact on air quality of air pollution control devices, fuels, propulsion systems, stationary sources, and transportation systems where thorough evaluation of emissions, emission constituents and reaction rates are required. This completed version of the model contains a mechanism involving 32 reactions, 12 accumulating species and 12 non-accumulating species. REM contains such user features as reverse and forward trajectory routines; automatic and objective interpolation from input emission inventory, meteorological and air quality data bases; a chemical dynamics routine capable of accomodating mechanisms based on elementary chemical reactions; and automatic estimation of mixing depth and solar irradiance based on input of local weather and sun angle data. REM has attained a running time which makes it cost-effective for practical use. The program also is user-oriented in that it provides simple input procedures, user documentation, receptor point and time-of-day selectivity, flexibility in treating specific problems, and ability to select any of an infinite number of trajectories on any number of days of interest.

17. Key Words and Document Analysis. 17a. Descriptors

Air pollution
Photochemical reactions
Mathematical models
Simulation
Chemical reactions
Kinetics
Turbulence
Irradiation
Chambers
Nitrogen oxides
Exhaust emissions
Carbon monoxide
Trajectories

17b. Identifiers/Open-Ended Terms

Reactive Environmental Simulation Model (REM)
Air pollution control
Environmental model
Photo-oxidation
Air pollution episodes

17c. COSATI Field/Group 13B

18. Availability Statement Unlimited

19. Security Class (This Report) UNCLASSIFIED

20. Security Class (This Page UNCLASSIFIED

21. No. of Pages ~~175~~ 176

22. Price $6.00

CONTROLLED EVALUATION OF THE REACTIVE ENVIRONMENTAL SIMULATION MODEL (REM)

VOLUME I: FINAL REPORT
EPA R4-73-013a

by

Lowell G. Wayne, Allan Kokin, and Melvin I. Weisburd
Pacific Environmental Services, Inc.
2932 Wilshire Boulevard (Suite 202)
Santa Monica, California 90403
(213) 829-3658

Contract No. 68-02-0345

Project Officer: Ralph C. Sklarew
Meteorology Laboratory
National Environmental Research Center
Research Triangle Park, North Carolina 27711

Prepared for

OFFICE OF RESEARCH AND MONITORING
ENVIRONMENTAL PROTECTION AGENCY
WASHINGTON, D.C. 20460

February 1973

This report has been reviewed by the Environmental Protection Agency and approved for publication. Approval does not signify that the contents necessarily reflect the views and policies of the Agency, nor does mention of trade names or commercial products constitute endorsement or recommendation for use.

TABLE OF CONTENTS

Page

ABSTRACT ix

CHAPTER I. MODELING PHOTOCHEMICAL POLLUTION I.1

- A. INTRODUCTION I.1
- B. APPROACH TO MODEL DEVELOPMENT. I.2
  - 1. Potential Uses of Models I.2
  - 2. Input-Output Considerations. I.2
  - 3. Principles of Simulation I.3
  - 4. Application for Control Strategy Purposes. . . . I.4
  - 5. Application for Short-Term Forecasting I.6
  - 6. Research, Training and Other Applications. . . . I.8
- C. RATIONALE OF THE REACTIVE ENVIRONMENTAL SIMULATION MODEL (REM) I.9
  - 1. General Approaches to Model Building I.9
  - 2. Reasons for Following the Conservative Approach. I.9
  - 3. Structure of the Simulation Process. I.11
- D. ROLE OF CHEMICAL REACTIONS IN DETERMINING AIR QUALITY. I.12
  - 1. Introduction I.12
  - 2. Principles of Chemical Kinetics in Relation. . . to Simulation of Air Quality I.14
  - 3. Distribution of Contaminants in the Atmosphere, Resulting from Chemical Reactions and Transport. I.16
  - 4. Chemical Reactions in the Atmosphere in Relation to Control Strategy Planning. I.24
  - 5. Formulation of a Chemical Reaction Mechanism in Terms of Elementary Reactions I.26
- E. ROLE OF ATMOSPHERIC TURBULENCE IN SIMULATION OF AIR QUALITY. I.31
- F. STATUS AND FUTURE DEVELOPMENT OF REM I.33
  - 1. History of REM I.33
  - 2. Current Project. I.36
  - 3. Recommended Improvements I.38
- G. EVALUATION CRITERIA. I.41

CHAPTER II. DESCRIPTION OF THE REACTIVE ENVIRONMENTAL SIMULATION MODEL (REM) II.1

- A. INTRODUCTION II.1
- B. GRID SYSTEM. II.4

Page
C. PROGRAM CODE AND MACHINE USE II.4
D. OPERATION OF REM II.4
E. CONTROL STRATEGIES II.6
F. REM MODULES. II.7
  1. Initialization Program II.7
  2. Numerical Integration. II.8
  3. Chemical Kinetics. II.8
  4. Meteorology. II.9
  5. Barrier Check. II.11
  6. Ultraviolet Module II.13
  7. Source Emissions II.13
  8. Output Routine II.21
  9. Plotting Routine II.21
  10. Reverse Trajectory Program II.21

CHAPTER III. SIMULATION OF IRRADIATION CHAMBER EXPERIMENTS. III.1
A. INTRODUCTION III.1
B. SIMULATION OF PROPYLENE-ETHANE-OXIDES OF NITROGEN SYSTEM III.7
  1. By Original Mechanism, M1. . . . . III.7
  2. By Revised Mechanism, M2 . . . . III.12
C. SIMULATION OF AUTO EXHAUST PHOTO-OXIDATION SYSTEMS . III.31
D. SIMULATION OF TOLUENE-CONTAINING SYSTEMS III.37
  1. The Toluene-Oxides of Nitrogen System. III.38
  2. The Toluene-Butane-Oxides of Nitrogen System . . III.41
  3. Discussion of Results with Toluene-Containing Systems. III.41
E. SIMULATION OF PHOTO-OXIDATION PRODUCTS IN THE IRRADIATION EXPERIMENTS. III.43
F. SUMMARY AND CONCLUSIONS. III.43

CHAPTER IV. SIMULATION OF PHOTOCHEMICAL AIR POLLUTION EPISODES . . . IV.1
A. INTRODUCTION IV.1
B. CARBON MONOXIDE SIMULATION IV.2
C. COMPLETE ATMOSPHERIC SIMULATIONS IV.14
  1. Simulation by Trajectories for 1330 PST Arrival. IV.15
  2. Extended Simulation of a Single Episode. IV.17
  3. General Accuracy of Atmospheric Simulations. . . IV.24
D. CONCLUSIONS. IV.30

APPENDIX RESULTS OF REM SIMULATIONS A.1

LIST OF FIGURES

Figure		Page
II.1	PES Reactive Environmental Model (REM)	II.2
II.2	Schematic of the PES Reactive Environmental Model (REM) .	II.3
II.3	REM Grid System for the Los Angeles Basin	II.5
II.4	Demonstration of Barrier Check Technique	II.12
II.5	Temporal Distribution of Daily Street Traffic	II.14
II.6	Temporal Distribution of Daily Freeway Traffic	II.15
II.7	Distribution of Street Traffic by Grid Area (thousands of vehicle miles per day)	II.16
II.8	Distribution of Freeway Traffic by Grid Area (thousands of vehicle miles per day)	II.17
II.9	Distribution of Reactive Hydrocarbon Emissions (average kilograms/hour) by Grid Area.	II.18
II.10	Distribution of Oxides of Nitrogen Emissions Taken as Nitric Oxide (average kilograms/hour) by Grid Area . .	II.19
II.11	Distribution of Less Reactive Hydrocarbon Emissions (average kilograms/hour) by Grid Area	II.20
II.12	Sample REM output	II.21
II.13	Digital Plot of Primary Pollutant Time vs. Concentration Histories	II.23
III.1	Concentration of Ethane Related to Time of Sampling, Experiment 321 (propylene, ethane, and oxides of nitrogen system).	III.5
III.2	Time Profiles of Nitrogen Dioxide Concentrations, Experiments 222 and 233 (diluted auto exhaust system). Smoothed experimental profiles.	III.6

LIST OF FIGURES

Figure		Page
III.3	Time Profiles of Contaminant Concentrations, Experiment 329. (Original Mechanism)	III.10
III.4	Time Profiles of Contaminant Concentrations, Experiment 325. (Original Mechanism)	III.11
III.5	Time Profiles of Contaminant Concentrations, Experiment 329. (Revised Mechanism)	III.15
III.6	Time Profiles of Contaminant Concentrations, Experiment 325. (Revised Mechanism)	III.17
III.7	Time Profiles of Nitrogen Dioxide Concentration Simulating Experiment 329.	III.19
III.8	Time Profiles of Oxidant (Ozone) Concentration Simulating Experiment 329.	III.20
III.9	Time Profiles of Contaminant Concentrations, Experiment 318.	III.21
III.10	Time Profiles of Nitrogen Dioxide Concentration Simulating Experiment 318.	III.23
III.11	Time Profiles of Oxidant (Ozone) Concentration Simulating Experiment 318.	III.24
III.12	Time Profiles of Nitrogen Dioxide Concentration Simulating Experiment 318.	III.25
III.13	Time Profiles for Oxidant (Ozone) Concentration Simulating Experiment 318.	III.26
III.14	Time Profiles of Nitric Oxide Concentration Simulating Experiment 318.	III.27
III.15	Time Profiles for Propylene Concentration Simulating Experiment 318.	III.28
III.16	Time Profiles of Contaminant Concentrations, Experiment 321.	III.30

Figure		Page
III.17	Time Profiles of Contaminant Concentrations, Experiment 222.	III.33
III.18	Time Profiles of Contaminant Concentrations, Experiment 233.	III.34
III.19	Time Profiles of Contaminant Concentrations, Experiment 231.	III.35
III.20	Time Profiles of Contaminant Concentrations, Experiment 224.	III.36
III.21	Time Profiles of Contaminant Concentrations, Experiment 250.	III.40
IV.1	Comparison of Calculated vs. Observed Values of Carbon Monoxide at Air Monitoring Stations on September 11, 1969.	IV.4
IV.2	Comparison of Calculated vs. Observed Values of Carbon Monoxide at Air Monitoring Stations on September 29, 1969.	IV.5
IV.3	Comparison of Calculated vs. Observed Values of Carbon Monoxide at Air Monitoring Stations on September 30, 1969.	IV.6
IV.4	Comparison of Calculated vs. Observed Values of Carbon Monoxide at Air Monitoring Stations on October 29, 1969.	IV.7
IV.5	Comparison of Calculated vs. Observed Values of Carbon Monoxide at Air Monitoring Stations on October 30, 1969.	IV.8
IV.6	Comaprison of Calculated vs. Observed Values of Carbon Monoxide at Air Monitoring Stations on November 4, 1969.	IV.9
IV.7	Comparison of Calculated vs. Observed Values of Total Oxidant and Carbon Monoxide at Downtown Los Angeles on October 29, 1969.	IV.18

Figure		Page
IV.8	Comparison of Calculated vs. Observed Values of Nitrogen Dioxide, Nitric Oxide, Total Oxidant and Carbon Monoxide at Azusa on October 29, 1969.	IV.19
IV.9	Comparison of Calculated vs. Observed Values of Nitrogen Dioxide, Nitric Oxide, Total Oxidant and Carbon Monoxide at Whittier on October 29, 1969. . . .	IV.20
IV.10	Comparison of Calculated vs. Observed Values of Nitrogen Dioxide, Nitric Oxide, Total Oxidant and Carbon Monoxide at Pomona on October 29, 1969.	IV.21
IV.11	Scatter Plot of Calculated vs. Observed Carbon Monoxide for the Atmospheric Simulations.	IV.25
IV.12	Scatter Plot of Calculated vs. Observed Nitrogen Dioxide for the Atmospheric Simulations.	IV.27
IV.13	Scatter Plot of Calculated vs. Observed Total Oxidant for the Atmospheric Simulations.	IV.29
A.1	Trajectories for September 11, 1969.	A.14
A.2	Trajectories for September 29, 1969.	A.15
A.3	Trajectories for September 30, 1969.	A.16
A.4	Trajectories for October 29, 1969.	A.17
A.5	Trajectories for October 30, 1969.	A.18
A.6	Trajectories for November 4, 1969.	A.19

LIST OF TABLES

Table		Page
III.1	Parameters Used for Simulation of Various Experiments . .	III.3
III.2	Irradiation Chamber Experiments in the Propylene-Ethane-Oxides of Nitrogen System.	III.8
III.3	Original Mechanism (M1) for the Chemical Dynamics Module (with Rate Factors for Exp. 329 and 325)	III.9
III.4	Revised Mechanism (M2) for the Chemical Dynamics Module (with Rate Factors for Exp. 329 and 325)	III.13
III.5	Irradiation Chamber Experiments with Automobile Exhaust Gases	III.32
III.6	Irradiation Chamber Experiments in the Toluene-Oxides of Nitrogen System	III.39
III.7	Irradiation Chamber Experiments in the Toluene-Butane-Oxides of Nitrogen System.	III.42
III.8	Comparison of Estimated vs. Observed Concentrations for Formaldehyde, Acetaldehyde, and Peroxyacetyl Nitrate (after 6 hours irradiation)	III.44
IV.1	Comparison of Estimated Mid-Hour Concentrations to Observed Hourly Average Concentrations for Carbon Monoxide, for Six Smog Days at Different Receptor Locations	IV.12
IV.2	Comparisons of Estimated Mid-Hour Concentrations to Observed Hourly Average Concentrations for Carbon Monoxide, for Four Receptor Locations on Different Smog Days	IV.13
IV.3	Comparison of Estimated Mid-Hour Concentrations to Observed Hourly Average Concentrations for Carbon Monoxide, Nitrogen Dioxide, Nitric Oxide and Ozone, for 1330 PST Trajectories	IV.16
IV.4	Comparison of Dosage of Various Contaminants as Estimated from Simulation Model to Dosage Estimated from Air Monitoring Data, Four Locations, Six Hours on October 29, 1969	IV.23

Tables		Page
A.1	Carbon Monoxide Simulations	A.2
A.2	Photochemical Pollutant Simulation Trajectories	A.9

ABSTRACT

The development and validation of an operational version of the Reactive Environmental Simulation Model (REM) ~~were completed~~ is presented. REM was specifically designed to handle large chemical mechanisms to assess the impact on air quality of air pollution control devices, fuels, propulsion systems, stationary sources, and transportation systems where thorough evaluation of emissions, emission constituents and reaction rates are required. The version delivered to the U.S. EPA under this contract contains a mechanism involving 32 reactions, 12 accumulating species, and 12 non-accumulating species. Larger or smaller mechanisms, also, can be readily inserted into REM for specified purposes.

REM is based on a Lagrangian moving coordinate system which enables the numerical simulation of the chemical reactions that take place in a parcel or column of air moving along a dynamic wind trajectory. The trajectory approach gives REM considerable flexibility and is adaptable for use in a number of practical operational situations. These include short-term air quality forecasting; analysis of the impact of sources of air pollution at various designated locations on the air quality at specified receptor points; interpolation of contaminant concentrations and dosages at locations not covered by air monitoring stations, and control strategy evaluations.

REM contains such user features as reverse and forward trajectory routines; automatic and objective interpolation from input emission inventory, meteorological and air quality data bases; a chemical dynamics routine capable of accomodating mechanisms based on elementary chemical reactions; and automatic estimation of mixing depth and solar irradiance based on input of local weather and sun angle data.

REM has attained a running time which makes it cost-effective for practical use. On an IBM System 370/155, the real-time-to-simulation ratio for the 31-step mechanism is 150:1; for carbon monoxide alone it is 3000:1; for some of the shorter mechanisms available it should run more than 300:1. The program, also, is user-oriented in that it provides simple input procedures, user documentation, receptor point and time-of-day selectivity, flexibility in treating specific problems, and ability to conveniently select any of an infinite number of trajectories on any number of days of interest. The modular construction of REM, also, makes it easy to add, replace, or delete individual modules. REM can be used as an unlimited receptor point model and to chronicle emission inputs contributing to the air quality at any receptor point.

The validation record of REM over a large number of runs may be summarized as follows:

- CO, less than a factor of 2 in more than 80% of the comparisons; 40% agreement within one part per million.
- O_3, within a factor of 2, 75% of the comparisons.
- NO, within a factor of 2, 75% of the comparisons; 90% agreement within .02 ppm.
- NO_2, within a factor of 2, 60% of the comparisons.

The shapes of predicted time profiles of contaminant concentrations are generally similar to those observed at air monitoring stations.

The ease and economy at which REM can be utilized under a variety of data availability situations make potential improvements in accuracy and application possible on a cost-effective basis.

Chapter 1

MODELING PHOTOCHEMICAL POLLUTION

A. INTRODUCTION

This final report covers the work performed under U.S. Environmental Protection Agency Contract 68-02-0345 to evaluate the Reactive Environmental Simulation Model (REM). REM originally was developed under Contract CPA 22-69-108, June, 1970. It was subsequently refined under Contract CPA 70-151, January, 1971.

The evaluation of atmospheric simulation models should consist of three major parts: (1) evaluation of the validity and applicability of the modeling approach; (2) validation of the model against known "real" world conditions, including field measurements; and (3) evaluation of the ease and economy of use of the model.

Given the uncertainties and complexities inherent in environmental modeling, confidence in a model and in its potentialities may be enhanced if it is based on established scientific principles to the maximum feasible extent, and if the empirical aspects are formulated in a plausible way, consistent with established principles as well as all available relevant data.

At the same time, the complexity of the problem of simulating air quality is such that a truly comprehensive air quality model for photochemical contaminants is, at present, out of reach. Further, if such a model were in existence, its use for most of the ordinary purposes of simulation would, in all likelihood, be prohibitively expensive. It is appropriate, in evaluating a model, to consider its characteristics in relation to its potential uses.

The evaluation of an air pollution model, therefore, must include a comprehensive understanding of the approach and its implications. It should include assessment of both the current status of the model and its projected line of development.

B. APPROACH TO MODEL DEVELOPMENT

1. Potential Uses of Models

Consideration of the intended use of a photochemical air quality model may indicate which aspects of the model should be emphasized--that is, developed in detail--and which may be de-emphasized in the interest of ease of operation or cost-efficiency. If an intended use is specified, model design may be optimized in view of the needs of the responsible user and in view of his ability to understand, apply, and adapt the model for this use.

Currently identified potential uses for air quality models fall generally into three categories, which are discussed below in further detail:

1. Control strategy evaluation
2. Short-term forecasting of air quality
3. Research, training and other applications

2. Input-Output Considerations

Any air quality model, for whatever intended use, has as its purpose the prediction of concentrations of contaminants in the atmosphere, based upon input information specific to certain situations of interest. Predicted concentrations will depend strongly on the time-frame involved. Thus, for control strategy evaluation, the appropriate time frame is likely to be a year or one of the seasons of a year, while forecasting of air quality for emergency warning systems requires a time-frame of hours.

Similarly, the spatial scale of predicted values is an important factor for model design. Predicting conditions in the immediate vicinity of a roadway or industrial pollution source may require a model substantially different from one to be used for evaluating the air quality of an air pollution control region.

Input factors consist, basically, of three types of data: contaminant emissions information, initial pollutant concentrations, and weather information. The time-frame and spatial scale of these input factors must be consistent with the requirements associated with the intended use of the model. Thus, a climatological summary of the weather for a given region will not be adequate input for use in a model for short-term forecasting of air quality.

3. Principles of Simulation

Operating on these elements, the model simulates the forces of nature which determine actual concentrations of contaminants in a real region. To the extent that these forces are predictable and understood, they can be represented by mathematical relations or simulated by numerical processes and the results may be used with confidence. To the extent that the relevant forces of nature are not predictable or not understood, the validity of simulation is unavoidably impaired. For these contingencies, empirical relations or processes are customarily devised and adjusted to produce results having more or less reasonable similarity to values observed in the atmosphere.

The greater the content of empiricism embodied in the simulation, the smaller is the validity of the model and the less confidence may be placed in the use of the results. For this reason, it is desirable to base the simulations on established physical and chemical laws whereve possible. Where necessary in the interest of cost reduction, the next preferred alternative is to use simplifications based on these laws. Least desirable, but sometimes necessary, is the resort to empiricism.

4. Application for Control Strategy Purposes

In evaluating alternative strategies for the abatement of air pollution problems, the user attempts to optimize estimated air quality subject to constraints imposed by nature and by society. His time-frame is often of the order of magnitude of years, in terms of implementation of the strategies to be compared. With respect to the common sources of photochemical contaminants, the applicable spatial scale is likely to be also rather large; for example, the transportation system for a large city or an entire region may be an important factor.

However, the selected strategy must provide for protection of the inhabitants of the region against concentrations of certain contaminants exceeding ambient air standards for periods as short as one hour. For simulating individual pollution episodes to this degree of detail, in view of ordinary minimum wind speeds of about 2 miles per hour, the appropriate spatial resolution is for characteristic distances of 2 miles.

For evaluating strategies for pollution abatement, an air quality model will be used in a comparative mode. That is, given certain fixed assumptions regarding the weather in the region under study, air quality parameters (i.e., contaminant concentrations) will be predicted for various hypothetical distributions of contaminant emissions, and the main interest of the exercise lies in comparing the predicted values of these concentrations. The model output, therefore, must be sensitive to differences in the details of the emission inventories which are provided as input, and it must reflect as accurately as possible the chemical processes in the atmosphere, which alter the concentrations by using up some of the contaminants and producing others.

On the other hand, the fact, that the required predictions refer to a hypothetical or indefinite future, ameliorates the necessity for realistic detail in regard to weather input. What is necessary is that the types of weather associated with high, moderate, and low pollution potential be known, so that hypothetical future weather conditions which are relevant to the smog problem can be furnished as input to the model. The most obvious way of accomplishing this, provided adequate weather and air quality records exist for the subject region, is to use historical weather data for days (or episodes) on which air quality was severely impaired or which showed other characteristics of special interest.

For example, in a region such as the South Coast Air Basin of California, where detailed records of both weather variables and contaminant concentrations are kept, the model user concerned with a control strategy would identify the occasion or occasions (within a recent period of interest) on which the highest oxidant levels were encountered at various monitored sites. Using the reverse trajectory routine associated with each of these high oxidant observations, and using the full model he would obtain model estimates for comparison with the observed concentrations. Assuming reasonable agreement existed, he would next rerun the model with the same trajectories and weather conditions, but with revised source emission input, corresponding to the strategies to be tested.

Estimates of the effects of each proposed control strategy could then be given for each of the selected high-oxidant observations. These estimates could be expressed either in relative terms, as percent reduction from the original model estimate, or in absolute terms, by comparing the predictions with air quality standards.* The net effect of this system is to yield, for any number of selected historical observations for hypothetical reoccurrences of the same weather patterns but with different emission patterns. Obviously, the same method of exploration can be extended to determine effects on lower oxidant levels, and on other contaminants as well.

---

*In this case, allowance may have to be made for statistically unavoidable uncertainty in the model estimates.

It is important to note that, when this system is used for the evaluation of proposed control strategies, elaborate simulation of the dynamics of air flow is not required, since any small errors introduced in a given model run by a simplified representation of the flow field are largely balanced by compensating errors in the comparison runs. On the other hand, the effects of chemical reactions in generating secondary contaminants are first-order, non-compensating effects which require simulation on an adequate theoretical basis. Fortunately, the principles necessary for developing such a simulation are known and, as explained below, they have been largely incorporated into the REM chemical dynamics module, which forms the core of REM.

5. Application for Short-Term Forecasting

The short-term forecast process consists of the prediction of pollution conditions up to perhaps 48 hours in advance in order to notify the public of expected air quality levels and to issue appropriate warnings and take appropriate temporary measures in the event than an air pollution emergency condition is predicted. The problem here is to predict air quality concentrations from forecasts of large-scale weather features within rather severe time constraints. Thus, both accuracy and speed are of crucial importance. In the future, photochemical simulation models may be linked to objective forecasting systems to assist in making such forecasts and to test the effectiveness of temporary emergency prevention measures.

The problem is complicated by model input requirements. To the extent that any air quality model depends for its operation on input of recorded weather data, that model will be inapplicable as an aid in forecasting air quality on the necessary day-to-day basis. If, on the other hand, a model can readily accept and utilize provisional approximate values of a small set of weather parameters, then prospects of incorporating the model in a short-term forecasting system would be considerably brighter.

Forecasting considers variables on the macroscale and mesoscale related to the general characteristics and flow of large air masses; while air quality models often require input conditions at specific measuring stations and receptor points on the microscale. Models which require more meteorological detail will have more difficulty in this regard than models which retain only the type of detail that is most compatible with current forecasting procedures.

A brief analysis of the forecast process will suggest the compatibility requirements. This essentially involves analysis of scale interrelationships, i.e., summarization of predictive information from the macroscale to the microscale.

a. Macroscale to Mesoscale

Large scale weather patterns are predicted from current weather information either manually or by means of National Weather Service Prognostic Models (barotropic or baroclinic), e.g., through the depiction of changes in height of a 500 millibar surface. From these data, predictions are made regarding general air flow characteristics, potential mixing heights and solar radiation (cloud cover) for the region of interest.

b. Mesoscale to Microscale

From this information, predictions must be made of air flow and mixing depth characteristics for specific areas within the region in order that the relationship to air quality can be properly made (and for a photochemical model to function). This involves the construction of appropriate trajectories by taking into account the relationship of the general flow of the air mass to the surface flow, and mapping of the predicted variations in mixing height for the region. This is usually accomplished by trained and experienced meteorologists who associate large and small scale conditions by use of long term historical, climatological and statistical records of weather and air quality conditions available to them in the region.

The question of the use of photochemical models in the forecast process thus will depend either on the establishment of an objective forecast system which incorporates the model (if the model is indeed needed), or incorporating the model with the manual procedures routinely employed by the forecast meteorologist.

In either case, the linkages between the model and the forecast procedure are the mixing depth variables, trajectory construction (which embodies both wind speed and direction) and cloud cover. The Lagrangian approach therefore seems especially adaptable and compatible with forecast procedures. REM, in particular, is founded on the trajectory approach and can accept exactly the kind of input that a forecast meteorologist would wish to supply to it. The trajectory model possesses flexibility and non-redundancy in application; only one or any number of trajectories can be tested. REM also will readily permit input of derived and hypothetical trajectories for rapid model computations.

6. Research, Training and Other Applications

Other uses of a model include interpolation of contaminant concentrations at locations not covered by an air monitoring network; calculation of receptor dosages; identification of source areas that contribute to the air quality of a receptor point; testing of postulated functions; and training of personnel. The trajectory model is especially and efficiently adapted to these uses.

C. RATIONALE OF THE REACTIVE ENVIRONMENTAL SIMULATION MODEL (REM)

1. General Approaches to Model Building

Two general approaches to model development may be characterized: Derivative and Conservative.

The derivative approach usually proceeds from the complex to the simple. It attempts to systematically model all functions--both first and second order--which the modeler believes must be accounted for in the total environmental system. The modeler may then modify, delete or simplify functions as necessary in the course of his effort to improve the workability of his model. The derivative approach in photochemical air quality modeling is currently characterized by the use of the "conservation-of-mass" equation, with elaborate procedures to take into account fine details of air flow in a three-dimensional field.

The conservative approach proceeds from the simple to the complex, as necessary, and emphasizes those functions that correspond most closely to observed atmospheric behavior and which utilize commonly available types of information. This approach focuses on major first order influences. Once the effects of these influences are established, second order effects are added if needed to improve the accuracy of the model. In photochemical modeling, this approach is exemplified by the Lagrangian (moving coordinate) system in which attention is focused on events which take place in any individual parcel of air as it follows a natural trajectory.

2. Reasons for Following the Conservative Approach

PES, since the beginning of its model development effort, has adopted a conservative, Lagrangian approach for the following reasons:

a. Because of the scarcity of relevant observational data, application of the derivative approach requires many empirical assumptions regarding the relation of detailed air movement to the observable surface conditions. Such assumptions must be furnished if the model is to be made operational; and, frequently, assumptions having no theoretcial basis may be used for reasons of computational convenience. In a detailed, all-inclusive model it is difficult to evaluate the actual effects of such speculative assumptions, singly and in combination, on the final results. Unless such effects can be isolated, speculative functions possess the danger of compounding errors.

b. The derivative approach tends to yield complex models which require comprehensive, detailed input information; in effect, a different model may be required for each day to be simulated. Such extensive and complex input data may restrict the flexibility of the model in its ready use for testing many days of the year. Similarly, the degree of detail needed to verify and apply the model is greater and front-end labor and costs tend to be significantly greater than for the simpler models.

c. Although the derivative approach initially tends to satisfy the sense of completeness, it may render the development effort problematical, requiring costly and expensive revisions. Another danger is that the effort to model one aspect comprehensively may also hinder the development of another important or needed mechanism. For example, should greater resolution be required in emission constituents and should verified chemical mechanisms be required which are larger than those currently in use, a complex model may be difficult to modify for these purposes.

d. Severe limitations in the availability of reliable and accurate emissions inventories and meteorological information limit the accuracy attainable in any model. Unless the comprehensive model is drastically simplified, to be usable with such input data, cost-effectiveness is likely to suffer.

3. Structure of the Simulation Process

The PES Reactive Environmental Model (REM) may be considered in two parts: (1) the "core model", i.e. those routines which express the fundamental, invariant principles which can be modeled; and (2) the validation, experimental and application routines which are for use in specific cases and experimental conditions. The heart of the PES approach has been to distinguish these two features of the simulation process. As explained below, consideration of the chemistry of a parcel of polluted air leads to an invariant paradigm which can be taken to be central, thus facilitating the isolation of effects due to the auxiliary routines which can be modified or improved as new information becomes available. The realization of the invariant paradigm thus permits the assessment of the importance of the effects of postulated functions.

The importance of the chemical mechanism in photochemical modeling in general, in its function in the "core model" and its role in control strategies is clear from a number of points of view that are taken up in other sections and chapters of this report. At the same time, the chemical module of any photochemical air pollution simulation model possesses a greater potential for achieving an invariant status and hence an acceptable degree of validity than do the meteorological or emission functions. As a body of theory, chemistry possesses a greater consistency and constancy of principles, with regard to predictability, than do other disciplines presently bearing on atmospheric modeling. Further, the large amount of unapplied chemical knowledge and increasing amount of experimental data available makes it possible to achieve an acceptable chemical module in a much shorter period of time and at considerably less expense than would be the case with the other functions of the model.

The basic parameters of elementary chemical reactions are invariant relative to changes in concentration and light intensity. Once they have been determined for any given reaction, they need not be reassessed for application in various concentration ranges. The body of data and knowledge available thus increases the probability of developing a valid chemical mechanism useful for purposes of atmospheric simulation.

The importance of the role of the chemical mechanism in models used for control strategy comparisons, also, is clear from the fact that since meteorological conditions are typified and then held constant, the reliability of the comparisons becomes a function of the validity of the chemical mechanism and the quality of the emission information employed. An adequate representation of the chemical mechanism, therefore, is particularly essential whenever the effects of new controls, fuels and propulsion systems which involve detailed information on emission constituents and reaction rates, are to be subjected to thorough testing.

The characteristics of the REM chemical module are further described below, and in Chapter II.

D. ROLE OF CHEMICAL REACTIONS IN DETERMINING AIR QUALITY

1. Introduction

In relation to non-reactive contaminants, air quality is determined by the rates of emission and the properties of air in motion. These properties have been subject of much study; theoretical formulations have been developed which account well for behavior of air as observed in the laboratory (under carefully controlled conditions).

But these formulations are not easy to apply to simulation of atmospheric conditions, because the necessary parameters are usually not observable. Therefore, in models which are intended to simulate the urban atmosphere, various simplifications are made. These attempt to preserve the formalism of the ideal case while recognizing (and avoiding) some of the complications of the real case.

One class of existing air quality models is based on "plume" formulas, which apply to steady wind conditions in wind tunnels, for example. Atmospheric and environmental conditions which interfere include fluctuating wind (both speed and direction); vertical turbulence; non-uniformity of wind with height above ground; roughness of terrain and intrusion of obstacles (such as buildings). Ignoring these factors usually leads to serious inaccuracies in predicting air quality, so various empirical adjustments are devised to account for them, or for some of them. These take the form, for example, of tables and graphs of vertical and horizontal diffusion parameters recommended for use in various typical weather conditions; summation over long periods of time to take advantage of the smoothing effect of averaging; "calibration" of the formulae by optimizing an arbitrary factor for best representation of observed data; in certain cases, optimizing an assumed "half-life", in analogy to radioactive decay processes.

Simulation of the air quality in an urban atmosphere, by this approach, requires the superposition of contaminant concentration patterns individually calculated for each of the large number of emission sources in the typical city. If enough degrees of freedom are provided in the form of arbitrary factors, and if the degree of detail required in the representation of air quality is kept low enough (e.g., restricting predictions to annual average contaminant level for a specified sensor location) the semblance of validation for an atmospheric model can be provided even without the substance. However, the irreducible requirement for plausibility with modeling of this sort is that concentrations of contaminants appear to decrease with distance from known sources. The behavior of photochemical product contaminants is incompatible with this requirement and, therefore, cannot be imitated successfully by diffusion models based on the plume formulation.

Determining factors for the concentrations of photochemical product contaminants are, at basis, the rates at which chemical reactions occur. These rates depend strongly on the concentrations of precursor contaminants and on the intensity of sunlight. Furthermore, the rates are joint functions of the concentrations; this implies that the observed concentrations of the products must depend upon interactions between contaminants emitted into the atmosphere at different locations, and that the effects of these various sources are not simply additive at any receptor location. This is especially obvious when the reaction between ozone and nitric oxide is considered: the first effect of injecting nitric oxide into an air mass laden with ozone is that ozone is consumed, with the production of nitrogen dioxide; later, if the sun is shining, ozone will again accumulate (but this will occur at a location perhaps far removed from the point where the nitric oxide was added).

Thus, for photochemical product contaminants, predicting the changes of concentration in an urban atmosphere requires more detailed information than for non-reacting contaminants. Further, unlike the non-reacting contaminants, photochemical products undergo changes of concentration which are in no way related to the mixing and transport of air; these changes can be demonstrated by studying synthetic atmospheres immobilized in irradiation chambers, under conditions such that non-reacting contaminant concentrations remain steady or change only by dilution. From this it follows that successful simulation of concentrations of the reactive contaminants and their products requires consideration of more factors than does simulation of non-reacting contaminants.

These additional factors basically involve the phenomena of chemistry and must be considered in that context.

2. Principles of Chemical Kinetics in Relation to Simulation of Air Quality

In the science of chemistry, kinetics is the branch which treats of the rates of occurrence of chemical changes. Modern gas phase kinetics is based on the well-established molecular collision theory of chemical reactions. According to this theory, most chemical change is the result of collisions between molecules, which cause rearrangement of the atoms which compose the molecules, thus giving rise to new molecules having different chemical characteristics.

Whether or not a reaction ensues when two chemical species are mixed depends, in the first instance, on whether an effective rearrangement of the atoms involved is chemically feasible. If a particular type of rearrangement is feasible, it will take place not on every collision between molecules of the two species, but for some fraction of such collisions; this fraction is called the "collision yield." It is important because it is universally characteristic of the molecular behavior of these two species when mixed in the gas phase (for example, in the atmosphere*). The collision yield is commonly a function of the temperature of the gas which contains the reacting molecules, but it is independent of the concentrations of the reacting species and of any other species present in the mixture, whether these extraneous substances are reactive or not. It is also independent of such atmospheric variables as wind, humidity, mixing height, barometric pressure and cloud cover.

The chemical change which takes place in this way, as a direct result of molecular collision, is known as an "elementary reaction." When two substances which react in this way are mixed, the rate at which they react is equivalent to the rate at which suitable molecular collisions occur, multiplied by the collision yield. The collision rate is proportional to the product of the concentrations of the reactants; it also depends (not strongly) on the temperature of the gas mixture, but it is essentially independent of the concentrations of other substances and of atmospheric variables such as wind, humidity, etc. The rate of reaction, since it is proportional to the collision rate, is therefore also independent of the concentrations of extraneous substances and of the atmospheric variables mentioned.

In a multicomponent system (such as an urban atmosphere), many different elementary reactions take place simultaneously, but each conforms to the kinetic principles just outlined, except for a very few rather minor complications. The resultant behavior of the system may be mathematically complicated because each of the rates of the elementary reactions, which cause the concentrations of the reactants to change, itself depends upon the concentrations of one or more of the reactants. This resultant behavior can, however, be calculated if all the elementary reactions and their collision yields are known. The modern high speed computer enables us to perform such calculations for some rather complicated systems.

---

*It should be noted that real atmospheres always contain particles of liquid and solid, which present surfaces where heterogeneous reactions can take place. Calculation of rates for such reactions is subject to similar, but slightly more complicated, rules.

The main difficulty in applying these principles to simulation of atmospheric photochemistry lies in the fact that our knowledge of the elementary reactions involved is incomplete, and our estimates of the collision yields are not very precise, even for those elementary reactions which are well recognized. The advantage of pursuing this approach, which is embodied in REM, is that the parameters involved are fundamental invariants of nature; they are required to be consistent with the entire body of chemical knowledge; they can be tested by experiment, not only in simulated smog irradiation chambers, but in many other ways; and since they are independent of many other atmospheric variables including concentrations, they may be expected to be useful in extending simulation to lower ranges of pollutant concentrations.

3. Distribution of Contaminants in the Atmosphere, Resulting from Chemical Reactions and Transport

To understand the behavior of contaminants in the atmosphere in terms of the changes of concentration with time, it is necessary to know not only the chemistry of the contaminants as it might be seen in an irradiation chamber, for example, but also the relevant facts concerning input of pollutants into the atmosphere and their dispersal and mixing by physical forces in the moving air. The principles involved in describing and simulating this behavior are the subject of this section.

A very general approach to the description of this behavior is the use of the "conservation of mass" equation[1]. This equation represents the changes in concentration of any contaminant at any point in the atmosphere. It states that the rate of change of concentration at that point is equal to the net effect of four processes: (a) the change due to chemical reactions; (b) the change due to emissions from pollution sources; (c) the change due to movement of the air; and (d) the change due to molecular diffusion.

---

[1] Darling, E.M. "Computer Modeling of Transportation-generated Air Pollution." Report No. DOT-TSC-OST-72-20, June 1972.

In the present state of the art, a general solution of the conservation-of-mass equation is not feasible, partly because of the complexity of the computations which would be involved but, even more importantly, because of the lack of some of the information required to compute the individual effects of the four processes. Deficiencies in present knowledge of the effects of chemical reactions are discussed in the preceding section of this chapter; in the PES model, these deficiencies are minimized by structuring the calculations in terms of elementary reactions, so that improvements in the understanding of the chemistry and in the precision of the parameters leads easily to an improvement of the representation of the chemical behavior.

The effects of changes due to emissions from pollutant sources are not difficult to compute, if rates of emission are known. However, the number of individual sources in an urban area is so large that a complete accounting is completely unfeasible, even if the necessary details of the behavior of each source were available. For practical purposes, therefore, these effects must be estimated in terms of average behavior for multitudes of small sources, with substantial detail only on a small number of very major sources. Thus, atmospheric modeling for air quality requires an emissions model for each region to which the model is to be applied. The PES atmospheric simulation model provides for separate emissions modules for several types of sources, namely, freeway traffic, non-freeway vehicular traffic, major industrial sources and aggregated other sources. Emission rates are estimated as a function of location and time. Obviously, the simulated detail resulting from the application of such an emissions model must be very different in many particulars from the real status of emissions at any moment chosen for simulation. This discrepancy, then, constitutes an inherent, serious limitation on the achievable accuracy of air quality modeling.

The effects of changes due to motion of the atmosphere have received much attention in some recent approaches to air quality modeling. It is common[*] to divide the motions of air into two types: a "transport" or advective component, which causes net geographical displacement of air (including both horizontal and vertical displacements beyond some minimum magnitude); and a "turbulent" component, which causes mixing of air from parcels in neighboring locations. Even when thus partitioned, however, the equations of motion remain intractable unless further simplifying assumptions are made.

For solving the equations of motion after the simplifying assumptions are introduced, there are two principal approaches, which differ in the choice of a calculational frame of reference. In one, called the "Eulerian" method, effects of all motions are computed with reference to a geographically fixed co-ordinate system. In the other method, called "Lagrangian", calculations are further simplified by computing only the advective effects relative to geographic co-ordinates, while the effects of turbulent motions are referred to a moving co-ordinate system (moving, specifically, with the velocity of the wind). The PES model utilizes the Lagrangian approach and focuses attention on processes occurring in a moving column of air.

The effects of molecular diffusion are quite generally assumed to be negligible, because the linear range of such effects has been shown by experiment to be small relative to both advective and turbulent atmospheric motions. This assumption is also implicit in REM.

To summarize and symbolize these concepts, we may write the conservation-of-mass equation in the form

---

[*] cf. Darling, loc. cit.

$$c_i' = R_i + S_i + A_i + T_i + M_i \qquad (1)$$

where c_i' is the rate of change of concentration of species $\underline{i}$;

R_i is the rate of change due to chemical reactions;

S_i is the rate of change due to pollutant emissions;

A_i is the rate of change due to advection;

T_i is the rate of change due to turbulence;

M_i is the rate of change due to molecular diffusion.

In large part, the problem in constructing a useful simulation model for air quality lies in identifying appropriate assumptions to simplify the computation of the various terms of Equation 1. As explained above, M_i can be taken as zero by assumption, leaving only four terms to be dealt with. By adopting the Lagrangian approach, A_i can be rendered tractable and effectively disengaged from the central problem of calculating concentrations, leaving for further consideration the terms $\underline{R_i}$, $\underline{S_i}$, and $\underline{T_i}$. These terms must be computed, explicitly or implicitly, for each parcel (i.e., each hypothetical volume element) of air within the compass of the model.

To develop a cost-effective model, it is desirable to minimize the computational effort involved in simulating those details of reality which are of little importance or relevance to the objectives of modeling. For example, any chemical reaction which could be shown to proceed to completion within a few seconds after the primary contaminant responsible is emitted into the air could be subsumed in the effects of sources and withdrawn from consideration in the more complicated chemistry represented by the term $\underline{R_i}$. Similarly, if any of the three terms $\underline{R_i}$, $\underline{S_i}$ and $\underline{T_i}$ could be shown to be negligible relative to the total, then computation for that term could be curtailed or eliminated. For purposes of the PES model, it is assumed that the effects of turbulence on rate of change of concentration are negligible, except in the vertical dimension. With respect to vertical turbulence, it is assumed that its effect is to produce homogeneity of contaminant concentration in the vertical dimension, from the ground to the mixing height. Combined, these assumptions obviate the necessity for performing calculations to determine T_i as a separate quantity, by defining the appropriate hypothetical volume element as an air parcel comprising a uniform column having height equal to the mixing depth of the urban atmosphere at the given time and location.

The effect of eliminating T_i as an essential term of the conservation-of-mass model is to make the calculational scheme for the model formally equivalent to that of an irradiation chamber of variable volume in which chemical reactions take place, and into which fresh quantities of reactants are continuously introduced. The simplified version of Equation 1, appropriate to the PES model, may therefore be formulated as

$$c_i' = R_i + S_i + H_i \qquad (2),$$

where H_i represents the rate of change of concentration of species $\underline{i}$ due to the variation of mixing height.

This formulation is appropriate, of course, only to the extent that the effects which have been ignored or subsumed are really small relative to those which have been retained. This is likely to be more nearly true in some circumstances than in others. We must, therefore, examine the typical state of an atmosphere in which photochemical smog is likely to develop, in order to justify the assumptions on which REM is based.

1. The assumption that the effect of horizontal components of turbulent motion is negligible. This assumption would be absolutely correct if there were no variation in concentration with geographical location, and it will be nearly correct whenever horizontal gradients of concentration are sufficiently small, so that the replacement of a small parcel of air within the postulated column by an equal parcel

from a short distance away would cause only a negligible change in the concentrations being calculated.

With regard to large scale inhomogeneities in the concentration of contaminants in the Los Angeles Basin, two comments are germane. First, the relatively slow progress of photochemical reactions, when combined with the rapid rate of small scale mixing such as caused by daytime breezes and vehicular traffic, tends to smooth out the differences in concentration of oxidant, ozone and other photochemical products, producing rather small concentration gradients over substantial areas within the urban region. A study of this situation, reported in an authoritative review[2] dealing with photochemical smog in the Los Angeles Basin, led the authors to conclude: "In spite of...lack of complete mixing, the maximum daily oxidant at stations within a 600 to 800 square mile area are directly proportional to each other in a predictable fashion."

Second, the scale of representation of inhomogeneities in the horizontal dimension, in the atmospheric simulation, cannot usefully be made any finer than the representation of inhomogeneities in the geographic variation of contaminant emissions. In the present state of the art, this effectively restricts the resolution to that available on emission inventory grids, on which the smallest differentiated areas are of the order of 4 square miles. Gradients permitted by such resolution are, beyond question, negligible in their effects on small air parcels subject to vertical mixing and chemical reaction.

2. The assumption that the effect of the vertical component of turbulent mixing is to establish uniform contaminant concentrations in a column of air between the ground and the mixing height. This assumption is in accord with the conventional meteorological explanation of

---

[2] Schuck, E.A., J.N. Pitts, Jr., and J.K.S. Wan. "Relationships Between Certain Meteorological Factors and Photochemical Smog," Air and Water Pollut. Int. J. 1966 Vol. 10, pp 689-711.

the establishment of normal lapse-rate conditions of vertical temperature structure below the subsidence inversion in the Los Angeles Basin, during sunlight hours. This follows from the vertical motion, due to buoyancy of air parcels warmed by contact with the ground and other surfaces heated by the sun; cooler air from above sinks to replace the rising air, and is in turn warmed. This convective effect soon results in a near uniform temperature gradient below the mixing height.

It is to be expected that this mixing mechanism should tend to distribute pollutants from sources near the ground (such as motor vehicles) in a similar manner, as any relatively cool, unpolluted air above the ground layer soon reaches the ground to receive heat from the ground and contaminants from the ground-based urban activities. Little is known of the actual distribution of contaminants under such circumstances, as few studies have been made.

However, one instance[3] investigated by a research team in the Los Angeles Basin substantially supports the assumption in question. Temperature, carbon monoxide and oxidant concentrations were measured at various altitudes above three air monitoring facilities during several ascents and descents, on a day (September 29, 1969) when photochemical smog prevailed in the Basin. The vertical distribution of contaminants showed a marked tendency toward uniformity, increasing as the day progressed and ground temperatures increased. For example, the report cites the following observations: at Commerce at 0810, a strong inversion base near 700 feet; at 700 feet, the CO is half the ground level; at 1000 feet, the CO is one tenth of the ground level. At 0900, the inversion had lifted slightly, and the CO at 700 feet had increased to 80 percent of the ground level. Near noon, the oxidant exceeded 20 pphm from ground level to 1700 feet at El Monte, but at Commerce it was 4 pphm or less at all points above 800 feet---with concentrations of 8 pphm from the ground to 750 feet. At 1300, the inversion was gone at El Monte; the temperature profile was close to the adiabatic lapse rate; the oxidant was nearly uniform from the ground to 2200 feet; CO was approximately the same at ground level, 700 feet, 1100 feet and 1500 feet.

---

[3] "1969 Atmospheric Reaction Studies in the Los Angeles Basin, Volume I" Final Report, Contract No. CPA 70-6 (Scott Research Laboratories)

Although these and other observations support the assumption that vertical turbulence tends to produce uniform concentrations throughout a vertical column of air, it is nevertheless clear that a finite time must be required for the operation of this mechanism. If the time required is long enough to be comparable with the characteristic time for development of photochemical products, then the concentrations of these contaminants should be expected to be substantially different near the top of the column than near the ground. No doubt the rate of mixing varies considerably from one day to another, and from one location to another. However, no method of estimating the effect of such variation has yet been offered. In the present state of the art, it appears likely that the assumption of uniform concentrations within the column is adequate for modeling purposes, under most of the conditions that give rise to photochemical smog.

As observed above, these assumptions regarding the effects of turbulent air motions render the calculational scheme for the PES model formally equivalent to that of an irradiation chamber, conceived as a chamber having variable volume and capable of receiving fresh contaminant input during the course of irradiation. Use of this structure for the model has the incidental advantage that it is readily adaptable for simulation of actual irradiation chamber experiments. Thus, testing of any proposed chemical reaction mechanism, with the aid of appropriately designed experiments, is facilitated. Chapter 3 of this report deals with the results of an extended series of irradiation chamber simulations, using data supplied by the contracting agency.

Another implication of the procedure of subsuming effects of turbulence under those of volume variation (cf. Equation 2) is that the effects of chemical reactions should be, in reality, more important than those of atmospheric turbulence. If this is true, then the changes in air quality as observed in the atmosphere should resemble, to an appreciable extent, the changes seen in chamber irradiations. The fact that they do so is well known and attested in the literature relating to photochemical smog. It has recently been reconfirmed in a statistical study by PES of Los Angeles air quality data for the years 1968 through 1970, dealing with the average diurnal variation of the photochemical contaminants. It is found that, on the average, nitric oxide concentration decreases continuously from the time of maximum morning vehicular traffic, while nitrogen dioxide increases to a maximum after about two hours and oxidant reaches a maximum after four or five hours (all at a particular receptor location in Los Angeles). Such observations tend further to confirm our contention that the PES model suffers no serious loss in plausibility from the assumptions used to obviate the calculation of $\underline{T_i}$ (Equation 1)--a calculation for which, in any event, only empirical approaches appear to be available.

4. Chemical Reactions in the Atmosphere in Relation to Control Strategy Planning

One of the principal uses of air quality models is the estimation of probable effects on urban air quality which would arise from various possible pollution abatement strategies. REM is designed to emphasize the importance of those aspects of the model which are most sensitive to changes in abatement strategy, namely, the effects of contaminant emissions and the effects of chemical reaction--the terms $\underline{S_i}$ and $\underline{R_i}$, respectively, of Equation 1.

The relevance of a cogent model of contaminant emissions is, of course, obvious; no model can produce estimates of air quality effects which are any more accurate than the supplied estimates of emissions. However, in some of the extant approaches to air quality modeling, emphasis is placed on detailed calculation of the effects of advection and turbulence--the terms $\underline{A_i}$ and $\underline{T_i}$--at the expense of a cogent model of the chemical reactions.

The importance of an adequate simulation of the chemical aspects of contaminant development should be particularly clear in the consideration of photochemical product contaminants like ozone, one of the most toxic constituents of photochemical smog. Referring again to the terms of Equation 1, it can be seen that, in this case, the term $\underline{S_i}$ is identically zero, since there are no ozone emissions. It is $\underline{\text{only}}$ through the term $\underline{R_i}$ that the effect of emissions of contaminants other than ozone can be taken into account in estimating air quality relative to ozone, and no amount of advection and turbulence can tend in the slightest degree of account for the production of ozone if the chemical simulation does not adequately do so.

It must be further observed, that the mode of use of an air quality model for control strategy planning is basically a comparative mode (in mathematical terms, a difference or ratio mode). That is, the question to be answered in applying the model for this purpose is, given such and such changes in the existing emission inventory for a given region, what changes in air quality can be expected to ensue? Viewed in this light, it can be seen that elaborate computational procedures for careful simulation of the atmospheric motions (terms $\underline{A_i}$ and $\underline{T_i}$) are unlikely to be cost-effective, since (a) there is no expectation that the processes of advection and turbulence will be in any way affected by changes in the existing emission inventory and (b) the accuracy of individual simulations is less critical than the relative accuracy of the comparison.

The relative importance of these aspects is reflected in the detailed structure of the terms of Equation 1, on closer examination. For example, the term $\underline{T_i}$ in the conservation-of-mass formulation, by either the Eulerian or the Lagrangian method, becomes[1]

$$\left(T_i = \frac{\partial(u'c_i')}{\partial x} + \frac{\partial(v'c_i')}{\partial y} + \frac{\partial(w'c_i')}{\partial z} \right) \qquad (3)$$

in which there is no requirement or provision for any information regarding contaminants other than species $\underline{i}$. Thus, in particular, the effect on ozone concentrations of a change in the emission inventory of nitric oxide would not be evidenced in any direct way by changes in the calculated value of $\underline{T_i}$.

With regard to the term $\underline{R_i}$, representing the rate of change of concentration of species $\underline{i}$ (ozone, say) as a result of chemical reaction, the situation is far different. The detailed form of $\underline{R_i}$ is expressed as a sum of terms for individual elementary reactions*; some of these terms are negative in magnitude and contain as a factor the concentration $\underline{c_i}$, but almost all contain, as additional factors, the concentrations of other constituents. (In the case of ozone, one of the negative terms contains the concentration of nitric oxide as a factor. Thus the behavior of the term $\underline{R_i}$ does reflect in a direct manner the influence of changes of nitric oxide emissions on ozone accumulation.)

For these reasons, when control strategy planning applications are envisaged, it is important to select an air quality model which (like REM) incorporates an adequately detailed chemical mechanism.

5. Formulation of a Chemical Reaction Mechanism in Terms of Elementary Reactions

Development of an adequate chemical reaction mechanism for simulating the time-profiles of concentrations of reactive contaminants and reaction products might be expected to be a relatively simple and straight forward process, in view of the basic simplicity of the kinetic principles discussed above (section 2 of this Chapter). The procedure does, however, contain pitfalls for the unwary, some of which will be discussed in this section.

One of the most common fallacies committed by would-be modelers who do not understand chemical kinetics is to confuse complex reactions with elementary reactions. For example, it is not uncommon, in discussing control strategy for photochemical contaminants, to encounter the argument that maximum ozone concentrations should be proportional to the product of maximum concentrations of hydrocarbons and oxides of nitrogen, since these are known to be precursor contaminants for ozone.

---

* For further detail, see Volume II of this report

That this relation does not hold true, in general, has been often demonstrated in irradiation chamber experiments with simulated smog. Nevertheless, it is sometimes felt that the assumption, that it is true in the urban atmosphere, will yield an adequate simulation for air quality with respect to ozone. This is thought to be plausible in view of (a) the superficial similarity of this relation to the corresponding expression of the rate law for elementary reactions and (b) the scarcity of relevant data regarding hydrocarbon concentrations in urban atmospheres.

The basic fallacy, here, is in contending that the rules for elementary reaction should hold when, in fact, there is no elementary reaction, between hydrocarbons and oxides of nitrogen, that has any appreciable collision yield. This should be obvious, incidentally, from the fact that these components do not react with each other in the absence of sunlight. As an indication of how unreliable such an assumption may be as a quantitative guide, we may cite the classical investigations of the kinetics of photochlorination of olefinic hydrocarbons (a somewhat parallel case). Here the rate of change of hydrocarbon concentration was found to be proportional to the concentration of chlorine gas, but almost completely independent of the hydrocarbon concentration--a clear-cut contradiction to the type of simple assumption advocated by these oversimplifiers.

Although elementary reactions are, in fact, responsible for the chemical changes which occur in both the photochlorination system and the photochemical smog system, most of these elementary reactions involve so-called "intermediate" species: very reactive molecules having a high content of chemical energy, such as free radicals and atoms--basically, molecular fragments produced in the system by the absorption of energy from sunlight. (In the photochlorination system, one such species is free atomic chlorine, produced by photolysis of ordinary diatomic molecules of chlorine gas; in the photochemical smog, or "photo-oxidation", system, such species include free atomic oxygen, from photolysis of nitrogen dioxide, and free hydroxyl radicals, as well as a wide variety of other free radicals). Because of their high reactivity, their concentrations always remain exceedingly small, and cannot be measured by methods currently available.

Thus, the adequate simulation of the photochemical smog system, whether in chamber experiments or in the atmosphere, depends on a reasonable understanding of the nature and properties of these intermediate species, and some reasonable estimates of the collision yields of the elementary reactions which involve them.

As previously mentioned, the state of the art of computer simulation of chemical kinetics is now such that, using available routines for numerical integration, concentration-time profiles of many components of a reaction system can be readily generated, starting with postulated initial concentrations and a mechanism of as many as a hundred individual reactions, perhaps more. Thus, if a complete mechanism is postulated, it may be readily tested for agreement with relevant data from chamber experiments. If, under a reasonably wide range of initial conditions, the results of computer simulation are in reasonable agreement with the results of experiment, then the postulated mechanism may be regarded as a fairly accurate description of the true chemistry of that reaction-system, provided that none of the postulated collision yields of the elementary reactions are known to be in serious conflict with other chemical information.

However, it is important to note that the postulated mechanism cannot be considered chemically adequate, unless all of the conditions listed above are met, using values for the collision yields which are invariant except for a temperature-dependence of a theoretically-permitted form. A mechanism is not satisfactory in a theoretical sense, if (a) different values of the collision yields (or related rate factors) are required for simulation of experiments with differing initial concentrations of various components; or (b) individual reactions, as written, are not compatible with established chemical principles, including stoichiometry; or (c) molecular formulas are written in generalized terms, corresponding to more than one chemical species. Each of these fairly common types of discrepancies invalidates a mechanism, at least in a theoretical sense, although in practice, some instances may be less damaging than others.

For a number of relatively simple systems, including the olefin-photochlorination systems cited above, theoretically adequate reaction mechanisms have been worked out. In most such cases a relatively small number of elementary reactions have been involved, usuually less than twenty.

The evident complexity of the photochemical smog system, however, ensures that a theoretically adequate, or nearly adequate, mechanism will involve a much longer list of elementary reactions. Complete determination of that list is not presently in sight. Therefore, to develop a satisfactory mechanism soon for practical purposes, some compromises with the purity of a theoretically satisfactory mechanism must be countenanced.

In developing the mechanism currently employed in REM, PES has utilized three types of compromises:

(a) Chain-terminating reactions, i.e., reactions between free radicals and between nitric oxide and free radicals, have been assigned common values of their rate factors, and the products have been assumed quantitatively negligible.

(b) Hydrocarbons other than propylene have been lumped into a single category, assumed to react with oxygen atoms with a single rate factor and with identical products.

(c) Rate factors for the chain-terminating reactions, and for the reaction of generalized hydrocarbons with oxygen atoms, have been occasionally allowed to vary, in the interest of improving simulation for certain irradiation chamber experiments.

These assumptions and the manner of their implementation are discussed below (Chapter 3) and in the final report[4] on an earlier project in which the main features of REM were developed.

At the same time, in developing REM, PES has avoided utilizing certain types of compromises, regarding chemical validity, which have been advocated by other modelers. These include:

(1) the use of chain-branching factors as invariants of the mechanism, in conflict with the fundamental nature of such factors as derived quantities inherently sensitive to concentration changes. E.g., "$OH + HC \rightarrow (b_2)RO_2$ where $b_2=4$ for propylene."

(2) the use of variable stoichiometric coefficients, in conflict with the principle of invariance of collision yields for elementary reactions in chemical kinetics. E.g., "$NO + RO_2 \rightarrow NO_2 + dOH$, where $d=1/2$ to $1/4$ for various concentrations."

Such parameters may in some cases facilitate the adjustment of simulation results to agree with reference data but, to the extent that they contravene the established principles of kinetics, they sacrifice generality and impair the credibility of the model for application to conditions other than those of the example simulated.

Thus, at the core of REM is a paradigm for the simulation of chemical kinetics which makes it rather easy to test proposed reaction mechanisms to determine whether they are compatible with results of chamber experiments and to utilize the best validated of such mechanisms in atmospheric simulation. At the same time, the PES approach minimizes the introduction of discrepancies which can arise from improper postulates as to the relation of the kinetic parameters to contaminant concentrations.

---

[4] Weisburd, M.I., L.G. Wayne, R. Danchick and A. Kokin, "Development of a Simulation Model for Estimating Ground Level Concentrations of Photochemical Pollutants." Final Report, Contract No. CPA 70-151 (January 1971)

E. ROLE OF ATMOSPHERIC TURBULENCE IN SIMULATION OF AIR QUALITY

REM is based on a relatively simple view of the motion of air over an urban area; namely, that air goes where the wind takes it, that in the process it picks up contaminants from the sources it moves over, and mixes them thoroughly in the vertical dimension, up to the mixing depth. Implementing this approach, REM focuses on hypothetical moving columns of air and integrates the effects of the emissions, the chemistry, and the changes in mixing depth as each such air parcel traverses its appropriate trajectory.

(Practically the same model for air movement was arrived at independently by Leahey[5], and validated for sulfur dioxide in New York City. Correlation between measurements, using an instrumented helicopter, and predictions, using the model, was 0.83 for 400 data pairs.)

The PES model calculates mixing depth for any given location and time as, to a good first approximation, a function of the temperature at ground level and of the vertical temperature structure of the atmosphere over cooler areas of the region. The temperature at ground level is approximated by interpolation from values observed at nearby measuring stations. As a result of motion along the trajectory, the elevation of the base of the air parcel changes because of topography, and the elevation of the top changes because of the changes in temperature at the ground. The net effect is of a change in volume of the air parcel; this may be a net increase or decrease, depending on circumstances. Whenever the volume is increasing, it is assumed that concentrations within the column decrease to maintain constant total mass; but whenever the volume decreases, it is assumed that concentration remains steady while total mass decreases (as if contaminants were being forced out through the top of the column).

---

[5] Leahey, D.M., "An Advective Model for Predicting Air Pollution within an Urban Heat Island," etc., J. Air Pollution Control Assoc. 22, 548-550 (1972)

The assumption of homogeneous mixing throughout the column is useful, in that it eliminates the necessity for repetitive computation of chemical reaction rates at various altitudes, to account for differences due to inhomogeneity. Another approach which has been advocated is to assume that the column comprises a number of vertically stacked cells, within each of which, mixing is instantaneous; then to provide a paradigm for transfer of material from each cell to the one above it by virtue of turbulent motions within the column.

This additional complication is likely to be useful only if (a) the differences in concentration between different levels of an actual sub-inversion air mass are large enough to cause very substantial deviations from the rates based on column-average concentrations, and (b) some plausible algorithm is known, by which the rate of upward diffusion due to turbulence can be estimated.

In regard to the first of these conditions, it is clear that real atmospheres are not really homogeneous in the vertical dimension. However, we have already adduced evidence (see section D.3 of this chapter) that, under conditions conducive to photochemical smog, the deviations from homogeneity are not inconsistent with an impressive degree of success in validating a model for sulfur dioxide in New York City (v.s.). It is of special interest, therefore, that in two photochemical air quality models currently under development, estimates of ground level concentrations based on the assumption of vertical homogeneity have been compared with other estimates based on the multilevel approach. Apparently, the differences found have not been very large.

As to the availability of a suitable paradigm for application to the problem of calculating rates of vertical diffusion, this has been addressed in the studies of another Environmental Protection Agency contractor[6], from which it appears that estimates of vertical diffusivity, in the present state of the art, rest on completely empirical formulations with an extremely sketchy experimental basis. When related to wind speed, estimates typically vary from observed values by a factor of three to ten, and sometimes more. When related to vertical temperature gradient, the spread of observed values is nearer to a factor of three, in the single literature source cited for this purpose.

---

[6] Contract No. 68-02-0336, Monthly Technical Progress Narrative, September 15, 1972

In view of these difficulties, it is pertinent to consider whether available data indicates that sub-inversion mixing is slow enough to require separate treatment in the model. Since the typical period required for development of photochemical smog from one phase to the next (e.g., from maximum NO to maximum NO_2) is about two hours, substantial mixing within a period of thirty minutes might be considered likely to produce a reasonable approach to vertical uniformity of atmospheric composition in the mixing layer. Studies recently published[7] showed that vertical velocities as high as 100 feet per minute are common in the subinversion layer in Los Angeles during the morning, and that constant-volume balloons were often displaced vertically as far as 1000 feet in a period of 15 minutes or less. Such vigorous motions within a mixing layer of, typically, 2000 feet or less, should provide good mixing.

We conclude that the assumption of vertical homogeneity, utilized in REM, is sufficiently plausible to be accepted for modeling purposes, at least until alternative formulations are based on more substantial theory and documented with better field information than is now possible.

F. STATUS AND FUTURE DEVELOPMENT OF REM

1. History of REM

The development of REM first began as a task under contract CPA 22-69-108 to the National Air Pollution Control Administration,

---

[7] Angell, J.K., D.H. Pack, L. Machta, C.R. Dickson and W.H. Hoecker, "Three-Dimensional Air Trajectories Determined from Tetroon Flights in the Planetary Boundary Layer of the Los Angeles Basin." J. Applied Meteorology, Vol. 11, p. 451-471 (April, 1972)

"Comprehensive Technical Report on All Atmospheric Contaminants Associated with Photochemical Air Pollution". This project concentrated on the preparation of the above report, preparation of the "Air Quality Criteria for Hydrocarbons" document (AP-49), statistical analysis of photochemical data for 6 CAMP cities and 11 SCAN stations, and development of an atmospheric pollution simulation model. This work was performed for the Bureau of Criteria and Standards. A completely operational version was validated and the program of the model, together with documentation and results of control strategy exercises (the first ever to be conducted with a photochemical simulation model), were delivered to NAPCA, June 1970. The results of this effort were reported in the Journal of the Air Pollution Control Association, Vol. 21, No. 6, June 1971.

The first version of the model contained a 31-step reaction mechanism (substantially different from the current version) and a stationary point source diffusion module based on standard diffusion principles. It utilized Hamming's linear, multistep predictor-corrector method for numerical integration purposes. With these exceptions, and subsequent optimizations and refinements, the design of this model has carried forward through the current project.

The next project was performed under Contract CPA 70-151, "Development of a Simulation Model for Estimating Ground Level Concentrations of Photochemical Pollutants," for the Bureau of Abatement, National Air Pollution Control Administration, July 1970 through January 1971. The work performed under this contract included a literature review of chemical mechanisms, chemical chamber simulations, program modifications to handle mixing depth information aquired from Scott Research Laboratories for September 29, 1969 at El Monte, Commerce and Hawthorne, revision of the source emission inputs, and conduct of 15 validation runs for September 29 and 30, 1969. Some 21 sensitivity tests and

11 control strategy exercises were also conducted in this project. The results of this effort were extensively reported in "Final Report: Development of a Simulation Model for Estimating Ground Level Concentrations of Photochemical Pollutants", January, 1971.

For 15 validation runs the percent deviations* by contaminant were as follows:

Contaminant	Ave.	Range	% Less than Factor of 2
Ozone	46%	5-79%	47%
Carbon Monoxide	47%	4-81%	54%
Nitric Oxide	52%	0-90%	64%
Nitrogen Dioxide	59%	5-100%	45%

Analysis of the results indicated that the "poor" runs contributing to these results were associated with the minimum mixing depth assumption used for surface inversion conditions (which had been set at 30 meters) and calculations of breaking inversions and that the "good" runs were associated with middle range mixing depths of 55-500 meters. Reruns of some of the poor runs with the minimum mixing depth assumption changed to 100 meters showed dramatic improvements. Rank order analysis of the data for nine runs involving four stations where the mixing depth calculations appeared to be reasonable yielded a positive rank correlation coefficient of .84, significant at the one percent level. These results indicated that further work was particularly needed on assumptions regarding mixing depth calculations. This work was carried forward into the current contract period.

A sensitivity analysis was also conducted to establish the relative importance of various design, input and program features of the model. The results are reported in detail in the above mentioned report. In general:

---

* Calculated as deviation over larger (calculated or observed) value. 0% = perfect agreement; 100% = maximum deviation possible.

1. Results are strongly sensitive to minimum mixing depth assumptions.

2. Results are strongly sensitive to traffic emission rates and to traffic behavior resulting from movement of the diurnal traffic curve two hours earlier. Concentrations are affected by as much as 50%.

3. Reductions in ozone are roughly proportional to reductions in uv intensities.

4. The results are sensitive to background concentrations (initial values at start of trajectory), but the degree of sensitivity is trajectory dependent.

5. Sensitivities to emission rate increases or decreases are highly trajectory dependent. Contaminant concentrations are never linearly proportional to emission reductions. In some instances, significant changes in air quality were shown to be highly refractory to small changes in emission rates.

6. The results exhibited notable sensitivity to assumptions concerning reaction rate constants for the production of singlet oxygen by reaction between ozone and nitric oxide; slight sensitivity to changes in certain rate constants; and moderate sensitivity to the density of the wind station network. The study indicated that the location of wind stations is as important as the density of such stations.

2. Current Project

The current project began in March, 1972, after more than a year in which no additional work had been conducted. The following was performed:

1. The existing REM program was completely reviewed and improved wherever possible from the standpoint of accuracy and efficiency.

2. Special interpolation routines were added for smoothing wind, relative humidity and temperature data (meteorological module) and emissions data (emissions module) to eliminate time-step and cross-grid discontinuities.

3. A sensitivity study was performed on the minimum mixing depth assumption and the minimum mixing depth value was set as an input parameter to 50 meters.

4. A new emissions module was developed which combines area and vehicular sources. New emissions data, supplied by Systems Applications Inc., were input to this module.

5. A new 32-step chemical mechanism was developed as a result of simulations of chamber data for 26 gaseous mixtures that had been supplied by EPA.

6. A new numerical integration mechanism was adapted to the model. This is the Adams option of the Gear routine. The back substitution option of the Gear routine was also made to work. This necessitated reducing the order of the chemical mechanism matrix from 11 to 7.

7. Carbon monoxide validations were performed on 67 trajectories at selected receptor points for 6 days in the Los Angeles Basin.*

8. Ground level concentrations for all photochemical contaminants were computed at four receptor points for 6 days (24 trajectories) in the Los Angeles Basin, and for an additional 8 trajectories for one of these days.*

9. A training session was successfully conducted by PES staff at EPA in the Research Triangle Park on October 25, 26 and 27, 1972. The model was easily operated by EPA personnel on the IBM System 370/165.

As a result of the above efforts, the new version of REM exhibited considerable improvement in speed and accuracy. For example:

- CO is less than a factor of 2 in more than 80% of the comparisons; 40% agreement within one part per million. The 80% figure may compared to 54% in the previous version.

- O_3 is within a factor of 2 in more than 70% of the runs as compared to 47% in the previous version.

- NO is in 90% agreement within .02 pphm. In a previous version, NO was within a factor of 2 in 64% of the comparisons.

---

* All simulations were conducted "hands-off", i.e., no runs were "fitted" or "calibrated", hence the validation results are not influenced by these kinds of manipulations.

- NO_2 is within a factor of 2 in 60% of the runs as compared to 45% in the previous version.

Continuous improvements in the speed and usability of REM were also attained. Computer speeds are expressed in terms of real-time-to-simulation ratios. For the IBM Systems 360/65 and 370/155, the following average ratios were attained:

1969, first contract	10:1	Hamming method
1970, second contract	50:1	Hamming method
1972, current project	150:1	Gear method, Adams option

When carbon monoxide simulations are conducted alone, REM runs at about 3000:1.* The type of computer used, of course, affects speed. On EPA's IBM System 370/165, a full chemical simulation of REM over 6 1/2 simulated hours ran at a speed of 550:1, or 40-45 seconds for a 6 1/2 hour trajectory. For carbon monoxide alone, the speed would be 11,500:1.

3. Recommended Improvements

The results of this and past projects indicate that REM is a more realistic, accurate and useful method for testing control strategies than are rollback or other available methods. Unlike the rollback technique, REM can determine the impact on air quality of various source reduction schemes, singly and in combination, by time and location taking into account varying configurations of point and area sources, both moving and stationary, and the chemical reactions that take place among air pollutants under varying physical and environmental influences.

The user may attain the confidence level he may require as an outgrowth of his use of the model. Through the normal processes of validating the model for any air quality control region, providing improved data or modifying input parameters, REM becomes highly adaptable to local conditions, and its accuracy can be continuously improved. REM is readily modified; for example, the chemical mechanism can be altered or replaced entirely, various transport and mixing assumptions can be attempted and modules can be deleted or added.

---

*Full chemical simulations can approach this speed depending on the chemical mechanism employed. Chemical mechanisms smaller than those used in this project are available. These would substantially improve running time.

The greatest spur to the practical refinement of the model, in fact, would be in its widespread use for control strategy and operational purposes since the natural uses of the model inherently involve validation and sensitivity testing, the results of which will indicate the further improvements that can be made to the model.

The degree of validation achieved by REM and possibly other photochemical models appears to be well within the degree of accuracy that has been attained by diffusion models. Further improvement in accuracy and speed by working with the model as it is now constituted, of course, is possible, but major improvements will depend on obtaining more and better field and chamber data.

A summary of desirable further work on photochemical modeling in general, and REM specifically, is described below:

1. In the future a closer interplay between chamber irradiations and simulations of chamber results should take place. New experiments should be designed to answer the questions about the mechanism that need answering, and continuous critique and feedback should be provided for.

2. An improved method of estimating mixing height for the eastern portions of the South Coast Air Basin should be developed. This will likely depend on more extensive field study of vertical temperature structure in the region.

3. An improved representation of the hydrocarbon mix for input to the chemical mechanism, and appropriate elementary reactions, should be studied and developed.

4. More experimental work is needed to determine the effects of water vapor and sulfur dioxide on the chemistry. Generation of aerosols by photochemical activity and the effects of aerosols on

photochemical activity should also be determined.

5. An option should be provided to utilize carbon monoxide as a ventilation index taking into account emissions input.

6. Additional elementary reactions should be explored (by cut-and-try methods) in an attempt to cut down the excessive simulated rate of conversion of NO to NO_2 and to reduce the overestimation of nitrogen dioxide in the current REM chemical mechanism.

7. Improvement of existing, and search for a new, numerical integration procedure should continue. This could include use of system identification methods, examination of tailor-made vs. general purpose procedures, further chemical mechanism parameter optimization, minimizing set size in validated mechanisms, and balancing accuracy vs. speed tests.

8. Alternative methods for inputting mixing height information, including multiple radiosonde information, aircraft monitoring data, and assumed mixing height information should be provided.

9. Photochemical models should be linked with routine 24-48 hour air pollution forecast and emergency warning procedures. This will require analysis of objective forecasting procedures, study of mega-meso-microscale relations, and linkage to air quality and meteorological data handling systems.

10. A synthetic trajectory application capability is required to permit use of the model in all data availability situations.

11. Automatic trajectory plotting or computer graphics to minimize manual plotting of trajectories from output would be desirable.

12. A universal U.V. Module which would generate solar angle as function of time, geographic location, and calendar date is desirable.

13. An improved version of the REM point-source diffusion routine should be developed.

14. Add user conveniences including displays of trajectory emissions output, automatic validation comparisons, summaries of emissions input to air parcels, etc.

15. Linkage of reverse trajectory routine to the main model, and packaging of REM as an automatic multi-receptor point episode model.

G. EVALUATION CRITERIA

The establishment of objective criteria for the evaluation of atmospheric simulation models, particularly photochemical models, is an extremely difficult matter. Both quantitative and qualitative factors must be considered, as well as subjective judgment. Further, it is difficult to evaluate models based on limited applications.

PES, throughout its experience in developing REM, has kept the following criteria in mind:

1. Cogency - the employment of fundamental and realistic principles consistent with knowledge of physical and chemical reality such that the model responds realistically and sensitively to the wide range of input conditions to which it may be subject. The question of cogency is described in greater detail in previous sections of this report.

2. Validation Accuracy - these criteria may be looked at from the standpoint of the statistician and the "responsible user" of the model. The statistical evaluation of REM is treated throughout this report. The responsible user is considered to be the air pollution control officer, urban planner or other individual with administrative responsibility who must decide whether or not to use the model and what degree of confidence can be placed in its use. Given the limits of modeling, the most important criteria that can be applied may be in part quantitative, in part qualitative. PES assumes the following criteria in their order of importance.

   a. The model should be capable of distinguishing among high and low oxidant days. It should exhibit a high degree of success in predicting episode days.

   b. The variation in predicted contaminant levels by time of day should be parallel to variation in the observed levels by time of day even if significant quantitative differences may occur; the model should exhibit similar results for dosage calculations.

c. The variation in predicted contaminants by general geographical location should be consistent with the observed values by location.

3. Potential for Improvement and Usability - these are very important criteria, particularly with respect to the current generation of photochemical models. The model should be (a) easy to use; (b) easy to modify; (c) adaptable to many urban areas; (d) adaptable to different degrees of data availability and conditions of use; and (e) economical to use.

Frequently, some of these criteria are ignored in model development. Yet, the accuracy of a model at any particular point in its stage of development may be misleading. Given a cogent and cost-effective model, further development in accuracy, speed, and application will depend more on its widespread use in practical situations than on a preconceived development program. For accelerated development to take place, the model should be easy to use and understand, and should be made available for general use.

Chapter II

DESCRIPTION OF THE REACTIVE ENVIRONMENTAL SIMULATION MODEL (REM)

A. INTRODUCTION

The REM effort has been directed towards the construction of a sophisticated photochemical mechanism which is capable of closely replicating smog chamber data and then extending this capability to the urban atmosphere. REM is based on a Lagrangian (moving coordinate) system. This system enables the numerical computation of the chemical reactions to take place in a moving parcel or column of air. The parcel is bounded by the inversion base above and the ground below. The locations of the base of the column at successive points in time describe the path or trajectory that the air parcel traverses across the region. The trajectory is computed by special routines contained in the REM program from wind velocity information contained in the data base as a function of time of day and location. An overview of the model's operation is presented in Figure II-1.

The computer program has been designed as a detailed episode model for chemical kinetics, with additional modules linked up to form a complete atmospheric system. The modules presently in the system determine the necessary meteorological parameters, the rate of absorption of actinic light by NO_2, and emissions due to traffic and area sources. A schematic diagram of REM appears in Figure II-2. The facility exists to incorporate modules to calculate the emissions due to large point sources and the effect of vertical diffusion should practical and effectual methods be found to perform these tasks. A mathematical description of REM may be found in Volume II of this report.

PHOTOCHEMICAL MODELING

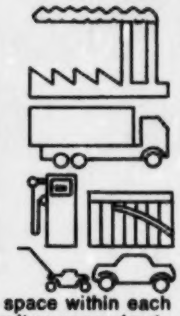

For pollution modeling, the air space within each geographic grid is assumed to emit an approximate mean value of pollutants for a given time. The model includes nitrogen oxides, high and low reactive hydrocarbons and carbon monoxide. Values are provided by local environmental control agencies.

Meteorological stations provide current data on winds, temperature, pressure, dew point, etc., to the model for predictive movement of air parcels through the various grids.

Pollutant monitoring stations measure types and amounts of pollutants, i.e., oxidants, hydrocarbons, nitrogen oxides, carbon monoxide.

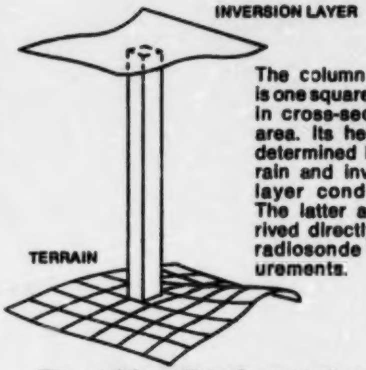

The column of air is one square meter in cross-sectional area. Its height is determined by terrain and inversion layer conditions. The latter are derived directly from radiosonde measurements.

The model predicts the amount and type of photochemicals present in a column of air as it traverses a computed trajectory path to a pollutant monitoring station. At this point predicted and observed values are compared.

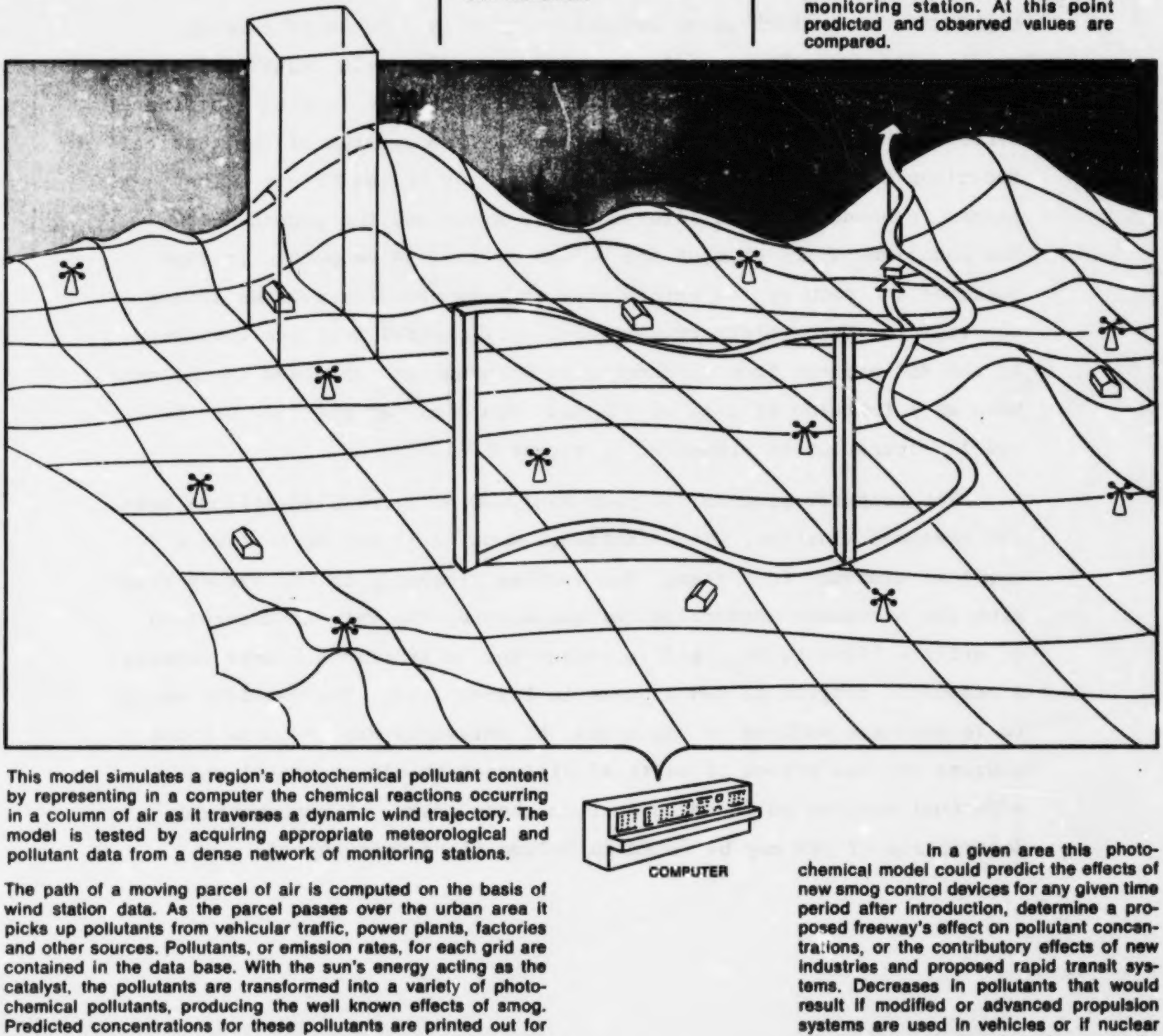

This model simulates a region's photochemical pollutant content by representing in a computer the chemical reactions occurring in a column of air as it traverses a dynamic wind trajectory. The model is tested by acquiring appropriate meteorological and pollutant data from a dense network of monitoring stations.

The path of a moving parcel of air is computed on the basis of wind station data. As the parcel passes over the urban area it picks up pollutants from vehicular traffic, power plants, factories and other sources. Pollutants, or emission rates, for each grid are contained in the data base. With the sun's energy acting as the catalyst, the pollutants are transformed into a variety of photochemical pollutants, producing the well known effects of smog. Predicted concentrations for these pollutants are printed out for points along the air parcel path and compared with values measured at actual air monitoring stations.

In a given area this photochemical model could predict the effects of new smog control devices for any given time period after introduction, determine a proposed freeway's effect on pollutant concentrations, or the contributory effects of new industries and proposed rapid transit systems. Decreases in pollutants that would result if modified or advanced propulsion systems are used in vehicles or if nuclear power plants are installed also could be predicted by the model.

Figure II-1. PES Reactive Environmental Model (REM)

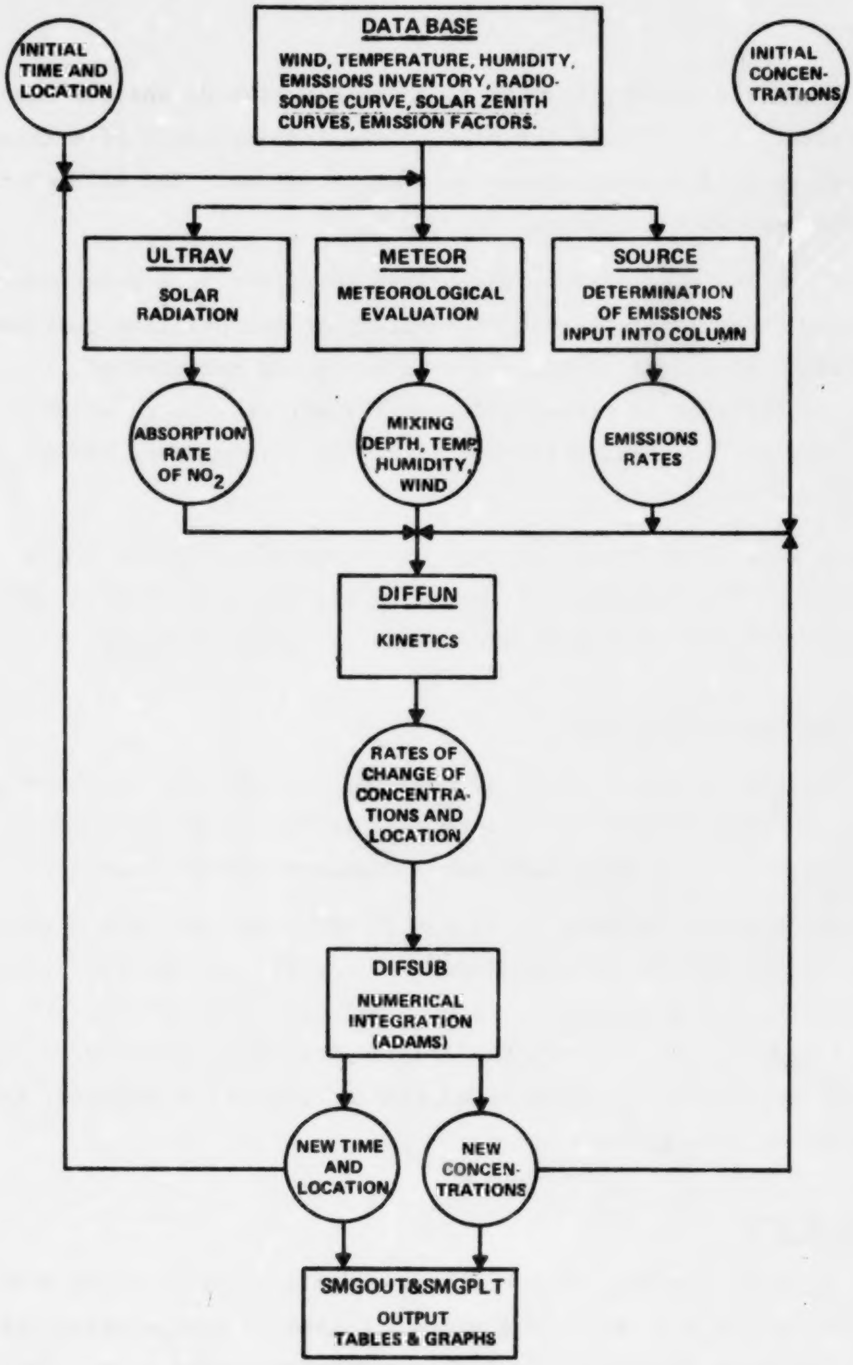

DATA BASE
WIND, TEMPERATURE, HUMIDITY, EMISSIONS INVENTORY, RADIOSONDE CURVE, SOLAR ZENITH CURVES, EMISSION FACTORS.
INITIAL TIME AND LOCATION
INITIAL CONCENTRATIONS
ULTRAV
SOLAR RADIATION
METEOR
METEOROLOGICAL EVALUATION
SOURCE
DETERMINATION OF EMISSIONS INPUT INTO COLUMN
ABSORPTION RATE OF NO2
MIXING DEPTH, TEMP, HUMIDITY, WIND
EMISSIONS RATES
DIFFUN
KINETICS
RATES OF CHANGE OF CONCENTRATIONS AND LOCATION
DIFSUB
NUMERICAL INTEGRATION (ADAMS)
NEW TIME AND LOCATION
NEW CONCENTRATIONS
SMGOUT&SMGPLT
OUTPUT TABLES & GRAPHS

Figure II.2. Schematic of the PES Reactive Environmental Model (REM)

B. GRID SYSTEM

The geometric setting for REM is a standard two-dimensionsl coordinate system. REM utilizes the mile as the standard unit of measure with all urban grid squares chosen as 4-square miles. The kilometer can also be used as the standard.

To set up the grid system, the origin is placed at a point such that the region of interest resides entirely in the positive quadrant. The coordinate positions of all air monitoring and meteorological stations are established in either miles or kilometers. These values are then fed into the model at execution time. In this manner, REM can be applied in any region.

Figure II-3 illustrates the grid system used by REM for the Los Angeles Basin. The locations of the air monitoring stations are designated as circles and the coordinate points are given in miles.

C. PROGRAM CODE AND MACHINE USE

REM is coded in the FORTRAN IV computer language and has operated with both the Level G and H compilers. It is thus operational on any computer system with 150K in core and a standard FORTRAN compiler.

The Los Angeles validation version of the model has been successfully run on the IBM System 360, Models 50 and 65, and the IBM System 370, Models 155 and 165. The ratio of simulation time to computer time used was approximately 150:1 on the 370/155 and 550:1 on the 370/165. In regions where much less data is available than in Los Angeles, REM will operate at even greater speeds.

D. OPERATION OF REM

REM has been designed to operate as a multi-receptor point model. The user is required to provide a minimum number of inputs after the data base has been prepared. In its execution mode, the model transports a parcel of air, bounded by the ground and the inversion layer,

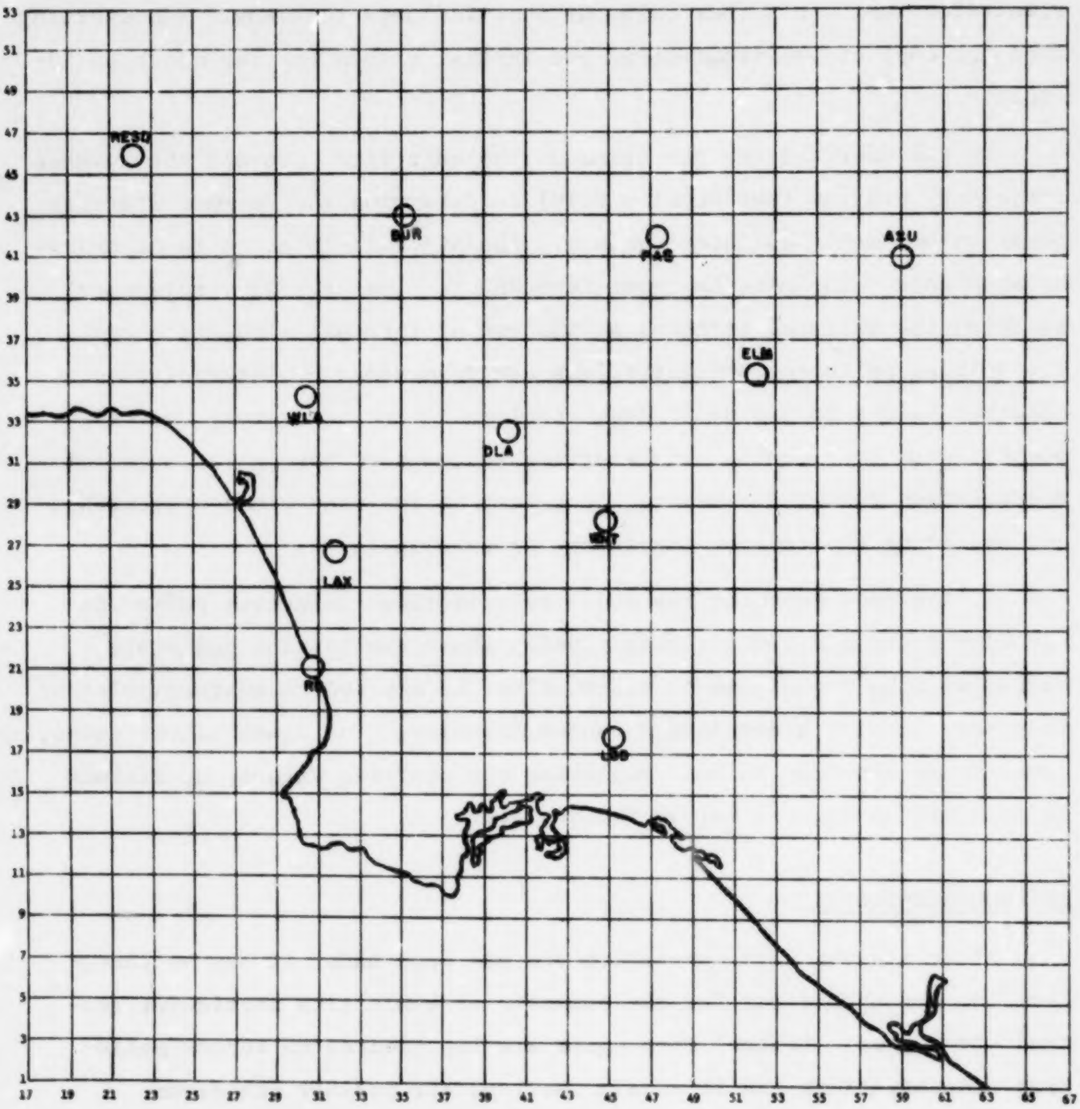
RESD
BUR
PAS
AZU
ELM
WLA
DLA
LAX
WHT
RB
LBO
53
51
49
47
45
43
41
39
37
35
33
31
29
27
25
23
21
19
17
15
13
11
9
7
5
3
1
17
19
21
23
25
27
29
31
33
35
37
39
41
43
45
47
49
51
53
55
57
59
61
63
65
67

Figure II.3. REM Grid System for the Los Angeles Basin

along a dynamic trajectory that is generated utilizing wind data from numerous meteorological stations. At each point along the path, the speed and direction of the trajectory are recalculated.

The user may select the starting point or the terminus for each simulation run. In either case, he must indicate the length and starting time (of day) of the simulation, and initial values for the major pollutants.

If the user selects the terminus, he must first operate the reverse trajectory program (see Section F.10) to determine the correct starting position and major pollutant values. The starting location is necessary because this point must be input into REM in order for the trajectory to reach the selected terminus at the end of the full simulation run. The initial pollutant concentrations are determined by interpolation of observed values at air monitoring stations to the trajectory starting point. Once the location and starting values have been calculated for a simulation run, the same trajectory may be run many times over without utilizing the reverse trajectory program again.

If the user executes the model by selecting a starting point, he may wish to choose a monitoring station where the initial pollutant values will be known. As an alternative, he may select another point of interest, or pick a completely random location. For these latter cases, some assumptions may be made regarding the starting values, or minimum or standard background values may be input.

E. CONTROL STRATEGIES

After a given full simulation run has been made, it may be considered as a standard run for the purposes of evaluating particular control strategies. Control strategies are implemented to reduce pollutant concentrations and to attain required air quality standards.

By varying any of the numerous emissions inputs to the REM, either individually or in combination, the possible effects of control strategies can be determined before they are actually implemented. These strategies may include for example: reducing total traffic, reducing traffic in specified areas, reducing emission rates, varying traffic patterns, or altering operating times of area sources.

F. REM MODULES

The modular construction of REM has facilitated the model's development and alteration, when necessary. Any given module may be unplugged and replaced as desired; or special modules may be created and added to handle special situations.

1. Initialization Program

The initialization program reads in the data base and the information needed for a complete simulation run. This program converts all of the data, except station locations, to the metric system for easy utilization by the other modules, and calls the numerical integration, output and plotting routines as required by monitoring the simulation time. At the end of the run, it checks to see if another simulation is to take place. To make additional runs, only control information must be input thereby facilitating the operation of REM for the user.

The initialization routine outputs the data base that has been read in to provide the user with a permanent record of the information employed in the simulation. A complete list of the data categories required for input follows:

- Trajectory start position and time of day;
- Length of simulation;
- Starting pollutant concentration values;

- Control parameters for numerical integration routine;
- Meteorological stations - location and elevation;
- Meteorological variables - hourly data (wind speed and direction, temperature, dew point);
- Emission factors for freeway and street traffic in grams per vehicle mile;
- Grid distribution of hourly area emissions;
- Radiosonde data - temperature vs. elevation profile; and
- Solar zenith angle as a function of time.

2. Numerical Integration

The numerical integration module is the heart of REM. This routine accepts as input derivatives calculated by the kinetics and meteorological modules and computes pollutant concentrations and the parcel position forward in simulated time. The kinetics module supplies the derivative of each of the photochemical pollutants computed as a function of time. The meteorological module provides wind velocity outputs as the time derivatives of the position vectors.

The economic use of REM is dependent upon the numerical integration routine. By attaining larger step sizes, the program will execute faster, use less computer time, and be less expensive to operate.

REM utilizes the Adams method of integrating ordinary differential equations of the Gear numerical integration package.[1] A sensitivity analysis has been conducted on the Adams routine in REM. As a result of this examination, it was found that the Adams method executes most economically with the maximum step size at 0.1 minutes and the error limit at .05 in pollutant concentration units.

3. Chemical Kinetics

The chemical kinetics module has operated on reaction mechanisms containing 13-41 reactions and is based on a set of stoichiometrically valid elementary reactions. The current version contains a 32-reaction mechanism that preserves the flexibility of chemical detail necessary for adequate simulation of both primary and secondary contaminants (see Chapter III). The set of elementary reactions, rate constants and chemical species is easily modified and expanded as required.

---

[1] C. W. Gear, DIFSUB for Solution of Ordinary Differential Equations, Communications of the ACM, Volume 14, Number 3, March 1971.

This routine calculates the elementary reaction rates and the derivatives of each of the accumulating chemical species as they change with time. It calls the meteorological, ultraviolet and emissions modules into operation, as necessary. The kinetics program adds the perturbations from the traffic and area sources to the derivatives computed for the chemistry for input into the numerical integration routine.

4. Meteorology

This module consists of a series of related routines that employ wind speed and velocity, temperature, relative humidity, elevation, and radiosonde data to calculate the meteorological values, mixing depth and rates of change in the wind at the pollutant column position.

a. Spatial Interpolation

Wind speed and direction, temperature, and relative humidity undergo both spatial and temporal interpolations from numerous meteorological stations to the trajectory location of the air parcel. The spatial interpolation is inversely proportional to the square of the distance from station to parcel. This procedure has two advantages over simply using a ratio inversely proportional to the distance involved. Firstly, it ensures that the meteorological values assigned to the trajectory position are more closely in keeping with the data at the nearest stations; and secondly, it permits the computer program to execute faster by eliminating the necessity of computing square roots.

b. Temporal Interpolation

The temporal interpolation is linear. The meteorological items for the current hour and the next hour are utilized in this process. The portion of each item contributing to the result is directly proportional to the number of minutes in the hour that have passed. For example, at 10:15 A.M. one-quarter of the value for hour 10 would be added to three-quarters of the value for hour 11.

c. Mixing Depth

The model calculates mixing depth on the basis of a temperature versus height profile derived from temperature soundings at various altitudes aloft recorded by radiosonde measurement or aircraft. The mixing height is taken as a function of temperature at the ground and the most recent vertical temperature soundings. The mixing depth is then obtained by subtracting ground elevation at the location of interest. The ground temperature is interpolated at the trajectory point from meteorological data at each station. In this technique the temperature versus height profile is assumed fixed during the day unless more frequent soundings are provided. The mixing depth changes with variations in ground temperature and elevation.

d. Trajectory Derivatives

The rates of change of the wind components at the air parcel position are utilized by the numerical integration routine to calculate the next trajectory position. Two differential equations are reserved for the trajectory calculat[illegible] They employ these derivatives in the same manner in which the integration of the differential equations for the chemistry occurs.

5. Barrier Check

A "barrier" is an imaginary line or set of connected line segments superimposed on the region of interest with the coordinate system for that area. Its purpose is to represent a topographical feature such as a mountain range which may serve to separate sections of an air quality region. The mountain range may tend to influence differing climatological characteristics and wind regimes. For example, on a given day in the Los Angeles Basin, the meteorological characteristics of the Westwood area are likely to differ from those in Van Nuys due, in part, to the intervention of the Santa Monica Mountains. Experience in the Los Angeles area has shown that significant temperature and wind regime differences between the San Fernando Valley and the central Basin tend to occur on any given day.

REM contains two such barriers. One bisects the Santa Monica Mountains and separates the San Fernando Valley from the main section of Los Angeles. The other barrier passes through the Puente and San Jose Hills at the east side of the Basin.

The main function of the barrier routine is to determine the "permissible" meteorological stations. Permissible stations are simply stations which are located in the same general section of the Basin as the trajectory point of interest, as defined by the barriers. That is, both the trajectory point and all stations to be used in the calculation of the trajectory path and the interpolated meteorological values at any trajectory point are located on the same side of each barrier. This is graphically shown in Figure II.4.

The barrier check is intended to ensure that a station which is very close in distance to a trajectory point of interest, but separated from the trajectory point by a mountain range does not exert any influence on the calculation of the trajectory path, temperature, and relative humidity at the trajectory point.

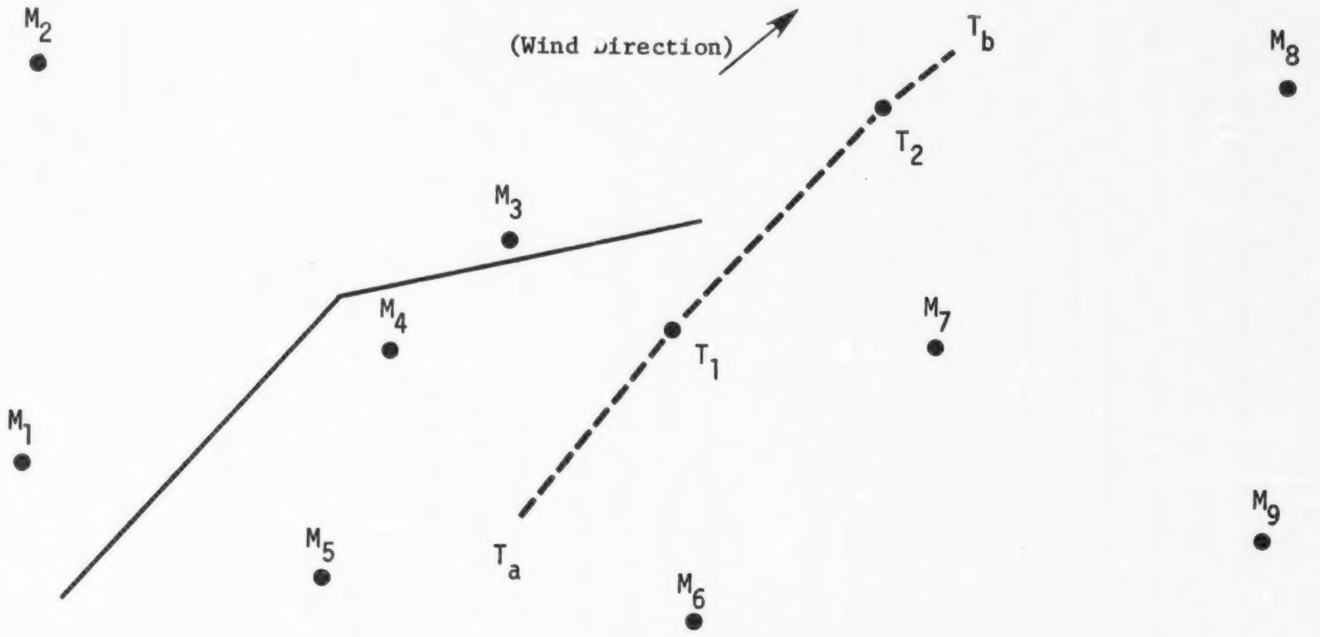
(Wind Direction)
M_1
M_2
M_3
M_4
M_5
M_6
M_7
M_8
M_9
T_a
T_1
T_2
T_b

Wind direction

Line T_a - T_b is the trajectory path

T_1 - T_a trajectory point of interest

T_2 - T_a downwind trajectory point along the same trajectory

M_i meteorological stations

P_1 Permissible meteorological stations for T_1 (M_4, M_5, M_6, M_7, M_8, M_9)

P_2 Permissible meteorological stations for T_2 (M_2, M_3, M_5, M_6, M_7, M_8, M_9)

Figure II.4 Demonstration of Barrier Check Technique

6. Ultraviolet Module

This module calculates a diurnal ultraviolet irradiance function based on measurement of sky cover, latitude and local calendar time. The irradiance determines the specific ultraviolet absorption rate of NO_2, which is used in the kinetics module.

7. Source Emissions

This routine computes emissions of NO, CO, reactive hydrocarbons and less reactive hydrocarbons for freeway and street traffic, and calculates emissions from area sources of NO, reactive hydrocarbons, and less reactive hydrocarbons.

The inputs to this program for vehicular sources include two diurnal traffic curves (see Figures II.5 and II.6),[2] emission factors for reactive hydrocarbons, less reactive hydrocarbons, CO and NO in grams per vehicle mile, and distributions of daily vehicle traffic on streets and freeways given in a system of 650 4-square mile grids that cover the Los Angeles Basin (see Figures II.7 and II.8).[2] The emissions of the above pollutants are computed as a function of time by applying their respective emission factors to the traffic levels at the air parcel location qualified by the daily traffic usage curve.

Emissions from area sources are also calculated as a function of time. A constant diurnal usage curve is applied to grid system distributions of hourly pollutant emissions of NO,[3] reactive hydrocarbons, and less reactive hydrocarbons (see Figures II.9, II.10 and II.11).[2]

---

[2] Appendix A, Development of a Simulation Model for Estimating Ground Level Concentrations of Photochemical Pollutants by P. J. W. Roberts, P. M. Roth and C. L. Nelson; Report 71SAI-6, March 1971, prepared by Systems Applications, Inc.

[3] Oxides of nitrogen taken as NO

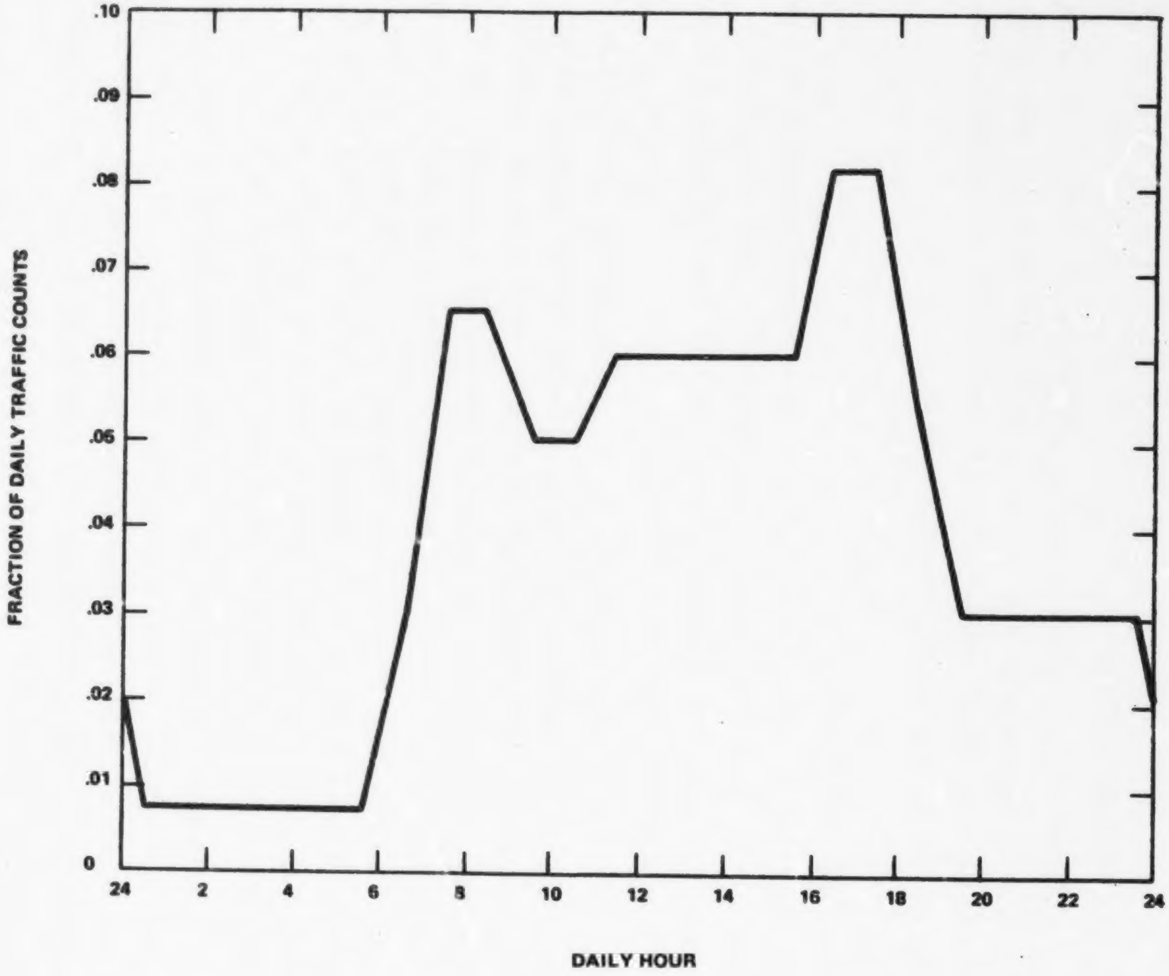

Figure II.5. Temporal Distribution of Daily Street Traffic (Interpreted from Data in Reference 2, pg. II.13)

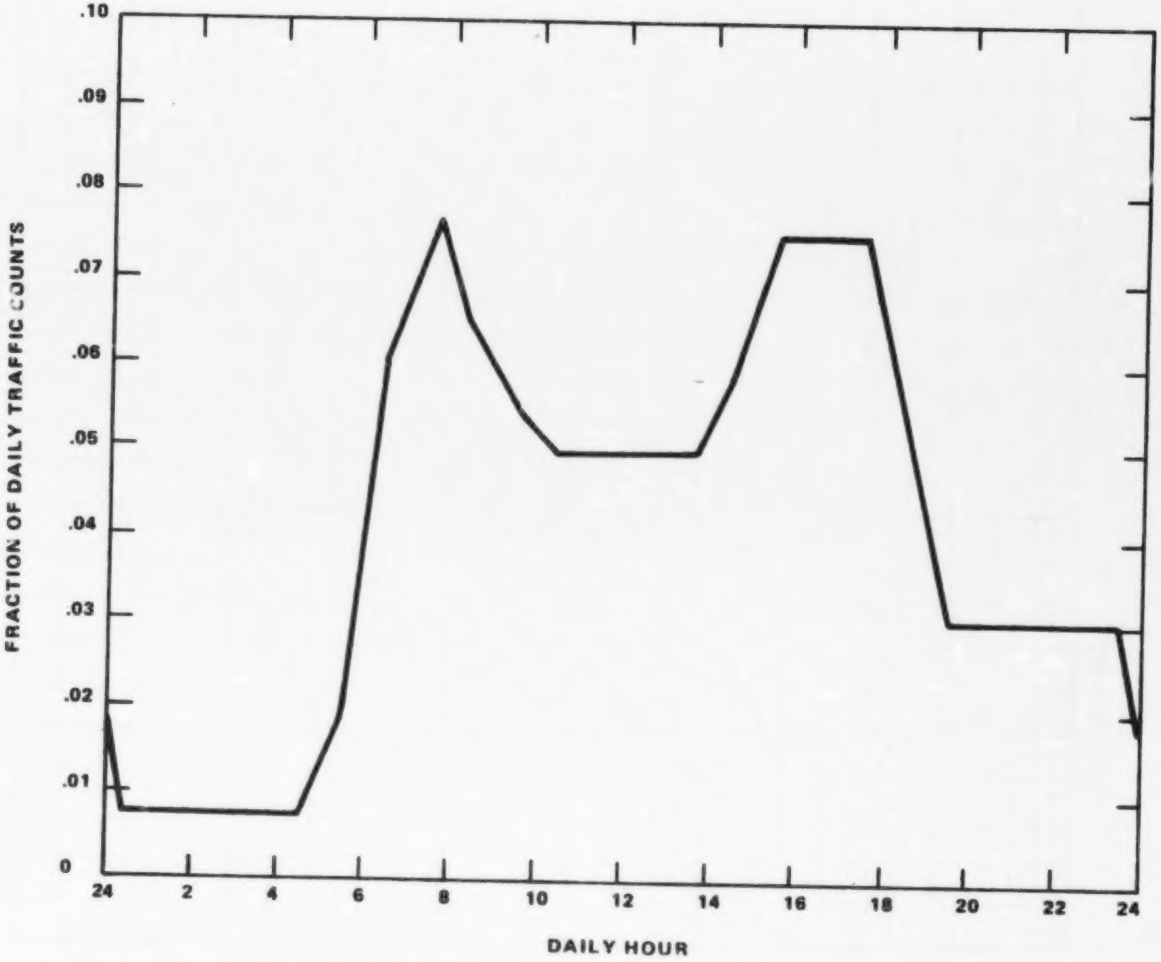

Figure II.6. Temporal Distribution of Daily Freeway Traffic (Interpreted from Data in Reference 2, pg. II.13)

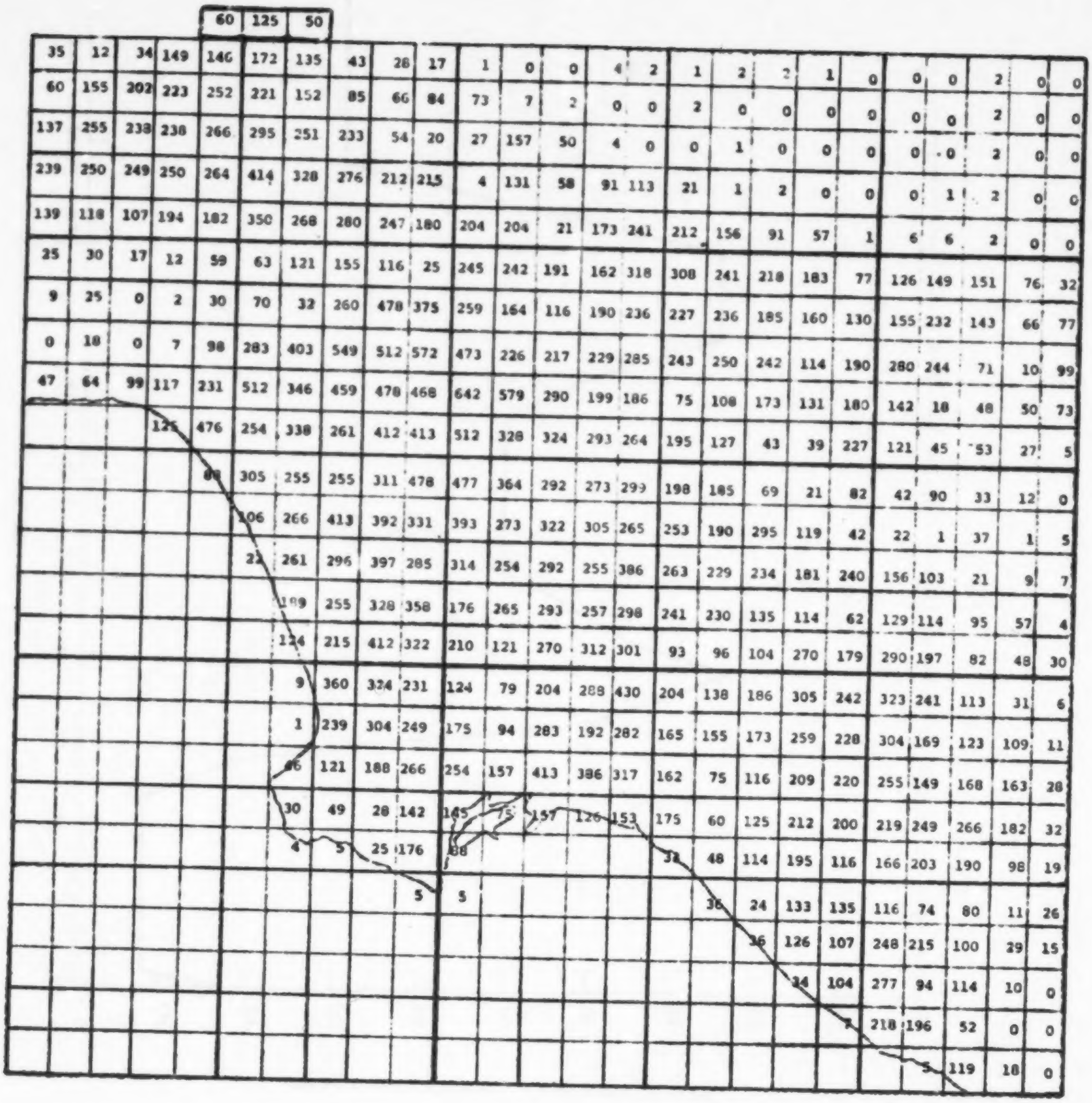

				60	125	50																		
35	12	34	149	146	172	135	43	28	17	1	0	0	4	2	1	2	2	1	0	0	0	2	0	0
60	155	202	223	252	221	152	85	66	84	73	7	2	0	0	2	0	0	0	0	0	0	2	0	0
137	255	238	238	266	295	251	233	54	20	27	157	50	4	0	0	1	0	0	0	0	0	2	0	0
239	250	249	250	264	414	328	276	212	215	4	131	58	91	113	21	1	2	0	0	0	1	2	0	0
139	118	107	194	182	350	268	280	247	180	204	204	21	173	241	212	156	91	57	1	6	6	2	0	0
25	30	17	12	59	63	121	155	116	25	245	242	191	162	318	308	241	218	183	77	126	149	151	76	32
9	25	0	2	30	70	32	260	478	375	259	164	116	190	236	227	236	185	160	130	155	232	143	66	77
0	18	0	7	98	283	403	549	512	572	473	226	217	229	285	243	250	242	114	190	280	244	71	10	99
47	64	99	117	231	512	346	459	478	468	642	579	290	199	186	75	108	173	131	180	142	18	48	50	73
			125	476	254	338	261	412	413	512	328	324	293	264	195	127	43	39	227	121	45	53	27	5
				88	305	255	255	311	478	477	364	292	273	299	198	185	69	21	82	42	90	33	12	0
					106	266	413	392	331	393	273	322	305	265	253	190	295	119	42	22	1	37	1	5
					22	261	296	397	285	314	254	292	255	386	263	229	234	181	240	156	103	21	9	7
						189	255	328	358	176	265	293	257	298	241	230	135	114	62	129	114	95	57	4
						124	215	412	322	210	121	270	312	301	93	96	104	270	179	290	197	82	48	30
						9	360	324	231	124	79	204	288	430	204	138	186	305	242	323	241	113	31	6
						1	239	304	249	175	94	283	192	282	165	155	173	259	228	304	169	123	109	11
						66	121	188	266	254	157	413	386	317	162	75	116	209	220	255	149	168	163	28
						30	49	28	142	145	75	157	126	153	175	60	125	212	200	219	249	266	182	32
						4	5	25	176	88					32	48	114	195	116	166	203	190	98	19
									5	5						36	24	133	135	116	74	80	11	26
																	36	126	107	248	215	100	29	15
																		34	104	277	94	114	10	0
																			7	218	196	52	0	0
																					5	119	18	0

Figure II.7. Distribution of Street Traffic by Grid Area
(thousands of vehicle miles per day)
[From Reference 2, pg. II.13]

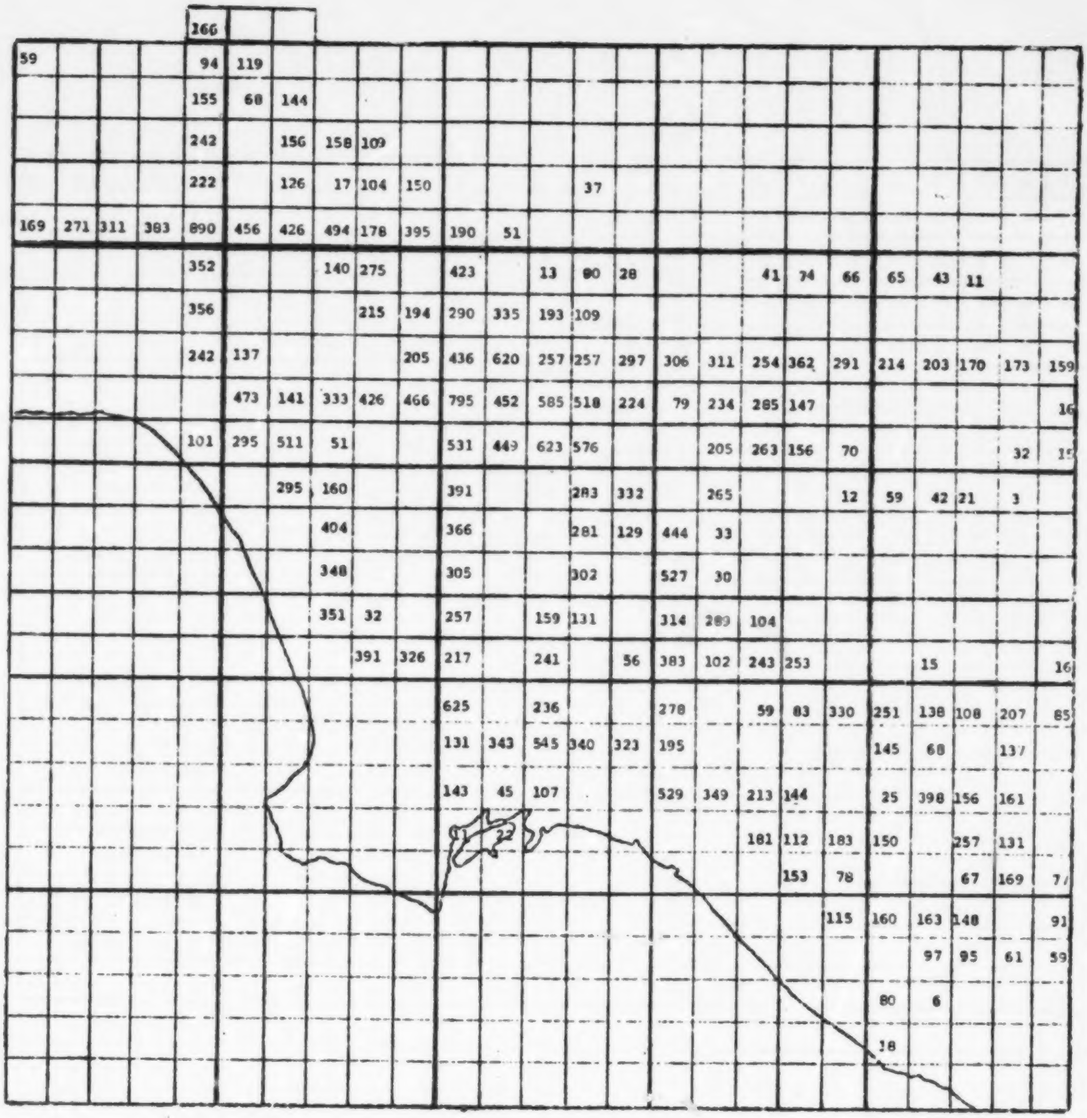
266
59 94 119
155 68 144
242 156 158 109
222 126 17 104 150 37
169 271 311 383 890 456 426 494 178 395 190 51
352 140 275 423 13 80 28 41 74 66 65 43 11
356 215 194 290 335 193 109
242 137 205 436 620 257 257 297 306 311 254 362 291 214 203 170 173 159
473 141 333 426 466 795 452 585 518 224 79 234 285 147
101 295 511 51 531 449 623 576 205 263 156 70 32
295 160 391 283 332 265 12 59 42 21 3
404 366 281 129 444 33
348 305 302 527 30
351 32 257 159 131 314 289 104
391 326 217 241 56 383 102 243 253 15
625 236 278 59 83 330 251 138 108 207 85
131 343 545 340 323 195 145 68 137
143 45 107 529 349 213 144 25 398 156 161
11 22 181 112 183 150 257 131
153 78 67 169
115 160 163 148 91
97 95 61 59
80 6
18

Figure II.8. Distribution of Freeway Traffic by Grid Area (thousands of vehicle miles per day) [From Reference 2, pg. II.13]

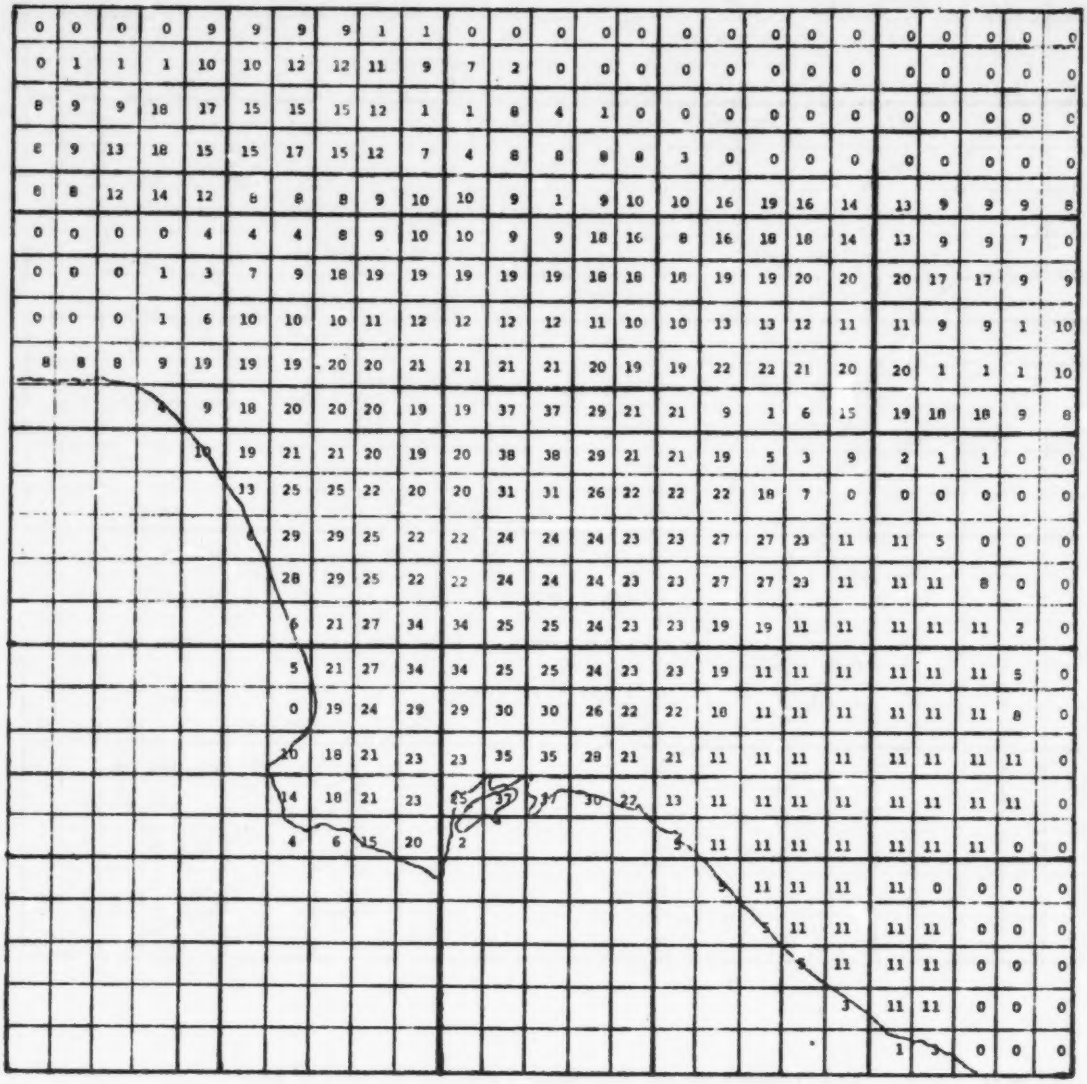

0	0	0	0	9	9	9	9	1	1	0	0	0	0	0	0	0	0	0	0	0	0	0	0	0
0	1	1	1	10	10	12	12	11	9	7	2	0	0	0	0	0	0	0	0	0	0	0	0	0
8	9	9	18	17	15	15	15	12	1	1	8	4	1	0	0	0	0	0	0	0	0	0	0	0
8	9	13	18	15	15	17	15	12	7	4	8	8	8	8	3	0	0	0	0	0	0	0	0	0
8	8	12	14	12	6	8	8	9	10	10	9	1	9	10	10	16	19	16	14	13	9	9	9	8
0	0	0	0	4	4	4	8	9	10	10	9	9	18	16	8	16	18	18	14	13	9	9	7	0
0	0	0	1	3	7	9	18	19	19	19	19	19	18	18	18	19	19	20	20	20	17	17	9	9
0	0	0	1	6	10	10	10	11	12	12	12	12	11	10	10	13	13	12	11	11	9	9	1	10
8	8	8	9	19	19	19	20	20	21	21	21	21	20	19	19	22	22	21	20	20	1	1	1	10
			4	9	18	20	20	20	19	19	37	37	29	21	21	9	1	6	15	19	18	18	9	8
				10	19	21	21	20	19	20	38	38	29	21	21	19	5	3	9	2	1	1	0	0
					13	25	25	22	20	20	31	31	26	22	22	22	18	7	0	0	0	0	0	0
					6	29	29	25	22	22	24	24	24	23	23	27	27	23	11	11	5	0	0	0
						28	29	25	22	22	24	24	24	23	23	27	27	23	11	11	11	8	0	0
						6	21	27	34	34	25	25	24	23	23	19	19	11	11	11	11	11	2	0
						5	21	27	34	34	25	25	24	23	23	19	11	11	11	11	11	11	5	0
						0	19	24	29	29	30	30	26	22	22	18	11	11	11	11	11	11	8	0
						20	18	21	23	23	35	35	28	21	21	11	11	11	11	11	11	11	11	0
						14	18	21	23	25	37	37	30	22	13	11	11	11	11	11	11	11	11	0
						4	6	15	20	2					5	11	11	11	11	11	11	11	0	0
																5	11	11	11	11	0	0	0	0
																	5	11	11	11	11	0	0	0
																		5	11	11	11	0	0	0
																			3	11	11	0	0	0
																				1	3	0	0	0

Figure II.9. Distribution of Reactive Hydrocarbon Emissions (average kilograms/hour) by Grid Area [From Reference 2, pg. II.13]

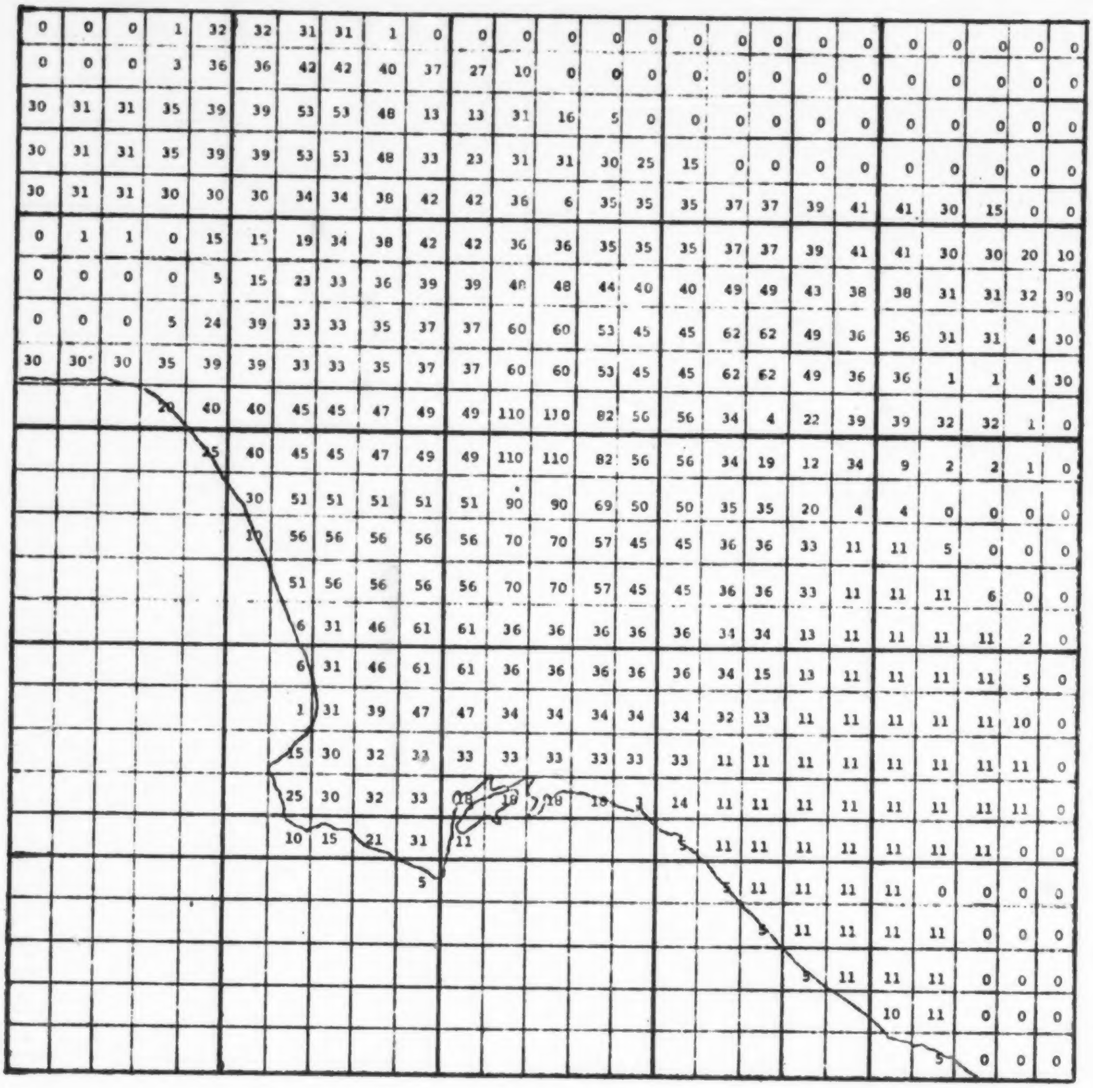

0	0	0	1	32	32	31	31	1	0	0	0	0	0	0	0	0	0	0	0	0	0	0	0	0
0	0	0	3	36	36	42	42	40	37	27	10	0	0	0	0	0	0	0	0	0	0	0	0	0
30	31	31	35	39	39	53	53	48	13	13	31	16	5	0	0	0	0	0	0	0	0	0	0	0
30	31	31	35	39	39	53	53	48	33	23	31	31	30	25	15	0	0	0	0	0	0	0	0	0
30	31	31	30	30	30	34	34	38	42	42	36	6	35	35	35	37	37	39	41	41	30	15	0	0
0	1	1	0	15	15	19	34	38	42	42	36	36	35	35	35	37	37	39	41	41	30	30	20	10
0	0	0	0	5	15	23	33	36	39	39	48	48	44	40	40	49	49	43	38	38	31	31	32	30
0	0	0	5	24	39	33	33	35	37	37	60	60	53	45	45	62	62	49	36	36	31	31	4	30
30	30	30	35	39	39	33	33	35	37	37	60	60	53	45	45	62	62	49	36	36	1	1	4	30
			20	40	40	45	45	47	49	49	110	110	82	56	56	34	4	22	39	39	32	32	1	0
				25	40	45	45	47	49	49	110	110	82	56	56	34	19	12	34	9	2	2	1	0
					30	51	51	51	51	51	90	90	69	50	50	35	35	20	4	4	0	0	0	0
					10	56	56	56	56	56	70	70	57	45	45	36	36	33	11	11	5	0	0	0
						51	56	56	56	56	70	70	57	45	45	36	36	33	11	11	11	6	0	0
						6	31	46	61	61	36	36	36	36	36	34	34	13	11	11	11	11	2	0
						6	31	46	61	61	36	36	36	36	36	34	15	13	11	11	11	11	5	0
						1	31	39	47	47	34	34	34	34	34	32	13	11	11	11	11	11	10	0
						15	30	32	33	33	33	33	33	33	33	11	11	11	11	11	11	11	11	0
						25	30	32	33	18	18	18	18	3	14	11	11	11	11	11	11	11	11	0
						10	15	21	31	11					5	11	11	11	11	11	11	11	0	0
									5							5	11	11	11	11	0	0	0	0
																	5	11	11	11	11	0	0	0
																		5	11	11	11	0	0	0
																				10	11	0	0	0
																					5	0	0	0

Figure II.10. Distribution of Oxides of Nitrogen Emissions Taken as Nitric Oxide (average kilograms/hour) by Grid Area [From Reference 2, pg. II.13]

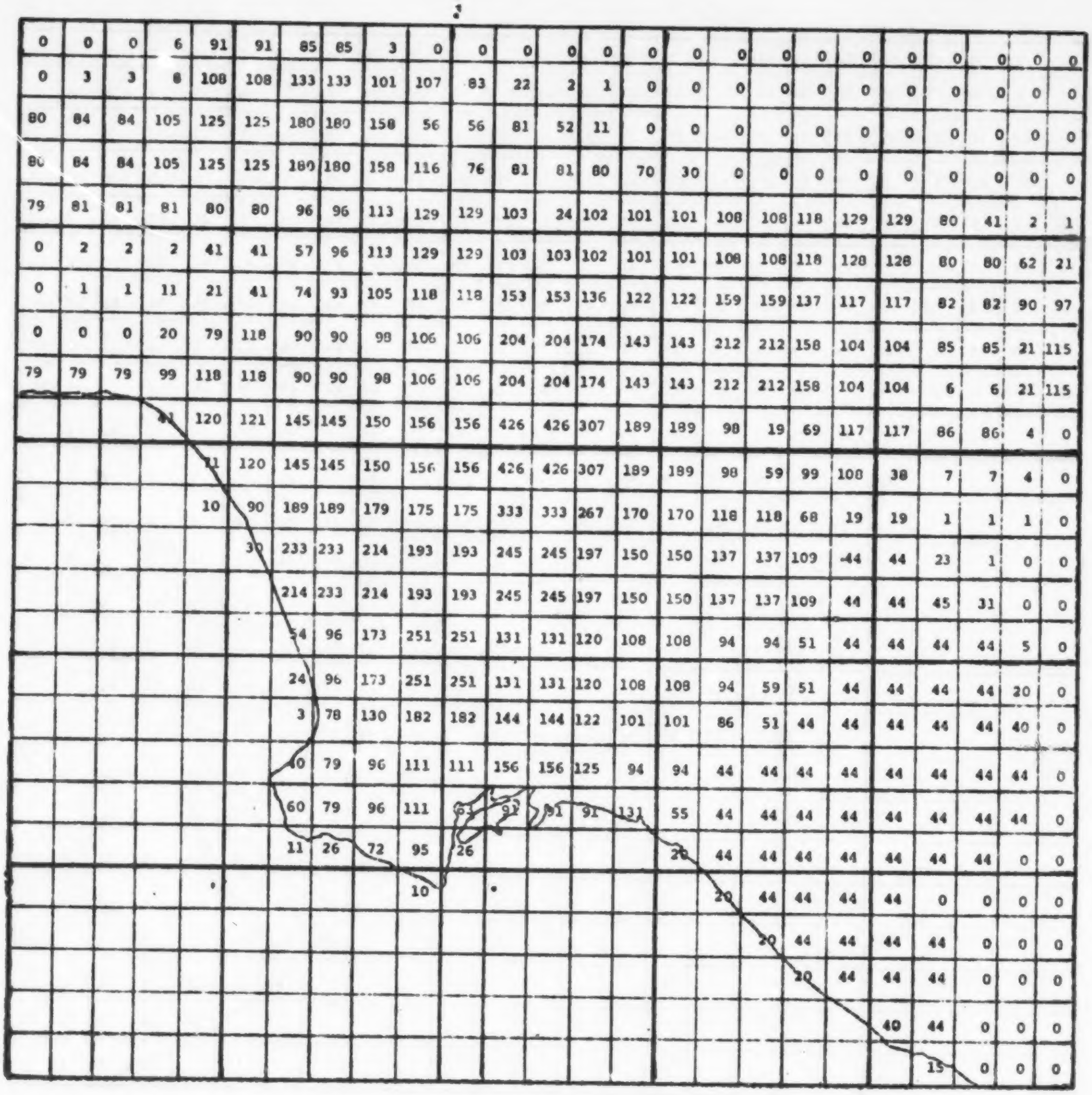

0	0	0	6	91	91	85	85	3	0	0	0	0	0	0	0	0	0	0	0	0	0	0	0	0
0	3	3	8	108	108	133	133	101	107	83	22	2	1	0	0	0	0	0	0	0	0	0	0	0
80	84	84	105	125	125	180	180	158	56	56	81	52	11	0	0	0	0	0	0	0	0	0	0	0
80	84	84	105	125	125	180	180	158	116	76	81	81	80	70	30	0	0	0	0	0	0	0	0	0
79	81	81	81	80	80	96	96	113	129	129	103	24	102	101	101	108	108	118	129	129	80	41	2	1
0	2	2	2	41	41	57	96	113	129	129	103	103	102	101	101	108	108	118	128	128	80	80	62	21
0	1	1	11	21	41	74	93	105	118	118	153	153	136	122	122	159	159	137	117	117	82	82	90	97
0	0	0	20	79	118	90	90	98	106	106	204	204	174	143	143	212	212	158	104	104	85	85	21	115
79	79	79	99	118	118	90	90	98	106	106	204	204	174	143	143	212	212	158	104	104	6	6	21	115
			41	120	121	145	145	150	156	156	426	426	307	189	189	98	19	69	117	117	86	86	4	0
				11	120	145	145	150	156	156	426	426	307	189	189	98	59	99	108	38	7	7	4	0
				10	90	189	189	179	175	175	333	333	267	170	170	118	118	68	19	19	1	1	1	0
					30	233	233	214	193	193	245	245	197	150	150	137	137	109	-44	44	23	1	0	0
						214	233	214	193	193	245	245	197	150	150	137	137	109	44	44	45	31	0	0
						54	96	173	251	251	131	131	120	108	108	94	94	51	44	44	44	44	5	0
						24	96	173	251	251	131	131	120	108	108	94	59	51	44	44	44	44	20	0
						3	78	130	182	182	144	144	122	101	101	86	51	44	44	44	44	44	40	0
						40	79	96	111	111	156	156	125	94	94	44	44	44	44	44	44	44	44	0
						60	79	96	111	63	91	91	91	131	55	44	44	44	44	44	44	44	44	0
						11	26	72	95	26					20	44	44	44	44	44	44	44	0	0
									10							20	44	44	44	44	0	0	0	0
																	20	44	44	44	44	0	0	0
																		20	44	44	44	0	0	0
																				40	44	0	0	0
																					15	0	0	0

Figure II.11. Distribution of Less Reactive Hydrocarbon Emissions (average kilograms/hour) by Grid Area [From Reference 2, pg. II.13]

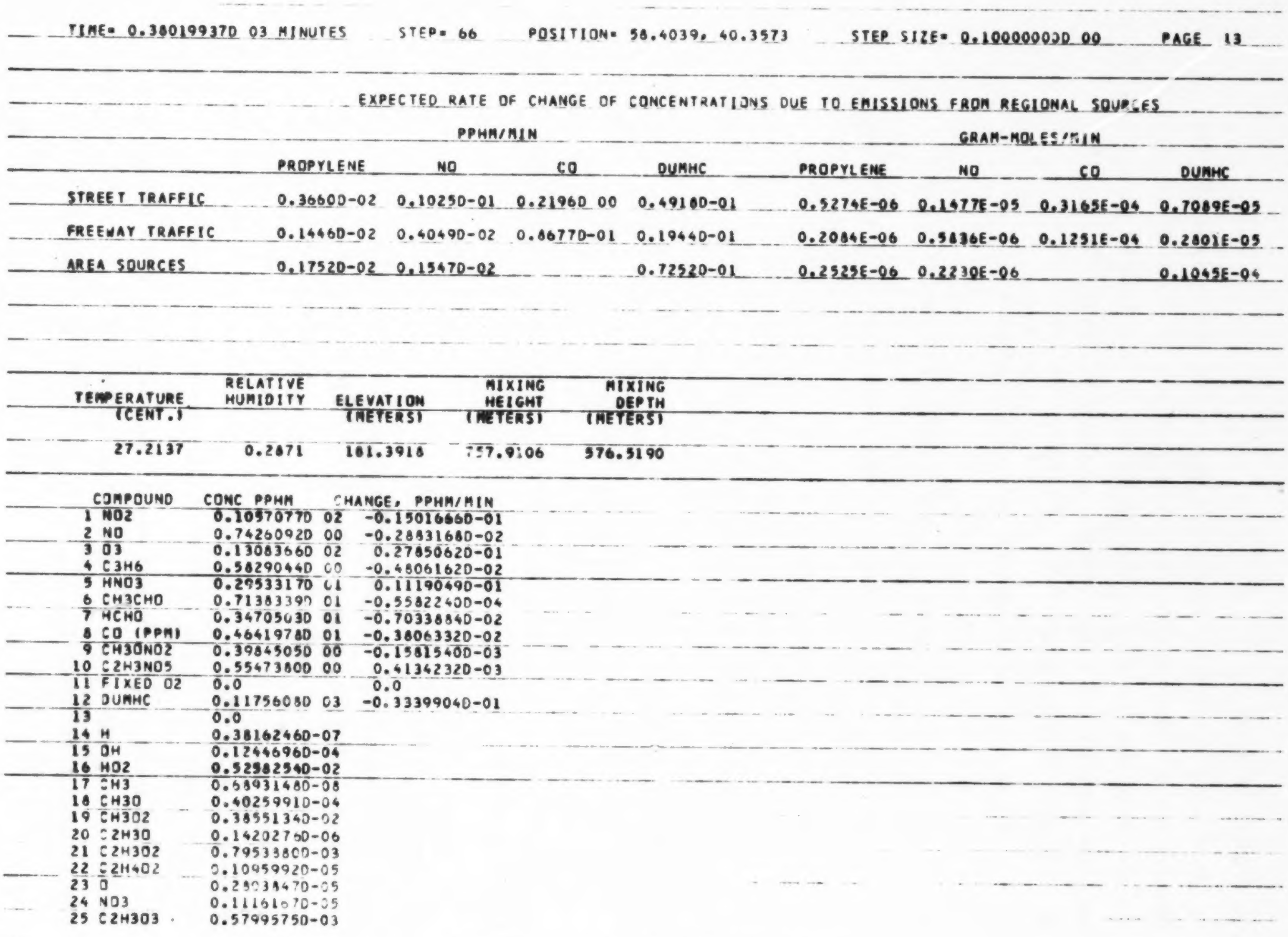

```
 TIME= 0.38019937D 03 MINUTES     STEP= 66    POSITION= 58.4039, 40.3573     STEP SIZE= 0.10000000D 00      PAGE  13

                      EXPECTED RATE OF CHANGE OF CONCENTRATIONS DUE TO EMISSIONS FROM REGIONAL SOURCES
                                        PPHM/MIN                                             GRAM-MOLES/MIN
                     PROPYLENE       NO          CO         DUMHC          PROPYLENE      NO          CO         DUMHC
 STREET TRAFFIC      0.3660D-02  0.1025D-01  0.2196D 00  0.4918D-01       0.5274E-06  0.1477E-05  0.3165E-04  0.7089E-05
 FREEWAY TRAFFIC     0.1446D-02  0.4049D-02  0.8677D-01  0.1944D-01       0.2084E-06  0.5836E-06  0.1251E-04  0.2801E-05
 AREA SOURCES        0.1752D-02  0.1547D-02              0.7252D-01       0.2525E-06  0.2230E-06              0.1045E-04



               RELATIVE                  MIXING       MIXING
 TEMPERATURE   HUMIDITY   ELEVATION      HEIGHT        DEPTH
   (CENT.)                 (METERS)     (METERS)     (METERS)

   27.2137      0.2871     181.3918     757.9106     576.5190

   COMPOUND      CONC PPHM       CHANGE, PPHM/MIN
   1 NO2         0.10570770 02   -0.1501666D-01
   2 NO          0.7426092D 00   -0.2883168D-02
   3 O3          0.1308366D 02    0.2785062D-01
   4 C3H6        0.5829044D 00   -0.4806162D-02
   5 HNO3        0.2953317D 01    0.1119049D-01
   6 CH3CHO      0.7138339D 01   -0.5582240D-04
   7 HCHO        0.3470503D 01   -0.7033884D-02
   8 CO (PPM)    0.4641978D 01   -0.3806332D-02
   9 CH3ONO2     0.3984505D 00   -0.1581540D-03
  10 C2H3NO5     0.5547380D 00    0.4134232D-03
  11 FIXED O2    0.0              0.0
  12 DUMHC       0.1175608D 03   -0.3339904D-01
  13             0.0
  14 H           0.3816246D-07
  15 OH          0.1244696D-04
  16 HO2         0.5298254D-02
  17 CH3         0.6893148D-08
  18 CH3O        0.4025991D-04
  19 CH3O2       0.3855134D-02
  20 C2H3O       0.1420276D-06
  21 C2H3O2      0.7953380D-03
  22 C2H4O2      0.1095992D-05
  23 O           0.2803847D-05
  24 NO3         0.1116167D-05
  25 C2H3O3      0.5799575D-03
```

Figure II.12. Sample REM Output

8. Output Routine

This program prints output data at various times along the trajectory route. The user may specify the times at which the printouts are to occur and the routine checks to see if a requested output time has been reached. A sample output is shown in Figure II.12. The primary data categories printed include:

- Time of output and trajectory position;
- Step size;
- Rate of change of concentrations from source routine in pphm/minute and in gram-moles/minute;
- Meteorological values at the trajectory point including mixing depth;
- Pollutant concentrations;
- Rates of change of accumulating (primary) pollutants; and
- Rates of the elementary reactions.

9. Plotting Routine

At the end of the simulation run, this program outputs three digital plots containing the history of each accumulating pollutant represented in time vs. concentration curves. An example of this output is shown in Figure II.13.

10. Reverse Trajectory Program

The reverse trajectory program calculates wind trajectories and interpolates initial concentration values for use by the simulation model. Its primary inputs consist of hourly average wind data monitored at a network of meteorological stations, and hourly average pollutant data recorded at a group of pollutant monitoring stations. The coordinate positions of these stations are also required.

In addition, the user must specify a coordinate position and the length of time for which the simulated trajectory is to be calculated. The program then considers the given coordinate position to be the

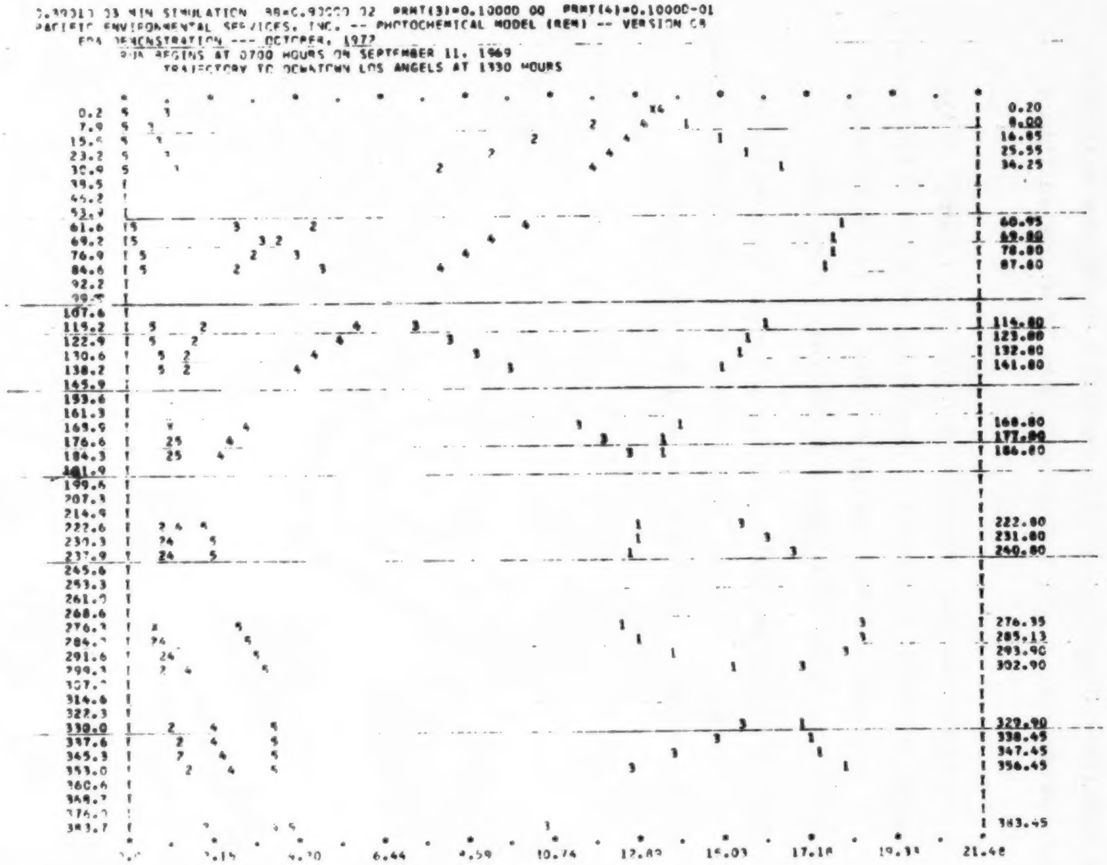

Figure II.13. Digital Plot of Primary Pollutant Time vs. Concentration Histories

Vertical axis represents time in minutes; horizontal axis depicts pollutant concentrations in pphm. The species plotted are as follows: 1 - NO_2, 2 - NO, 3 - O_3, 4 - C_3H_6, and 5 - HNO_3.

terminus of the trajectory, and computes consecutive points along the trajectory in a direction opposite to that of the wind. At the conclusion of the trajectory (the determination of the starting point), an interpolation routine calculates initial concentrations for nitrogen dioxide, nitric oxide, ozone and carbon monoxide from the pollutant data.

Although its primary use has been for calculating reverse trajectories, the program may also be used for computing forward trajectories. In this case, the pollutant interpolation routine would yield concentration values which could be considered as validation points.

Theoretically, the program could operate with one meteorological and one pollutant station. However, the greater the number of stations utilized, the more realistic and accurate will be the results.

Chapter III

SIMULATION OF IRRADIATION CHAMBER EXPERIMENTS

A. INTRODUCTION

An important aspect of the evaluation of the model was the exploration of the adequacy of the chemical mechanism in terms of available information from irradiation chamber experiments. Since rates of elementary reactions in the gas phase are, to a good first approximation, determined only by the concentrations of the reacting species (and the temperature of the system), the chemical mechanism can be applied to atmospheric simulation with greater confidence if it can be shown to be consistent with laboratory observations on similar systems.

For this purpose the contracting agency furnished kinetic data from twenty-six experiments in which air containing hydrocarbons and oxides of nitrogen was irradiated and time-profiles of the concentrations of various constituents were determined. These data were to be used to test the simulation capability of the mechanism under conditions uncomplicated by variations in weather variables and emission rates.

The twenty-six experiments fell into four distinct systems, differing in their hydrocarbon constituents: six using propylene and ethane; ten using only toluene; six using toluene and n-butane; and four using auto exhaust gases containing small proportions of a large number of different hydrocarbons.

The mechanism incorporated in the atmospheric simulation model had been designed to test the possibility of simulating propylene photo-oxidation kinetics accurately, and of simulating other systems as if their hydrocarbon constituents consisted solely of propylene and a second, hypothetical, hydrocarbon of less reactivity than propylene. The simulation of the propylene-ethane system was appropriate for approaching the first of these objectives, while simulating the auto exhaust systems could be expected to furnish information more directly relevant to the atmospheric simulation problem, especially for the required validation on Los Angeles data. Simulation of the toluene-containing systems further tested the flexibility of the approach.

These tests showed that all four systems could be simulated reasonably well with only two rate factors reserved as adjustable parameters. The values selected are shown in Table III-1 and discussed in detail in following sections.

A problem arises in evaluating the success of simulation of the laboratory data, in that these data are subject to uncertainty due to random error introduced in preparation, irradiation, sampling and analysis of the chamber contents. Such random errors may have perturbing effects of two types. First, time-profiles for individual contaminants may appear irregular, as random errors affect successive analytical results to different degrees or in different directions. Second, time-profiles for the same constituent in different experiments may be subject to systematic distortion due to unrecognized or undocumented variation in the conditions which may occur in the interim between the experiments (e.g., change in irradiance of the lamps).

Errors of the first sort may be roughly estimated by examining the degree of variation between duplicate analyses. Errors of the second sort could be investigated by systematic study of the agreement between replicate experiments. No assessment of errors of either type was furnished by the contracting agency; however, some relevant evidence was contained in the data.

The data for oxides of nitrogen included many sets of duplicate determinations for total NO_x, as well as a smaller number of duplicate sets for NO_2. NO was determined by subtracting NO_2 from NO_x and was therefore subject, presumably, to somewhat larger resultant errors. For NO_x, differences between duplicates were on several occasions as large as 0.4 ppm, when the total concentration was 2 ppm or less. The root-mean-square difference between duplicates, for NO_x in the range

Table III-1

Parameters Used[a] for Simulation of Various Experiments

Hydrocarbon System	Exp't No.	K31	Z2
Propylene + ethane	329, 325	3.5	0.0
	318, 336	3.5	0.3
	321, 334	3.5	0.25
Auto exhaust	222, 233	7.0	0.0
	224, 231	3.5	0.1
Toluene	250, etc.	7.0	0.0
Toluene + n-butane	251, etc.	7.0	0.0

[a] Effects of variation of Z1 and Z2 are illustrated in Figures III-10 to III-17. All other rate factors were as listed in Table III-4.

1 to 1.5 ppm, was 0.19 ppm; this corresponds to 95% confidence limits at about 0.27 ppm above and below the value from each individual determination.

Regarding the individual oxides of nitrogen, since nitric oxide was determined by difference, the 95% confidence interval cannot be less than that for NO_x and is presumably larger (ca. 0.3 ppm). The precision of replicate analyses for NO_2 appears to have been substantially better, giving 95% limits at 0.1 ppm (or less) on each side of a given determination.

Duplicate analyses were not reported for other constituents of the system; therefore, corresponding estimates of error in the analytical process for these constituents are not available. However, a related error estimate can be derived from the deviations of the observed values from a smoothed time-profile. A cursory review of deviations of this sort indicated that the 95% confidence limits surrounding individual determinations of propylene and ethylene are of the order of magnitude of 5 pphm or less.

Systematic errors are more difficult to detect, but evidence of such errors is seen in some of the chamber data. For example, Figure III-1 shows the ethane data for experiment 321, plotted against time of sampling. The points for the first 100 minutes and the last 100 minutes together determine a smooth, self-consistent time-profile for ethane, but all the intervening points fall below that profile with deviations of 8 to 12 pphm.

Other evidence pointing to the possibility of systematic errors is apparent in the comparison of results of separate experiments having similar initial conditions. Since there was no exact replication of initial conditions in these experiments, we cannot accurately evaluate the variance between replicates for this type of error. However, the comparison between nitrogen dioxide time-profiles for experiments 222 and 233 (see Figure III-2) strongly suggests that this type of error may be important. In this case an increase of only 20 percent in

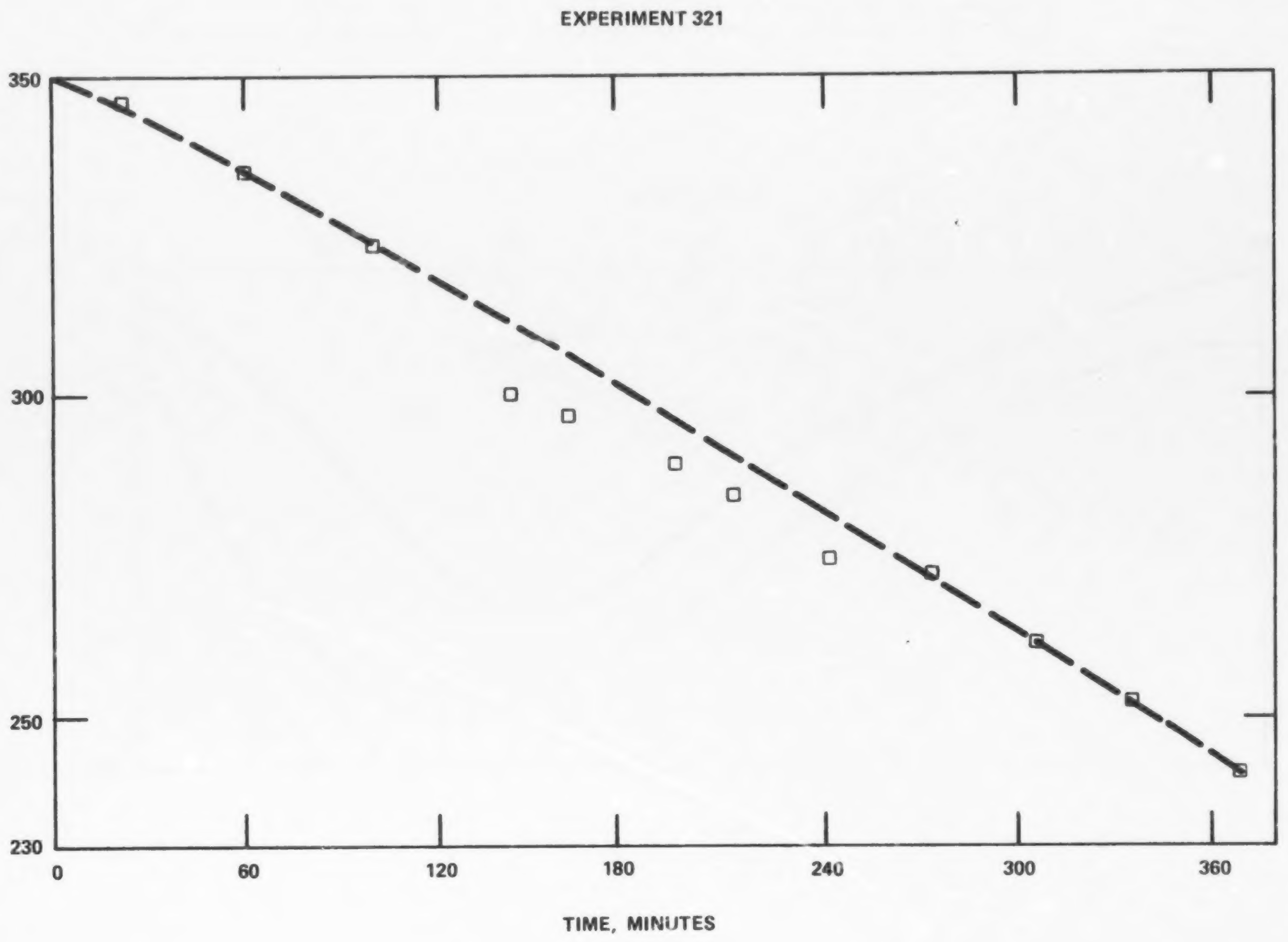

Figure III.1. Concentration of ethane related to time of sampling, Experiment 321 (propylene, ethane, and oxides of nitrogen system).

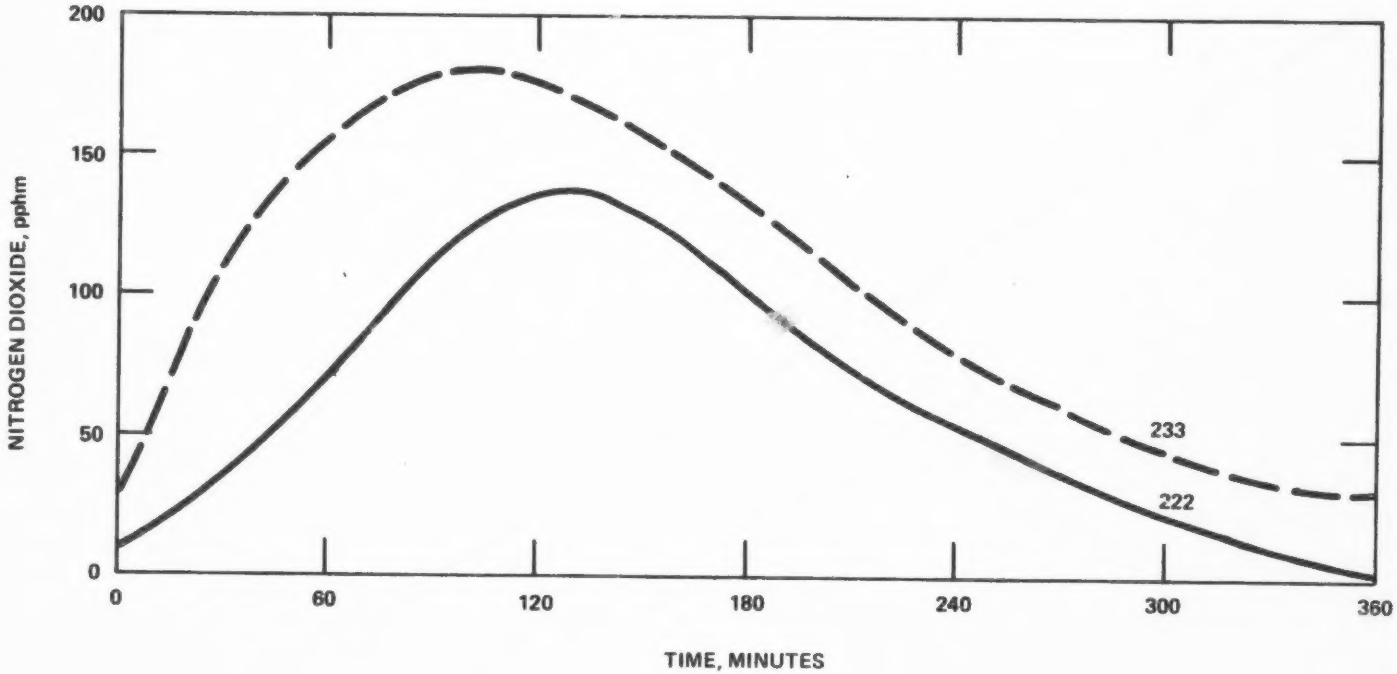

Figure III.2. Time profiles of nitrogen dioxide concentrations, Experiments 222 and 233 (diluted auto exhaust system). Smoothed experimental profiles. Experiment 222: ——; Experiment 233: — —.

initial NO_x appears to cause a fourfold increase in the rate of initial oxidation of nitric oxide and an increase of more than 75 percent in the total dosage of nitrogen dioxide over the six-hour irradiation period. Unless due to systematic error, this indicates a very unexpected sensitivity to the initial nitrogen dioxide concentration.

B. SIMULATION OF PROPYLENE-ETHANE-OXIDES OF NITROGEN SYSTEM

1. By Original Mechanism, M1

The propylene-ethane-oxides of nitrogen system was represented in the experimental data by six irradiation chamber runs. These are listed in Table III-2, with summary information about their initial conditions and the findings which resulted.

The first simulation tests utilized mechanism M1, shown in Table III-3, which was substantially the mechanism reported in the final report of Contract CPA 70-151, submitted to EPA in January, 1971.

In these tests, the most difficult part of the task of simulating observed time profiles of concentrations from chamber runs appeared to be the prediction of appropriate levels of ozone. Since only two of the experimental irradiations for this sytem had generated any substantial ozone levels, the initial simulation tests were directed at these runs (experiments 329 and 325).

Results achieved using mechanism M1 are illustrated in Figures III-3 and III-4, showing time profiles for Experiments 329 and 325 respectively. With the best choice of rate factors resulting from these tests, discrepancies of 20 percent or less (between observed and calculated values) could be maintained for more than an hour for ozone and propylene concentrations, and for more than 100 minutes (the entire length of the simulation) for nitric oxide and nitrogen

Table III-2

Irradiation Chamber Experiments in the Propylene-Ethane-Oxides of Nitrogen System

Exp't No.	Concentrations, pphm Initial				Comparisons (est/obs) at				
					360 minutes				maximum
	NO_2	NO	C_3H_6	C_2H_6	NO_2	NO	C_3H_6	O_3	NO_2
329	4	30	24	322	12/7	0/0	0/2	41/42	28/27
325	2	34	45	269	9/4	0/0	0/4	50/46	30/27
318	6	115	51	289	78/88	2/1	2/8	43/0	102/89
336[a]	10	110	61	328	78/62	2/14	2/10	43/3	102/83
321	11	130	28	350	89/58	12/35	8/6	7/0	89/60
324[a]	9	125	26	273	89/49	12/34	8/5	7/0	89/54

[a] Runs 336 and 324 were not separately simulated; they are compared with simulations for 318 and 321, respectively.

Table III-3

Original Mechanism (M1) for the Chemical Dynamics Module (with Rate Factors for Exp. 329 and 325)

```
 1   NO2+HV       =NO+O                  0.27000000D 00
 2   O+O2+M       =O3+M                  0.14000000D 07
 3   O3+NO        =NO2+O2 S              0.50000000D-01
 4   NO2+O3       =NO3+O2                0.10000000D-02
 5   O2 S         = O2                   0.10000000D 03
 6   NO3+NO       =2NO2                  0.24500000D 03
 7   C2H4O2+O2  =CH3CHO+O3               0.10000000D 02
 8   NO+HO2       =NO2+OH                0.10000000D 02
 9   H+O2+M       =HO2+M                 0.10000000D 07
10   DUMHC + O2S = CH3OOH                0.20000000D 02
11   CH3OOH + HV = CH3O + OH             0.15000000D-01
12   NO2+OH       =HNO3                  0.10000000D 04
13   OH+O3        =HO2+O2                0.10000000D 03
14   OH+CO        =H+CO2                 0.30000000D 01
15   CH3+O2+M     =CH3O2+M               0.14000000D 07
16   CH3O2+NO     =CH3O+NO2              0.10000000D 03
17   CH3O+O2+NO  =CH3O2+NO2              0.10000000D 0[illegible]
18   C2H3O+O2+NO=C2H3O2+NO2              0.10000000D 02
19   C2H3O2+NO    =C2H3O+NO2             0.10000000D 03
20   C2H4O2+NO =CH3CHO+NO2               0.10000000D 03
21   CH3O+O2      =HCHO+HO2              0.10000000D 03
22   C3H6+O       =CH3+C2H3O             0.35000000D 02
23   C3H6+O3      =HCHO+C2H4O2           0.50000000D-04
24   C3H6+O+O2    =HCHO+C2H4O2           0.17500000D 02
25   C3H6 + O2S =CH3O + C2H3O            0.10000000D 01
26   C3H6+HO2     =CH3O+CH3CHO           0.20000000D 01
27   C3H6+MEO2=CH3+MEO+C2H3O             0.10000000D 00
28   C2H3O+M      =CH3+CO+M              0.10000000D 02
29   CH3O+NO2     =CH3ONO2               0.10000000D 01
30   C2H3O+O2+NO2=C2H3O3NO2              0.20000000D 01
31   DUMHC+O      =CH3+C2H3O             0.70000000D 01
32   HCHO + HV = H + H + CO              0.50000000D-02
33   NO2 +NO3 +H2O = HNO3+ "             0.10000000D 02
```

EXPERIMENT 329

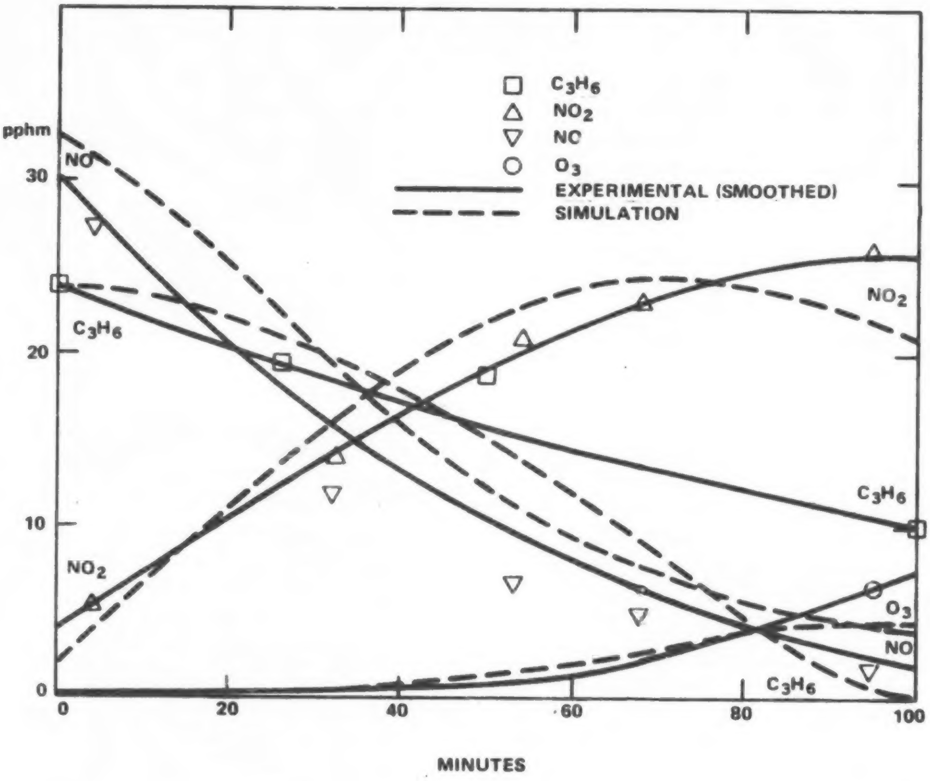

Figure III.3

Time profiles of contaminant concentrations, Experiment 329 (propylene, ethane and oxides of nitrogen system). Simulation results using original mechanism (MI), compared with experimental data points and smoothed profiles. Experimental points, □; C_3H_6; △ : NO_2; ▽: NO; ○: O_3 Smoothed profiles: —— ; simulation results: – – .

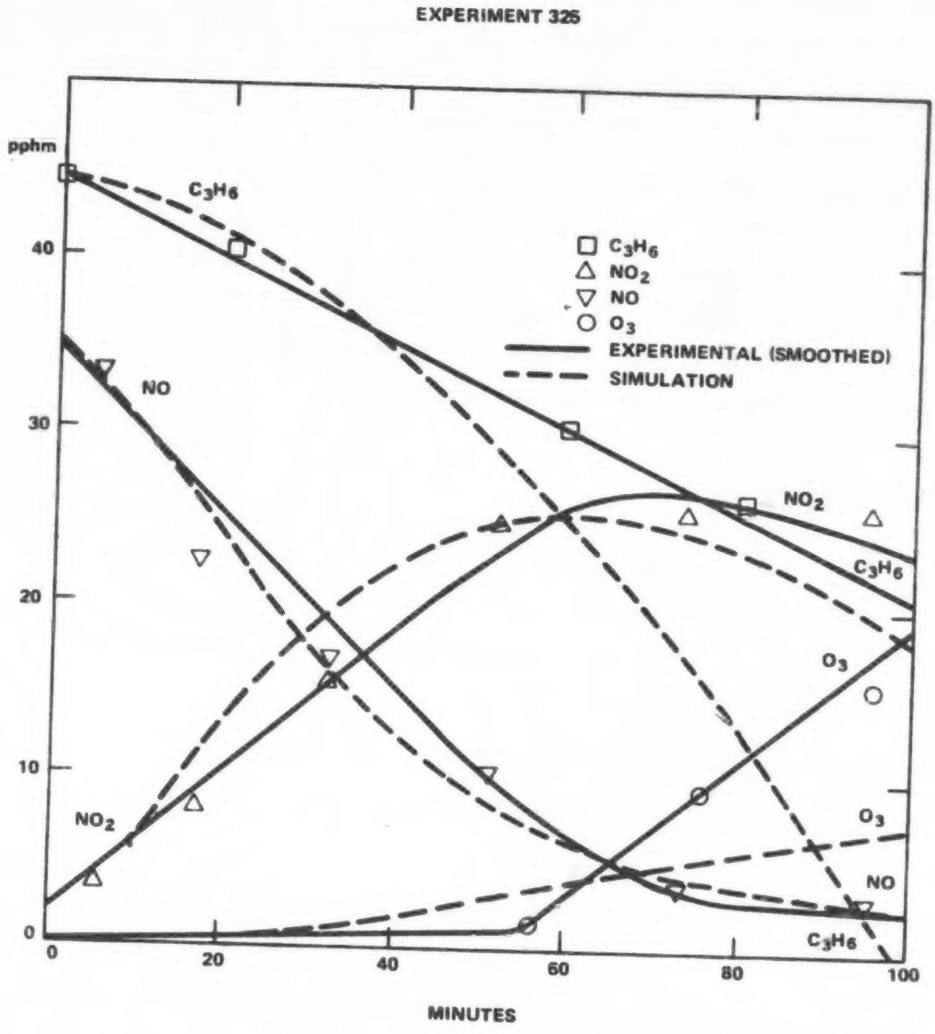

Figure III.4

Time profiles of contaminant concentrations, Experiment 325 (propylene, ethane and oxides of nitrogen system). Simulation results using original mechanism (MI), compared with experimental data points and smoothed profiles. Experimental points, □ ; C_3H_6; △ : NO_2; ▽: NO; ○: O_3 Smoothed profiles: —— ; simulation results: — — .

dioxide. In both runs, simulation of propylene concentration was reasonably good for the first hour, but thereafter the simulated propylene decreased too rapidly and virtually vanished after 100 minutes. Ozone simulation was within experimental error for the entire 100 minutes for experiment 329, but the rapid accumulation of ozone observed after about 50 minutes in experiment 325 was not successfully simulated*.

Apparently the underestimation of ozone in experiment 325 was associated with the overestimation of the propylene consumption rate. As described below, this sort of difficulty was largely overcome by a revision of the mechanism. The revision, approved by the project technical officer, Dr. Sklarew, incorporated several suggestions by Dr. Dodge of the Division of Physics and Chemistry.

2. By Revised Mechanism, M2

Satisfactory simulation of experiments 329 and 325 was soon achieved using the revised mechanism M2, whose most essential new feature was reaction of propylene with hydroxyl radicals. Mechanism M2 is set forth in Table III-4, together with the appropriate rate parameters as optimized for experiments 329 and 325.

In mechanism M2, the following revisions were incorporated:

a. All reactions attributed to singlet molecular oxygen were eliminated.

b. Reaction 7 (consumption of propylene by hydroxyl radicals) was added.

c. Reactions previously written as termolecular, involving molecular oxygen and acetyl radicals, were eliminated in favor of accounting for the adduct, peroxyacetyl radical. Thus reactions 18 and 30 of M1 were dropped, and new reactions 10, 18, 25 and 30 incorporated in M2.

---

* In simulating exp. 325, the same parameters were used as for exp. 329, inasmuch as the objective was to find a single set of parameters uniformly applicable for this system.

Table III-4

Revised Mechanism (M2) for the Chemical Dynamics Module (with Rate Factors for Exp. 329 and 325)

1	NO2+HV =NO+O	0.40000000D 00
2	O+O2+M =O3+M	0.14000000D 07
3	O3+NO =NO2+O2	0.40000000D 00
4	NO2+O3 = NO3+O2	0.10000000D-04
5	C2H3O3 + O2= C2H3O2 + O3	0.20000000D 02
6	NO3+NO =2NO2	0.24500000D 03
7	C3H6+OH = CH3CHO+CH3	0.10000000D 04
8	NO+HO2 =NO2+OH	0.10000000D 02
9	H+O2+M =HO2+M	0.10000000D 07
10	C2H3O + O2 = C2H3O3	0.10000000D 06
11		0.0
12	NO2+OH =HNO3	0.10000000D 03
13	OH+O3 =HO2+O2	0.10000000D 02
14	OH+CO =H+CO2	0.30000000D 01
15	CH3+O2+M =CH3O2+M	0.14000000D 07
16	CH3O2+NO =CH3O+NO2	0.20000000D 01
17	CH3O+O2+NO =CH3O2+NO2	0.10000000D 02
18	C2H3O3+NO = C2H3O2+NO2	0.25000000D 01
19	C2H3O2+NO =C2H3O+NO2	0.20000000D 02
20	C2H4O2+NO =CH3CHO+NO2	0.10000000D 03
21	CH3O+O2 =HCHO+HO2	0.20000000D 03
22	C3H6+O =CH3+C2H3O	0.35000000D 02
23	C3H6+O3 =HCHO+C2H4O2	0.50000000D-04
24	C3H6+O+O2 =HCHO+C2H4O2	0.17500000D 02
25	C2H4O2+O2 = C2H3O3+OH	0.30000000D 03
26	C3H6+HO2 =CH3O+CH3CHO	0.10000000D 01
27	C3H6+MEO2=CH3+MEO+C2H3O	0.10000000D-01
28	C2H3O+M =CH3+CO+M	0.10000000D 02
29	CH3O+NO2 =CH3ONO2	0.10000000D 01
30	C2H3O3+NO2 = C2H3O3NO2	0.20000000D 00
31	DUMHC+O =CH3+C2H3O	0.35000000D 01
32	HCHO + HV = H + H + CO	0.30000000D-02
33	NO2 +NO3 +H2O = HNO3+ "	0.10000000D 03

d. To allow for ozone accumulation to exceed initial oxides of nitrogen input, the new reaction 5,

$$C_2H_3O_3 + O_2 = C_2H_3O_2 + O_3,$$

was incorporated.

At the same time that these changes were made, the chemical dynamics module was also adjusted to allow for use of the chain termination rate factor, Z, as an input parameter, so that its effect on the simulation could be more easily explored.

Although the reaction set shown in Table III-4 was not further altered in the course of the project, there were subsequently two further adjustments of the chemical dynamics module. We shall designate the module in the state just described as M2a. The further alterations, giving modules M2b and M2c, were the following:

M2b was derived from M2a by allowing for radical chain termination by reaction of radicals with nitric oxide. The rate factor Z thereupon became Z1, and the new rate factor was made Z2.

M2c was derived from M2b by incorporating a term for chamber dilution (at a rate of .007 min^{-1}) in the differential equation for each of the non-steady-state species involved in the numerical integration procedure.

a. Module M2a

Figure III-5 shows the simulation results achieved for Experiment 329 by module M2a, using the rate factors listed in Table III-4 and with Z taken to be 100 $\text{pphm}^{-1}\ \text{min}^{-1}$. The initial concentration of ethane was used as the input value of dummy hydrocarbon (DUMHC) and the rate factor for reaction 31 (attack on dummy hydrocarbon by oxygen atoms) was taken as 3.5 $\text{pphm}^{-1}\ \text{min}^{-1}$. Concentrations predicted over the six-hour period of irradiation were within 0.08 ppm of those indicated by the experiment for the four main reacting species, nitrogen dioxide, nitric oxide, propylene and ozone.

The largest discrepancies were for nitrogen dioxide, and correspond to a consistent overestimation. A rough correction for chamber

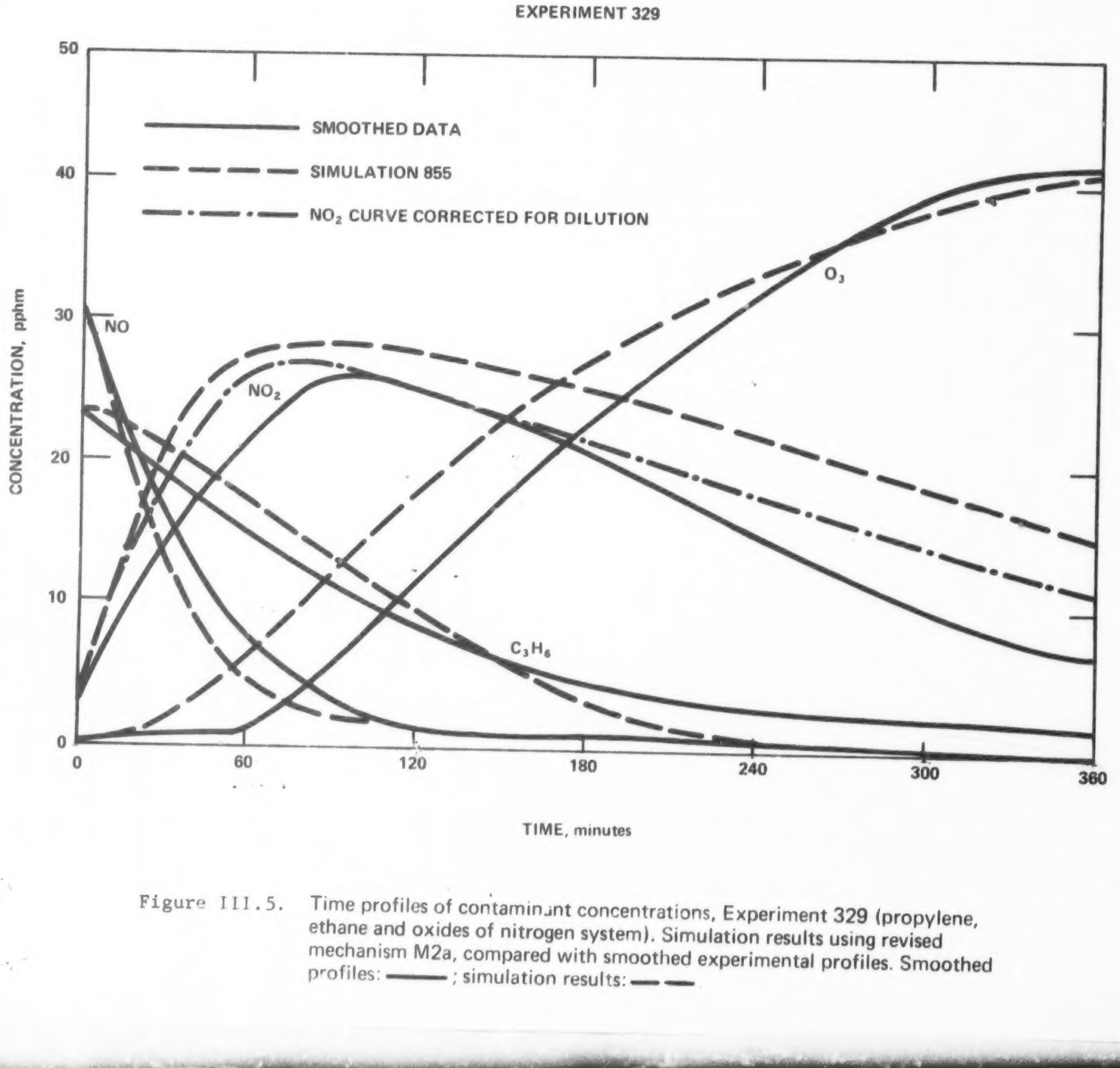

Figure III.5. Time profiles of contaminant concentrations, Experiment 329 (propylene, ethane and oxides of nitrogen system). Simulation results using revised mechanism M2a, compared with smoothed experimental profiles. Smoothed profiles: ——— ; simulation results: — —

dilution* (not incorporated in M2a) indicated, as shown in the figure, that dilution could approximately account for the major part of these discrepancies.

Ozone concentrations predicted were within 0.06 ppm of observed values throughout the irradiation period. The largest discrepancies arose from the fact that a buildup of 0.06 ppm was estimated for the first hour of reaction, as compared with only 0.01 ppm observed. After three hours, the difference between predicted and observed values became appreciably less.

Nitric oxide concentrations were consistently estimated within 0.04 ppm of the observed (smoothed-curve) values, and propylene within 0.03 ppm. There was, however, a marked difference between the estimated initial rate of consumption of propylene and the initial rate indicated by the smoothed data curves, the estimated initial rate appearing too low by a factor of 4 or 5. After the first twenty minutes of simulation, the estimated and observed rates were approximately equal.

Figure III-6 shows simulation results for experiment 325 by M2a, using the same rate factors and other conditions specified in the preceding paragraphs for experiment 329. In this case the discrepancies between estimated and observed values of nitrogen dioxide are higher--up to 0.16 ppm before correcting for dilution, and up to 0.12 ppm after correction. In other respects, however, the results are quite similar to those just discussed.

b. Module M2b

Simulations of experiments 329 and 325 by module M2a, as shown in the preceding discussion, were for the most part within experimental error of the data furnished. However, when applied to simulation of other experiments of the propylene-ethane-oxides of nitrogen system,

---

* This correction was based on a simple reduction of nitrogen dioxide concentration, proportional to the loss of material from the chamber assuming steady dilution at a relative rate of 0.007 min^{-1}.

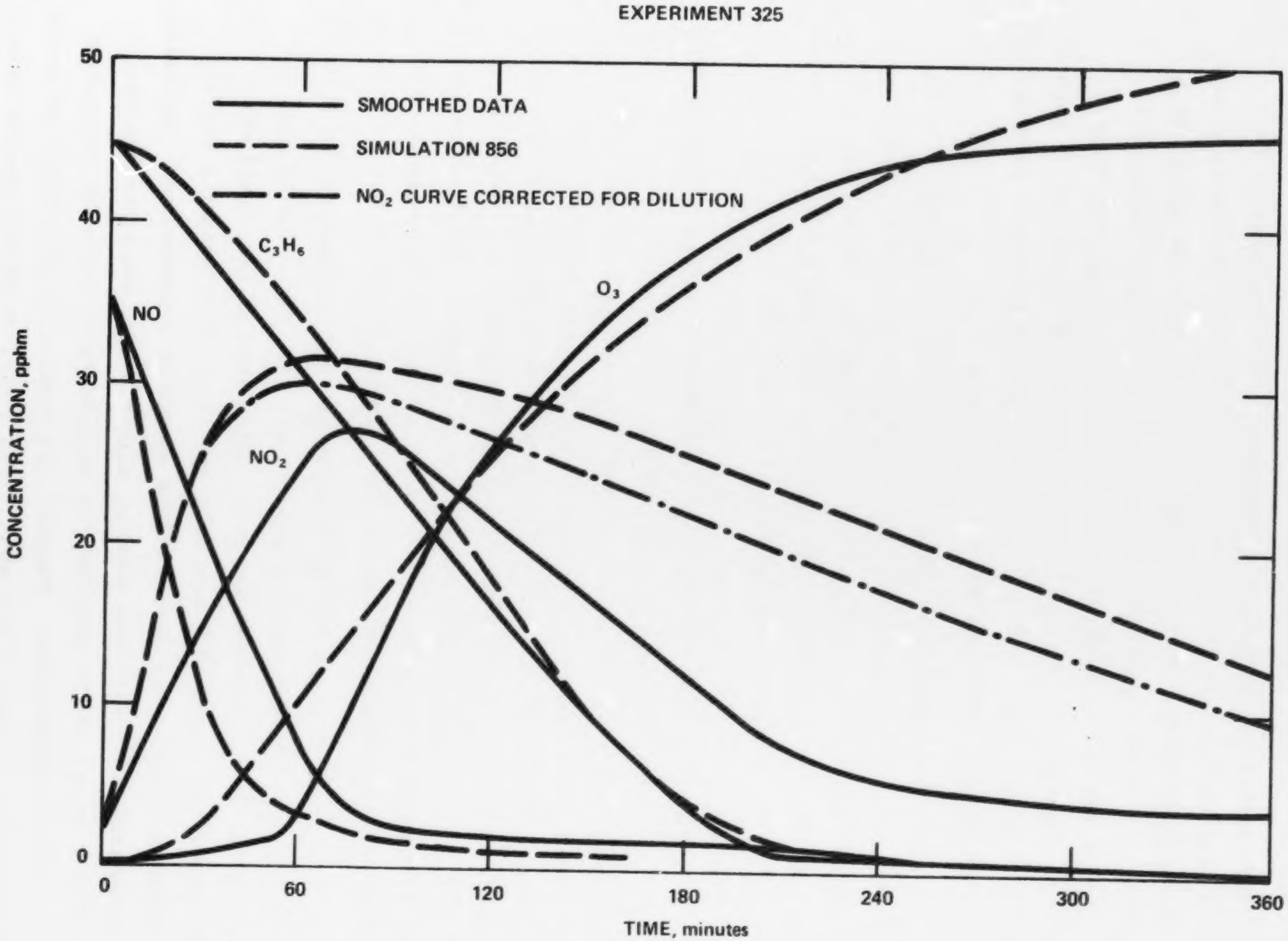

Figure III.6. Time profiles of contaminant concentrations, Experiment 325 (propylene, ethane and oxides of nitrogen system). Simulation results using revised mechanism M2a, compared with smoothed experimental profiles. Smoothed profiles: ——— ; simulation results: — — .

the same set of rate factors predicted ozone levels which were seriously in error, indicating premature accumulation of ozone, when in fact very little oxidant was found within the six-hour irradiation period in those experiments. Module M2b allowed us to test the effect of a hypothetical chain-terminating reaction in which nitric oxide could react with any chain-carrying radical to remove it from the system. The rate constant for this reaction, it was found, could not be greater than 0.5 $pphm^{-1}$ min^{-1} without unduly retarding the overall progress of photo-oxidation in the simulations.

A series of simulations based on experiment 329 showed that the effects of variation of Z1, the rate factor for radical recombination, was small relative to the effect of introducing Z2, the rate factor for chain termination by nitric oxide. Figure III-7 shows nitrogen dioxide time-profiles as calculated for Z2 = 0.3 $pphm^{-1}$ min^{-1} with values of Z1 ranging from 15 to 300 $pphm^{-1}$ min^{-1}; the NO_2 profile from Figure III-5 is also included for comparison. The major effect of introducing Z2 at this value is a drastic reduction in the initial rate of nitrogen dioxide accumulation due to photo-oxidation of nitric oxide. Both the time required for half-conversion and the time required to attain maximum nitrogen dioxide concentration were extended by more than an hour by this change, while the effect of changing Z1 was relatively slight. Figure III-8 shows the ozone time-profiles for the same set of simulations from which it is seen that the onset of accumulation of ozone is substantially delayed by the assumption of Z2 = 0.3.

Figure III-9 shows the application of these parameters (Z1 = 100, Z2 = 0.3) to the simulation of experiment 318. Here, the initial concentration of nitric oxide was much larger than in the experiments previously discussed (329 and 325), and larger discrepancies between estimated and observed time-profiles emerge as a consequence. Estimated concentrations of nitrogen dioxide, nitric oxide, and propylene were within 0.25 ppm of the experimental smoothed-profile values throughout the six-hour irradiation. However, the simulation predicted substantial accumulation of ozone after about three hours, an effect clearly absent

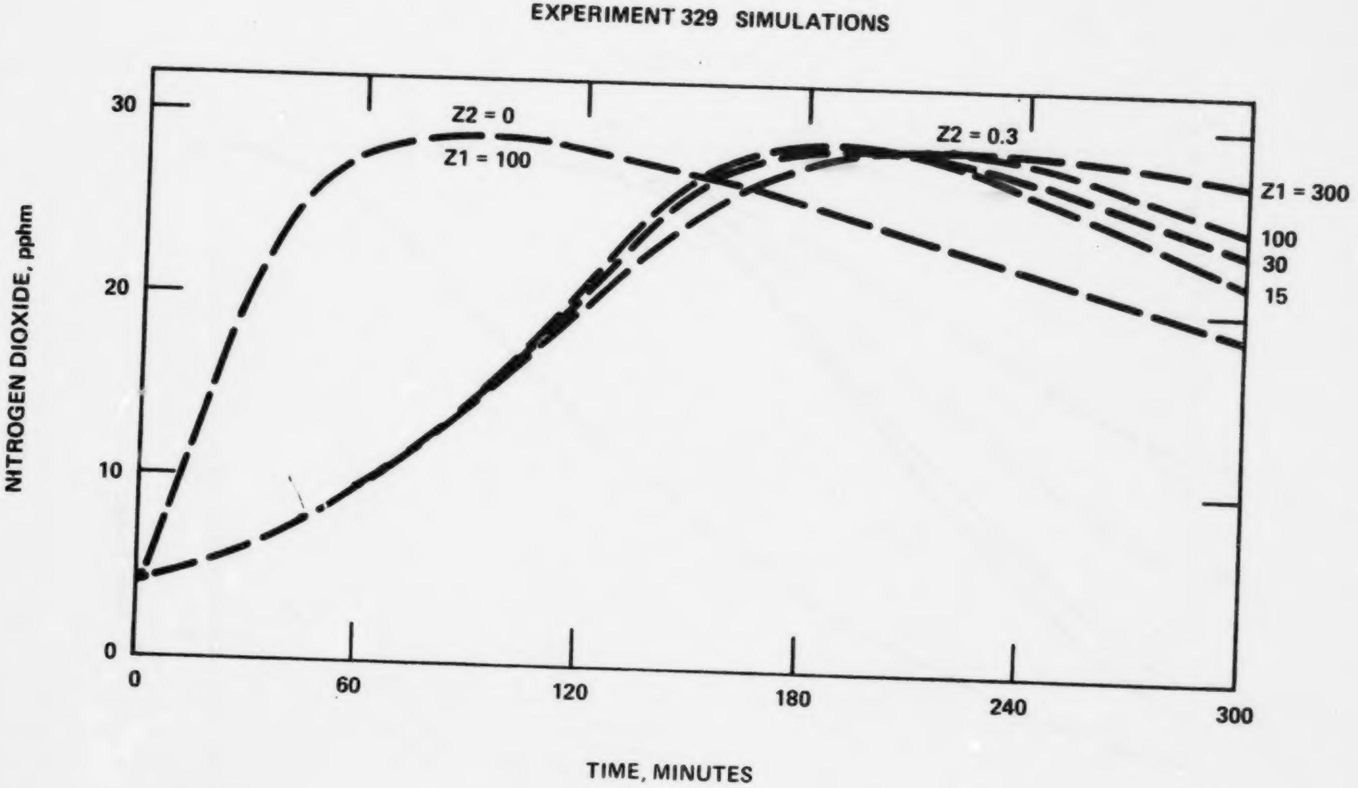

Figure III.7. Time profiles of nitrogen dioxide concentration simulating Experiment 329 (propylene, ethane and oxides of nitrogen system). Results using revised mechanism M2a and M2b, with various values of chain-terminating parameters Z1 and Z2.

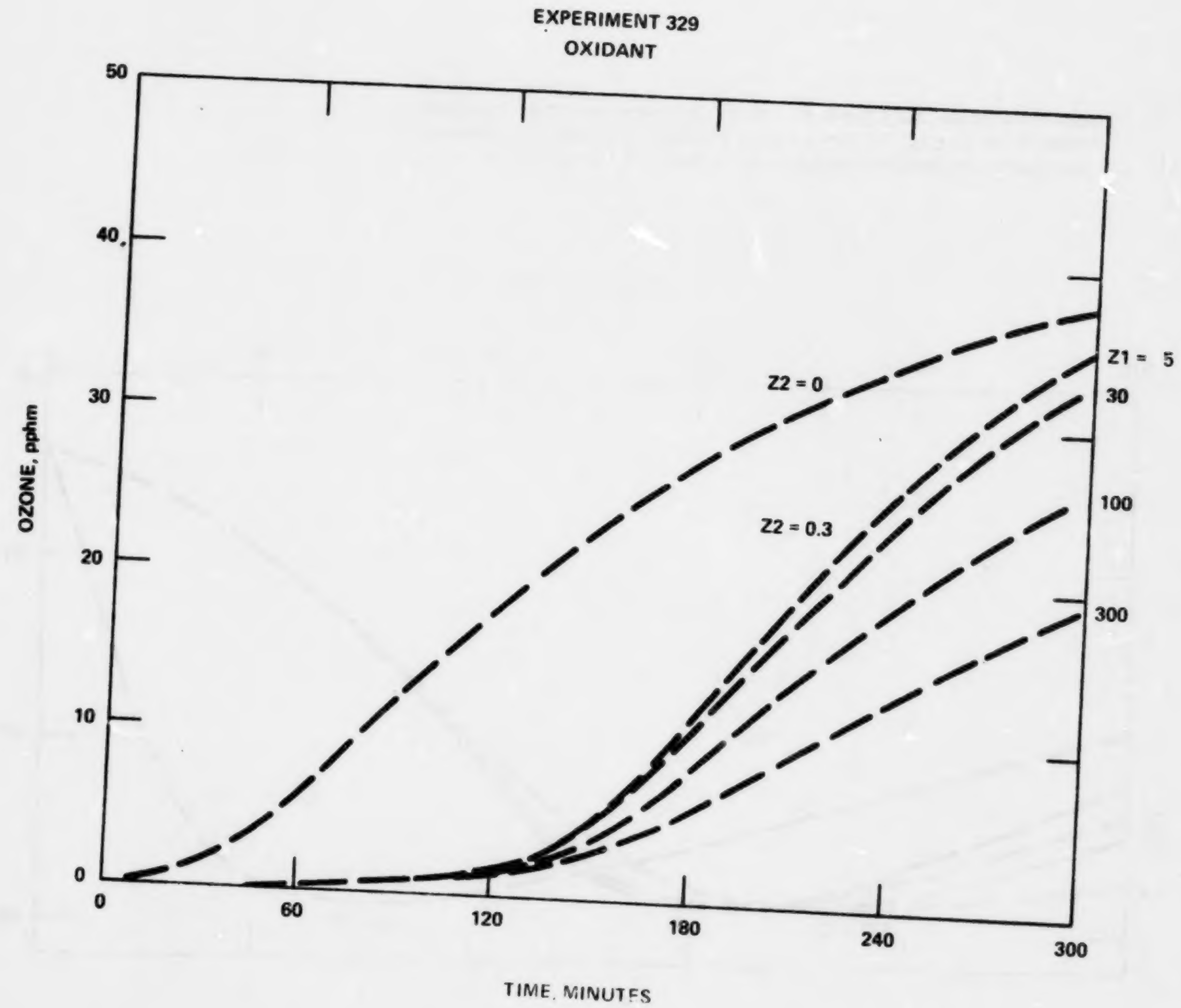

Figure III.8. Time profiles of oxidant (ozone) concentration simulating Experiment 329 (propylene, ethane and oxides of nitrogen system). Results using revised mechanism M2a and M2b, with various values of chain-terminating parameters Z1 and Z2.

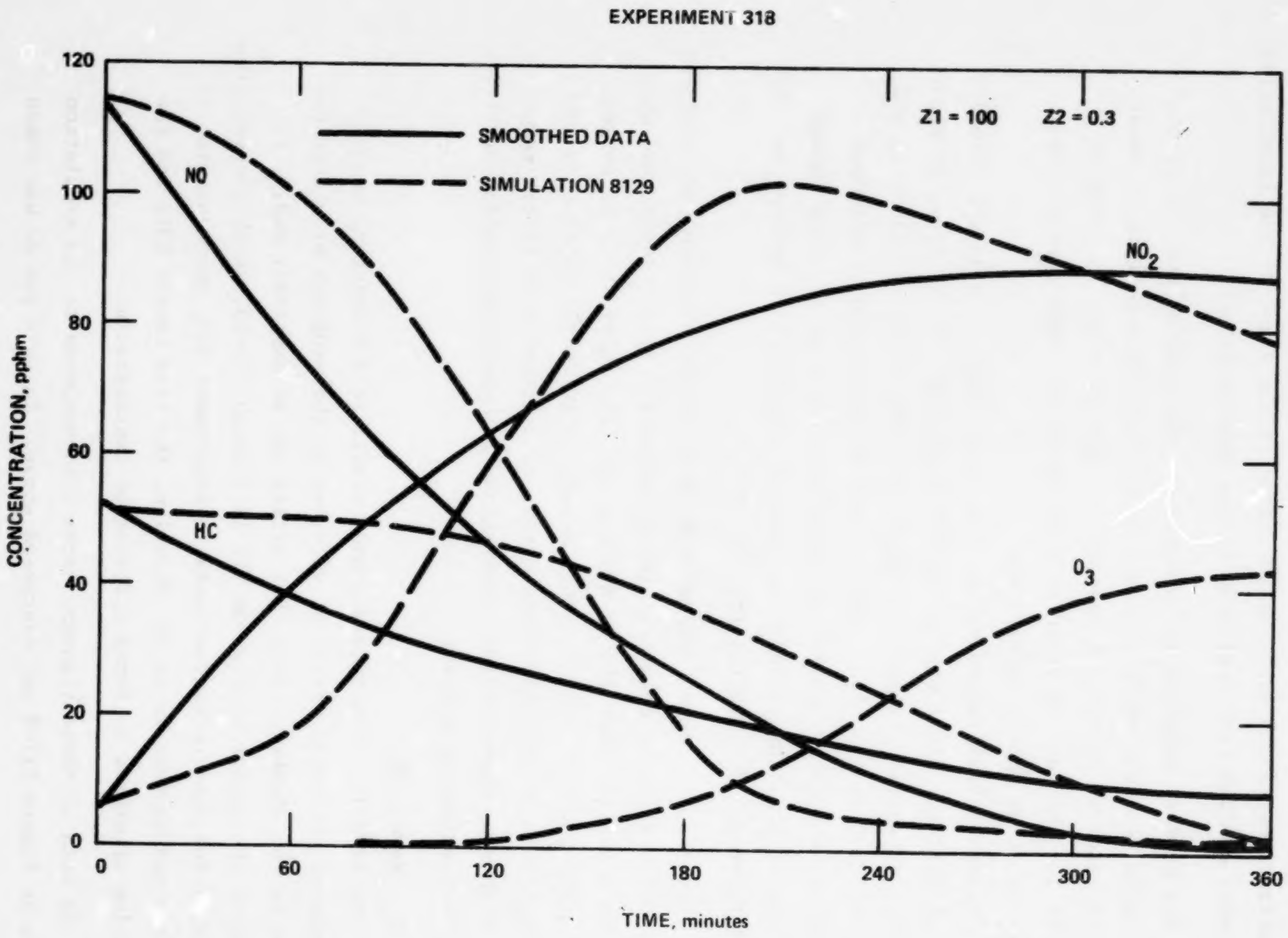

Figure III.9. Time profiles of contaminant concentrations, Experiment 318 (propylene, ethane and oxides of nitrogen system). Simulation results using revised mechanism M2b, compared with smoothed experimental profiles. Smoothed profiles: ——— ; simulation results: — — .

in the experiment. Furthermore, the predicted rates of change of concentrations of the other contaminants at the start of the irradiation were much smaller than indicated by the chamber data.

Any further suppression of ozone (in the simulations) by further increasing Z2 would evidently lead to greater discrepancies in these initial rates of change. Therefore, it appears that, in order to account for the lack of ozone in experiment 318, more extensive modifications in M2 should be explored.

Further detail regarding the effect of varying Z2 on the simulation of nitrogen dioxide profiles for experiment 318 is shown in Figure III-10. Shown are estimated profiles for the series of values Z2 = 0, 0.05, 0.15, 0.3, 0.4, 0.5. The maximum concentration of nitrogen dioxide is not much affected by these variations of Z2, even though the time of reaching the peak is delayed from about 75 minutes for the first to around 300 minutes for the last.

Figure III-11 shows the corresponding series of ozone time-profiles. It is interesting to note that these curves all rise steeply, and with approximately the same slope, after an initial delay which is longer, the larger the value of Z2. This mechanism evidently implies an inhibitory effect of initial nitric oxide, in at least qualitative agreement with many experimental observations in hydrocarbon-oxides of nitrogen photo-oxidation systems.

c. Module M2c

The creation of module M2c made available a convenient means of estimating the total effect of dilution on the progress of photochemistry in the chamber. That this effect is, as expected, small, is shown by the curves in Figures III-12 through III-15, which present time-profiles for various contaminants in experiment 318, corresponding to various assumptions as to Z2, dilution, the rate factor K31, and the relation of ethane to dummy hydrocarbon concentration.

In each of these figures, curve 1 corresponds to the simulation shown in Figure III-9 and discussed above. In this run Z2 was taken

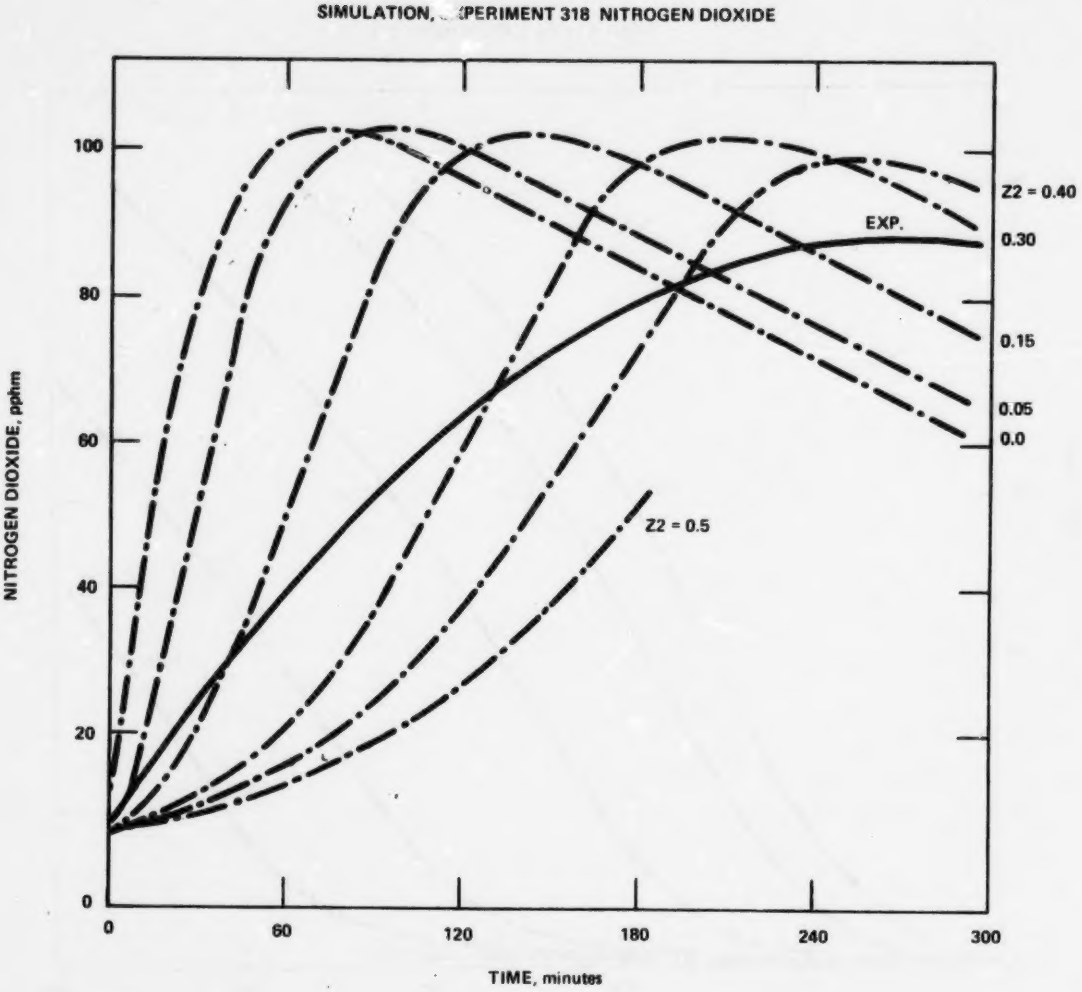

Figure III.10. Time profiles of nitrogen dioxide concentration simulating Experiment 318 (propylene, ethane and oxides of nitrogen system). Results using revised mechanism M2a and M2b, with various values of chain-terminating parameter Z2.

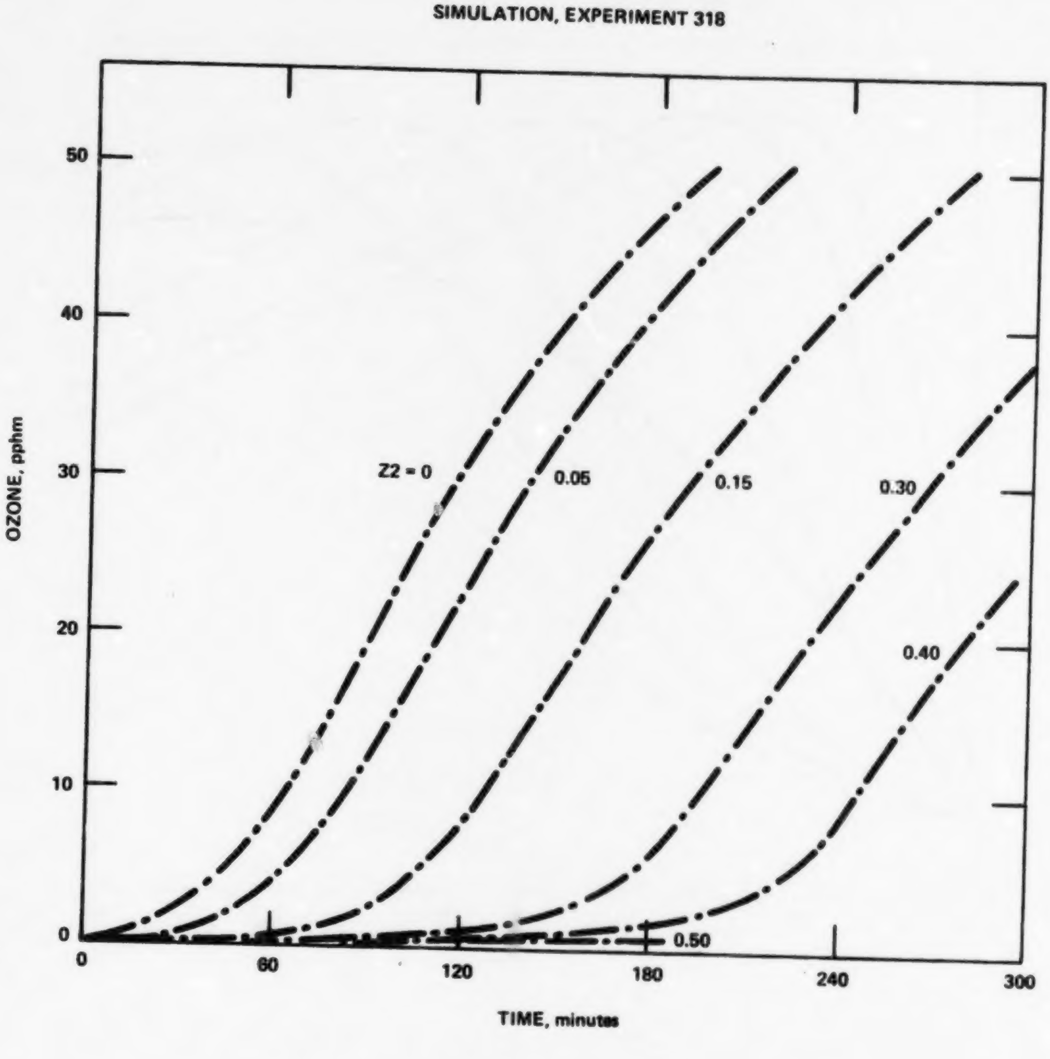

Figure III.11. Time profiles of oxidant (ozone) concentration simulating Experiment 318 (propylene, ethane and oxides of nitrogen system). Results using revised mechanism M2a and M2b, with various values of chain-terminating parameter Z2.

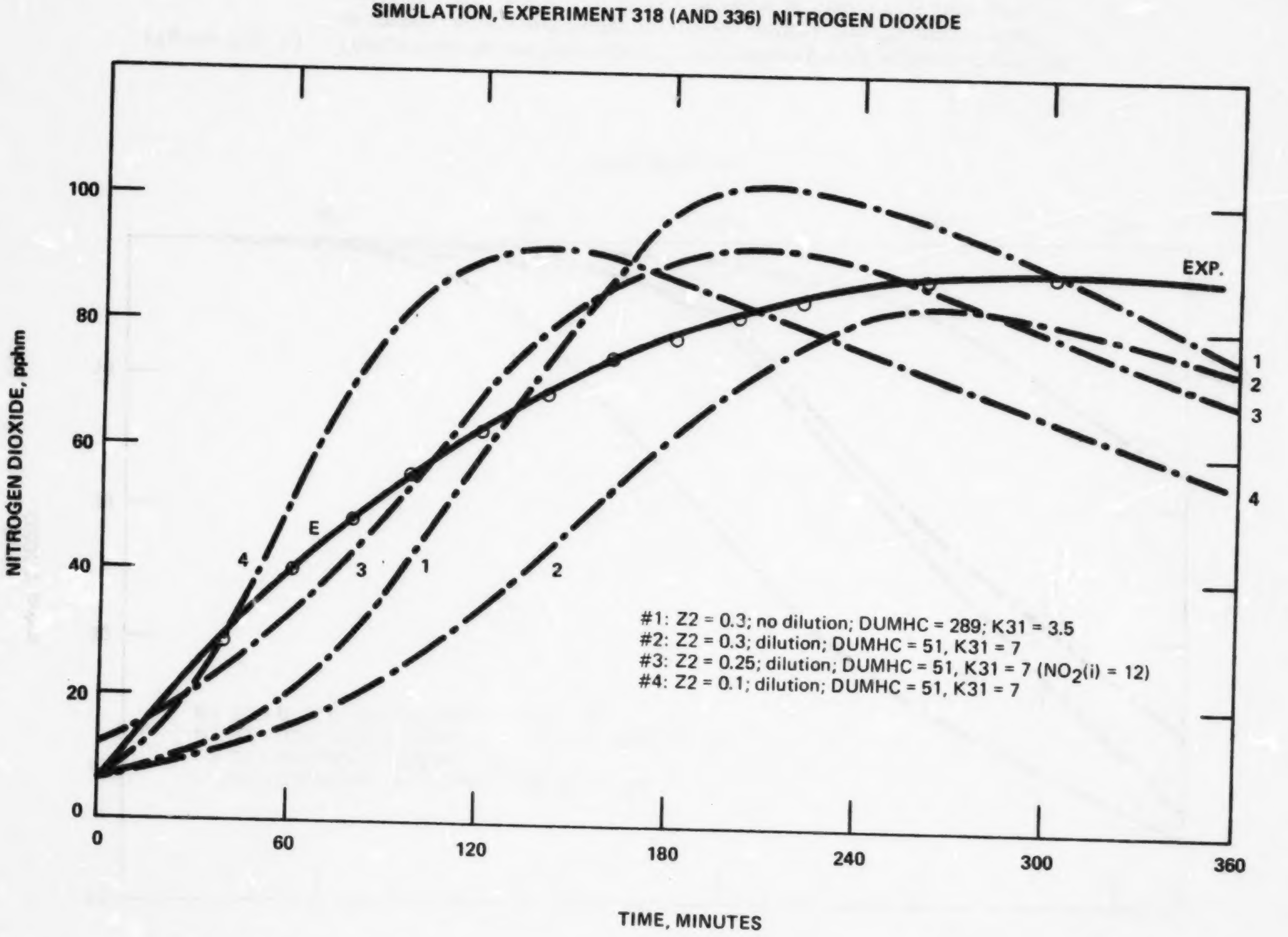

Figure III.12. Time profiles of nitrogen dioxide concentration simulating Experiment 318 (propylene, ethane and oxides of nitrogen system). Results using revised mechanism M2b and M2c, with various values of chain-terminating parameters and parameters for unreactive hydrocarbon.

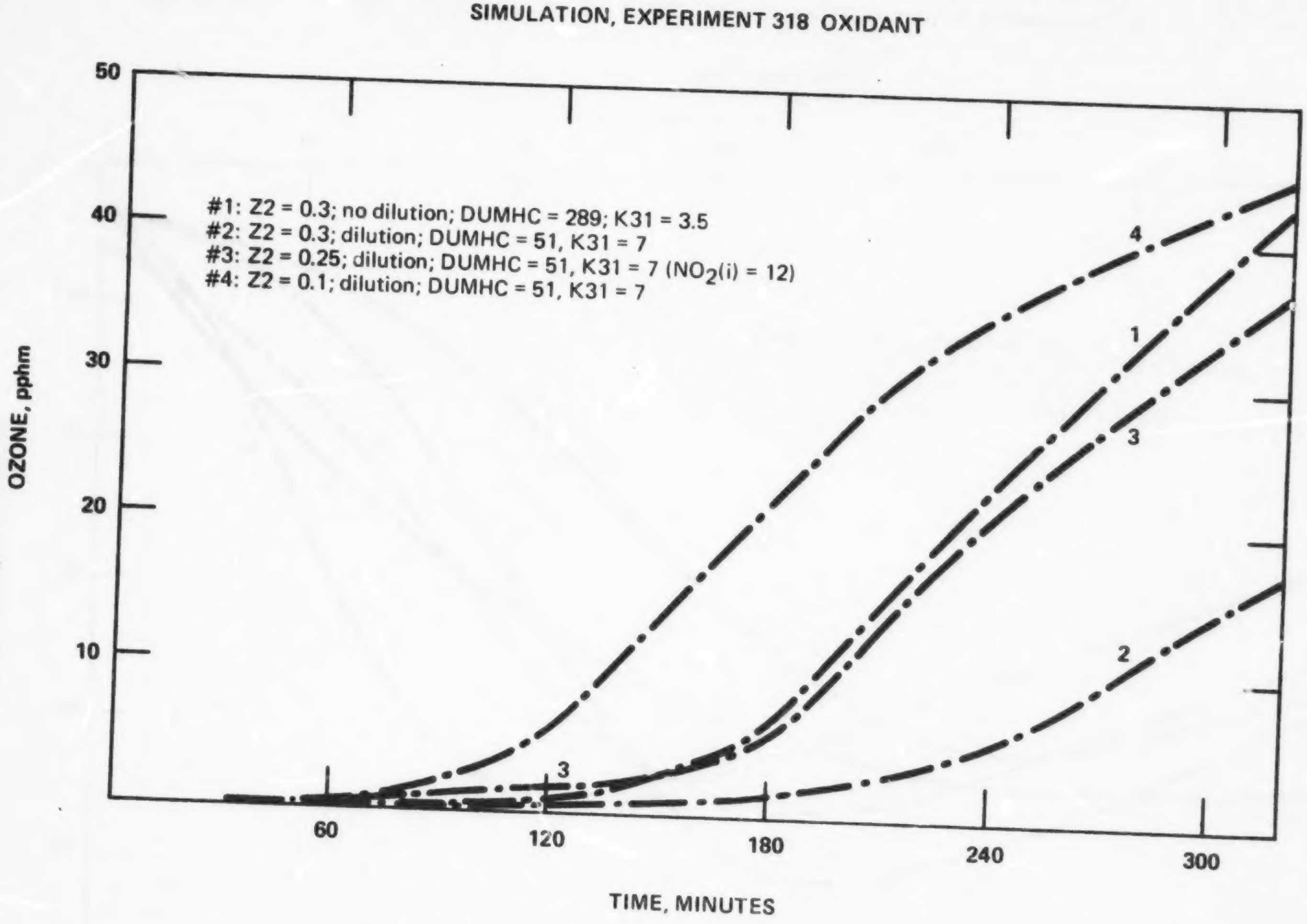

Figure III.13. Time profiles for oxidant (ozone) concentration simulating Experiment 318 (propylene, ethane and oxides of nitrogen system). Results using revised mechanism M2b and M2c, with various values of chain-terminating parameters and parameters for unreactive hydrocarbon.

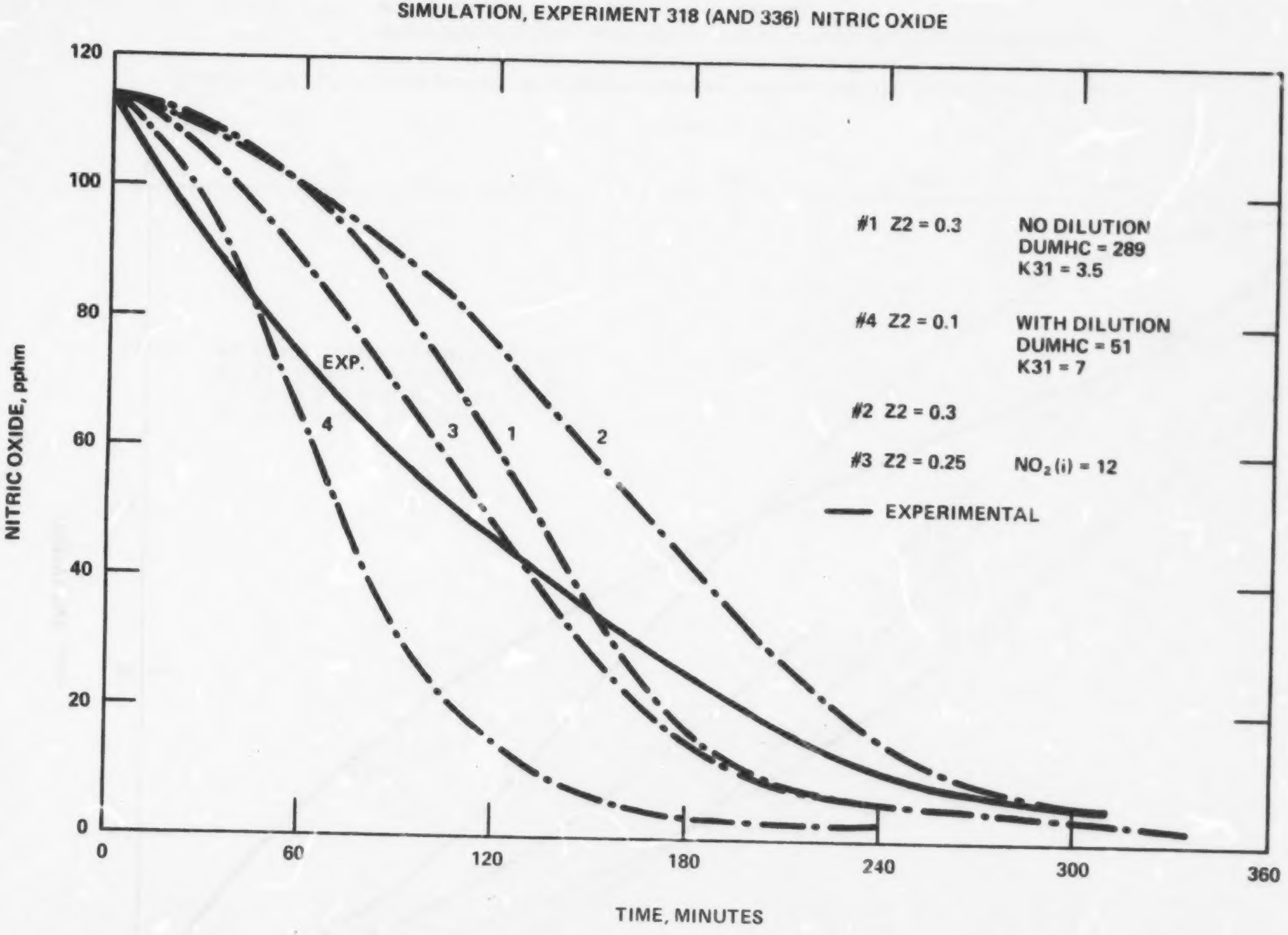

Figure III.14. Time profiles of nitric oxide concentration simulating Experiment 318 (propylene, ethane and oxides of nitrogen system). Results using revised mechanism M2b and M2c, with various values of chain-terminating parameters and parameters for unreactive hydrocarbon.

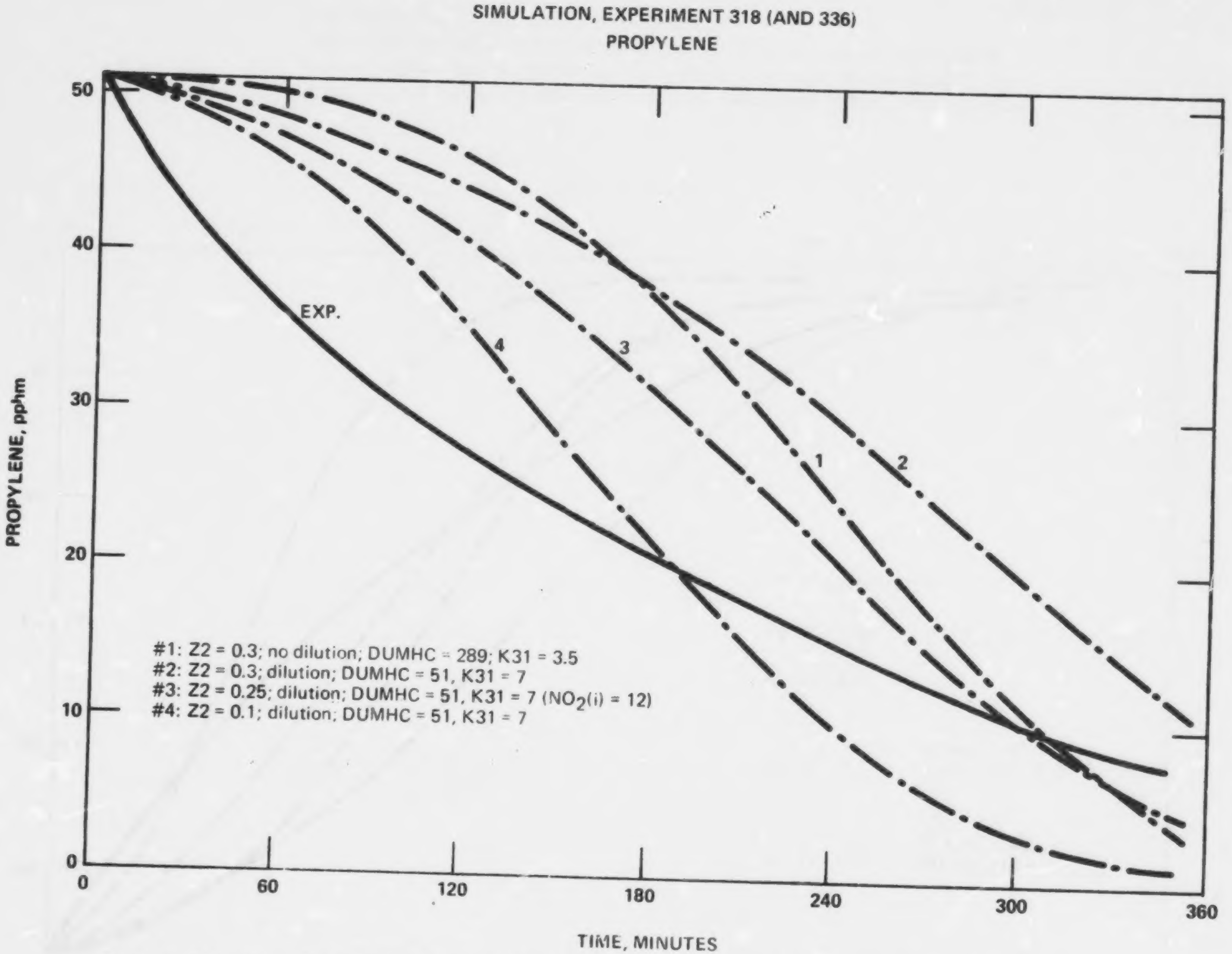

Figure III.15. Time profiles for propylene concentration simulating Experiment 318 (propylene, ethane and oxides of nitrogen system). Results using revised mechanism M2b and M2c, with various values of chain-terminating parameters and parameters for unreactive hydrocarbon.

as 0.3 $pphm^{-1}$ min^{-1}; K31 was 3.5; each mole of ethane was assumed equivalent to one mole of dummy hydrocarbon; and dilution was ignored.

Curve 2 was from a simulation with Z2 = 0.3; K31 = 7; one mole ethane = 0.18 mole DUMHC; and dilution assumed.

Curve 3 was from a simulation having Z2 = 0.25, K31 = 7; one ethane = 0.18 DUMHC; dilution assumed; and initial NO_2 taken as 12 pphm (twice the amount specified in the experimental data).

Curve 4 was for Z2 = 0.1; K31 = 7; one ethane = 0.18 DUMHC; and dilution assumed.

Z1 was taken at 100 $pphm^{-1}$ min^{-1} throughout.

Comparison of the curves with the experimental smoothed profiles also shown in the figures indicates that the conditions which permit optimum simulation are not the same for all contaminants. Thus, the nitrogen dioxide and nitric oxide data are perhaps best simulated by curve 3; the ozone data, by curve 4, and the propylene data, by curve 2. It is clear that, unless further modifications to the mechanism are explored and substantiated, any choices for the values of parameters to be used in simulation of the propylene-ethane-oxides of nitrogen system will have to be in the nature of a reasonable compromise, in view of the requirements of the particular case.

Although the set of rate factors used for the simulation of experiment 318 (shown in Figure III-9) was inadequate to predict suppression of ozone in that experiment, it was somewhat better relative to experiment 321, as shown in Figure III-16. In this case the predicted ozone after six hours was less than 0.1 ppm. In spite of the use of module M2c, which includes the adjustment for chamber dilution, the concentration of nitrogen dioxide at the end of the experiment was overestimated by about 0.3 ppm, and the nitric oxide underestimated by about 0.2 ppm. For the first three hours, however, there were no discrepancies above 0.05 ppm; and for propylene, the discrepancies were less than 0.05 ppm throughout.

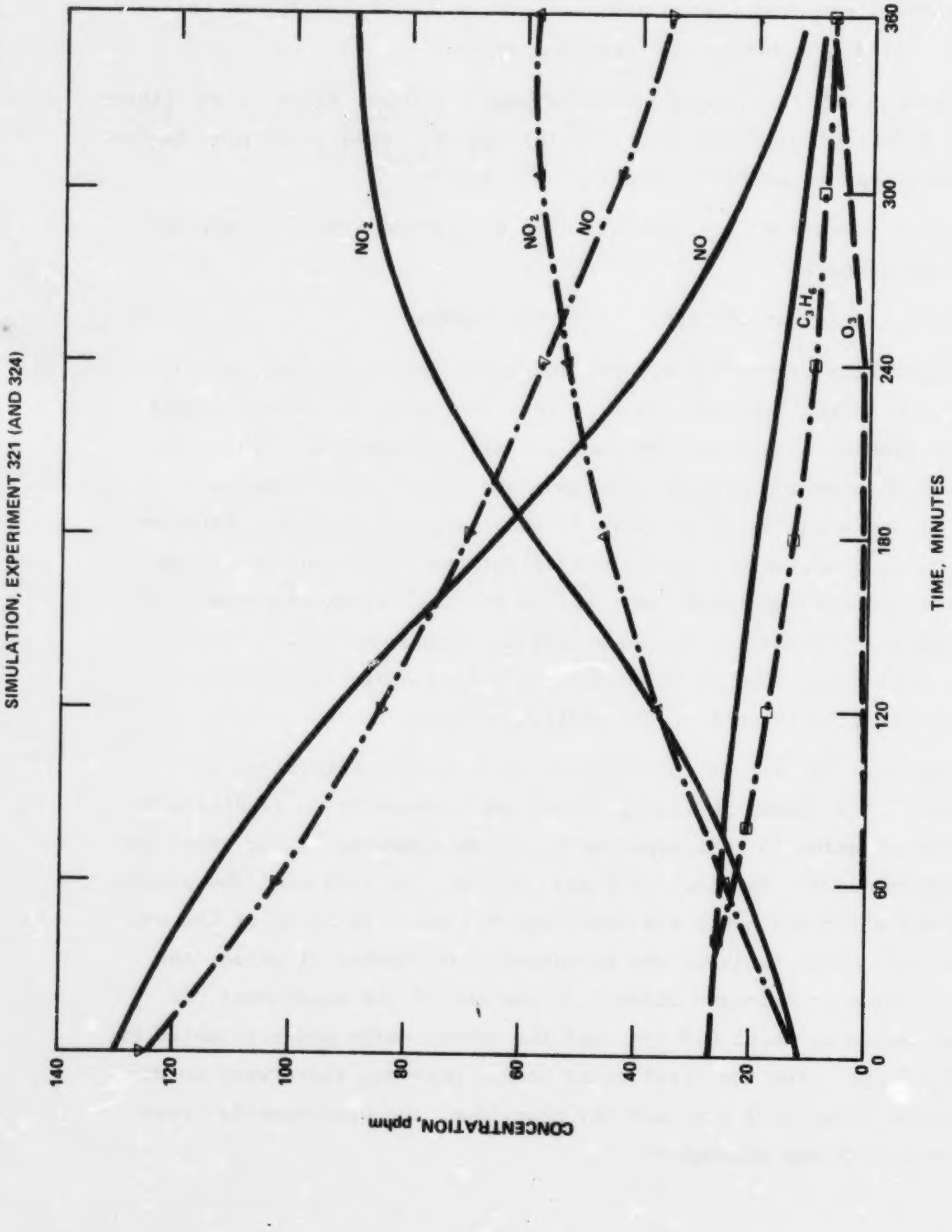

Figure III.16. Time profiles of contaminant concentrations, Experiment 321 (propylene, ethane and oxides of nitrogen system). Simulation results using revised mechanism M2c, compared with smoothed experimental profiles. Smoothed profiles: ——, simulation results: —·—·.

C. SIMULATION OF AUTO EXHAUST PHOTO-OXIDATION SYSTEMS

Diluted auto exhaust gases were irradiated in four chamber experiments, under the conditions indicated in Table III-5.

Figures III-17, III-18, III-19 and III-20 show the results of simulation of the auto exhaust experiments, using module M2b. The rate factors used in these simulations were the same as those shown in Table III-4, with the exception that in the first two, K31 was increased by a factor of two, to 7 $\text{pphm}^{-1}\ \text{min}^{-1}$.

For convenience in discussion, we consider these chamber tests in two pairs: experiments 222 and 233, in which high levels of ozone were produced, and experiments 224 and 231, in which ozone was essentially absent.

Since the intention in the atmospheric model was to simulate auto exhaust as a mixture of propylene and an arbitrary less reactive hydrocarbon, it was desirable to adjust the relative amounts of these hypothetical surrogate species so as to optimize the simulation of NO, NO_2, and O_3 without attempting to simulate the hydrocarbon concentration profiles. Degrees of freedom for the simulation were, therefore, the initial concentrations of propylene and of the dummy hydrocarbon, and the rate factor for reaction 31 (attack on dummy hydrocarbon by oxygen atoms). We chose to set the initial concentration of propylene equal to that found for propylene in the experiment in each case, and to let the dummy hydrocarbon be higher by an order of magnitude, to simulate the remainder of the hydrocarbon portion of the exhaust gases. The parameter Z2, for rate of chain termination by nitric oxide, was also allowed to vary.

The effect of variation of Z2 is seen in Figure III-17, where experiment 222 is simulated by three sets of curves, with successive values 0, 0.05 and 0.1 for Z2. The main effect is to produce a delay in the early progress of photo-oxidation, so that the simulated time for oxidation of half the nitric oxide is increased from about 20 to about 40 minutes, and the production of NO_2 and ozone are correspondingly

Table III-5

Irradiation Chamber Experiments with Automobile Exhaust Gases

Exp't No.	Concentrations, pphm Initial				Comparisons (estimated/observed) at 360 Minutes				Maximum
	NO_2	NO	C_3H_6	DUMHC[a]	NO_2	NO	C_3H_6	O_3	NO_2
222	10	195	21	480	59/4	0/0	0/0	85/91	165/140
233	22	220	25	600	68/32	0/0	0/0	85/102	200/185
224	20	320	12	200	210/140	22/20	3/2	7/4	205/140
231	20	285	10	150	180/95	45/65	3/2	5/3	180/105

a. Concentrations of DUMHC were taken from the total hydrocarbon concentrations, assuming a carbon number of 2.9. The rate factor for reaction of DUMHC with oxygen atoms was taken as 7 pphm^{-1} min^{-1} for Experiments 222 and 233, 3.5 pphm^{-1} min^{-1} for Experiments 224 and 231.

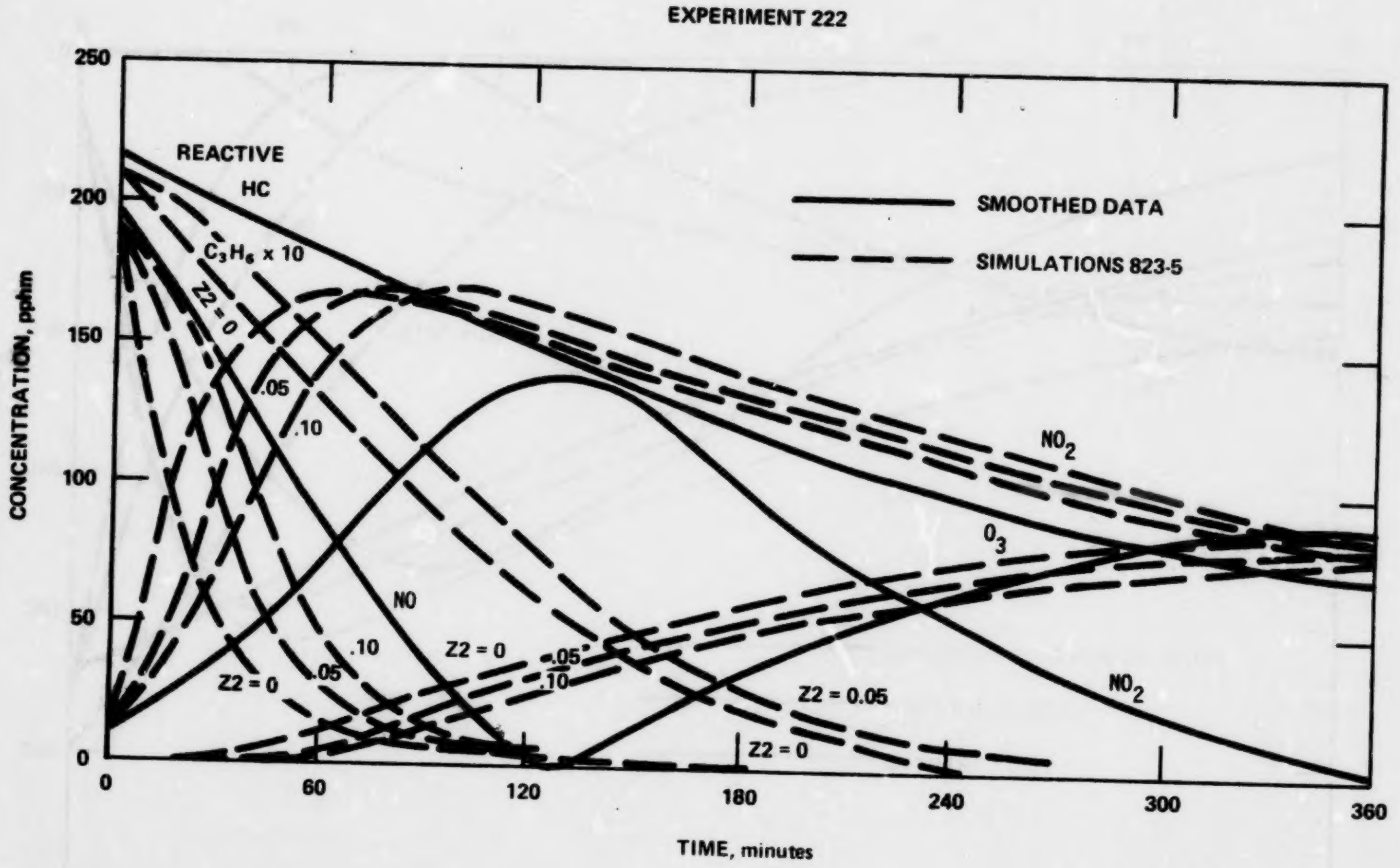

Figure III.17. Time profiles of contaminant concentrations, Experiment 222 (diluted auto exhaust system). Simulation results using revised mechanism M2b, with various values of chain-terminating parameters Z2, compared with smoothed experimental profiles. Smoothed profiles: ——— ; simulation results — — .

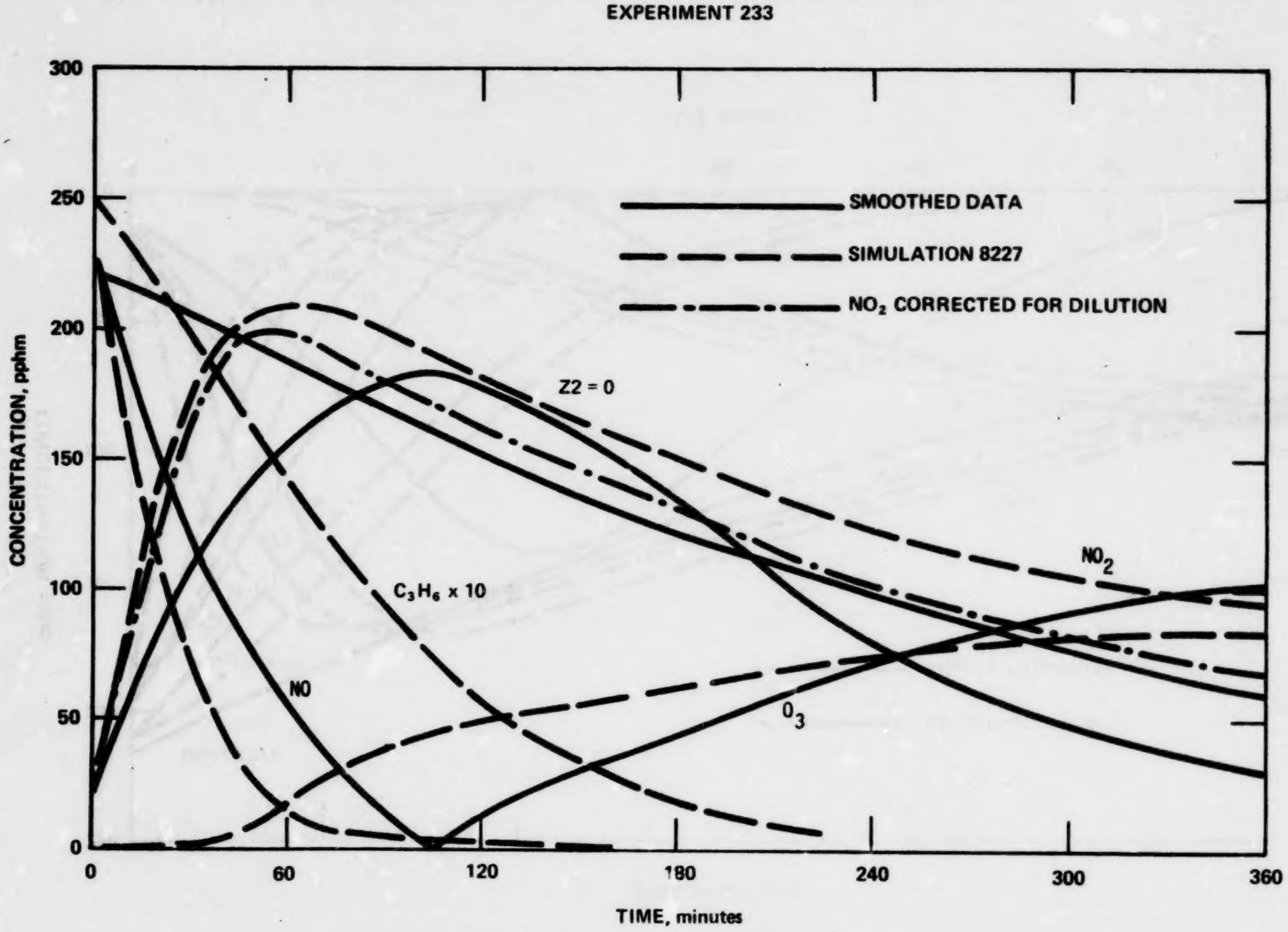

Figure III.18. Time profiles of contaminant concentrations, Experiment 233 (diluted auto exhaust system). Simulation results using revised mechanism M2b, compared with smoothed experimental profiles. Smoothed profiles: ——— ; simulation results: — — .

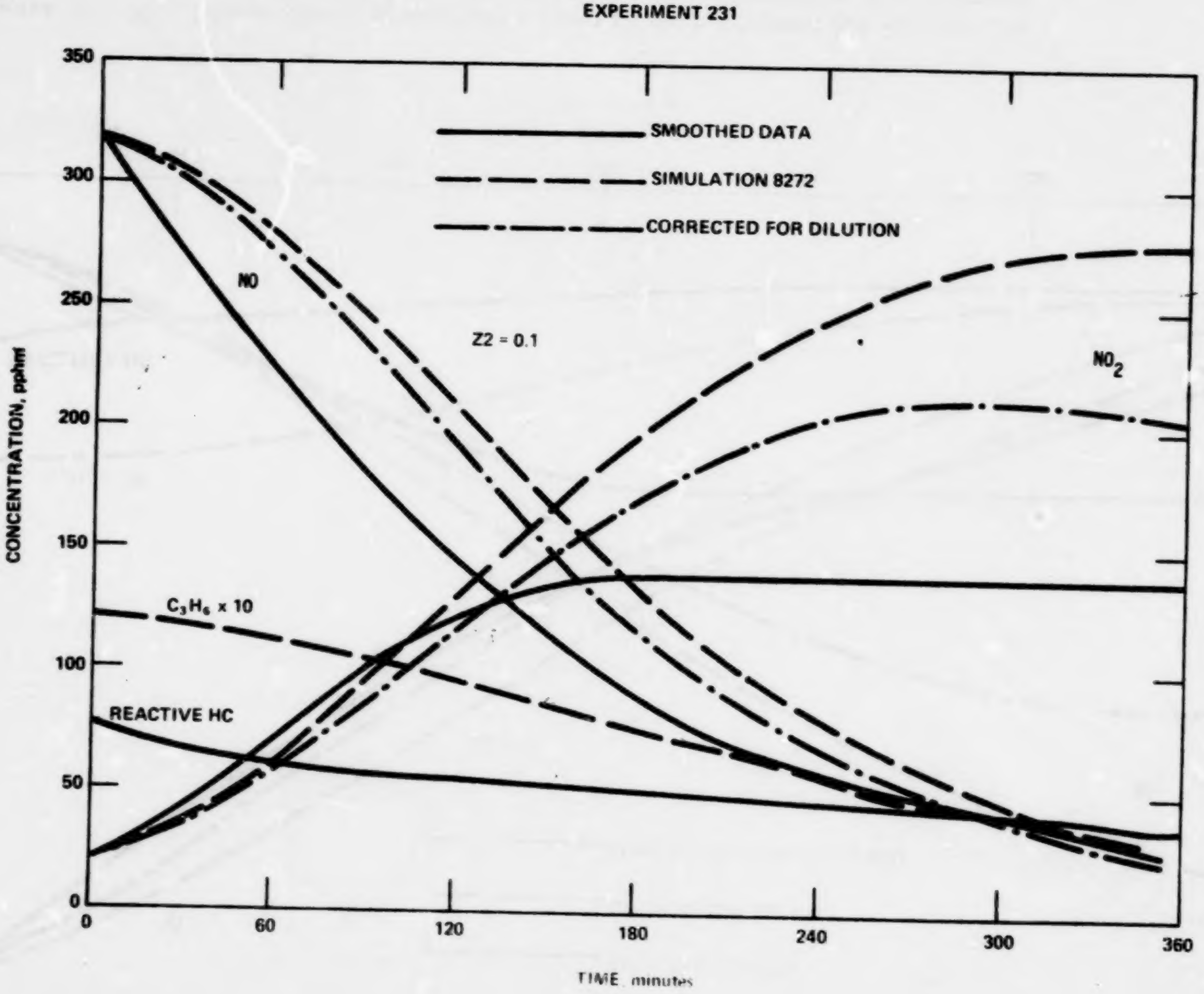

Figure III.19. Time profiles of contaminant concentrations, Experiment 231 (diluted auto exhaust system). Simulation results using revised mechanism M2b, compared with smoothed experimental profiles. Smoothed profiles: ———; simulation results: — —.

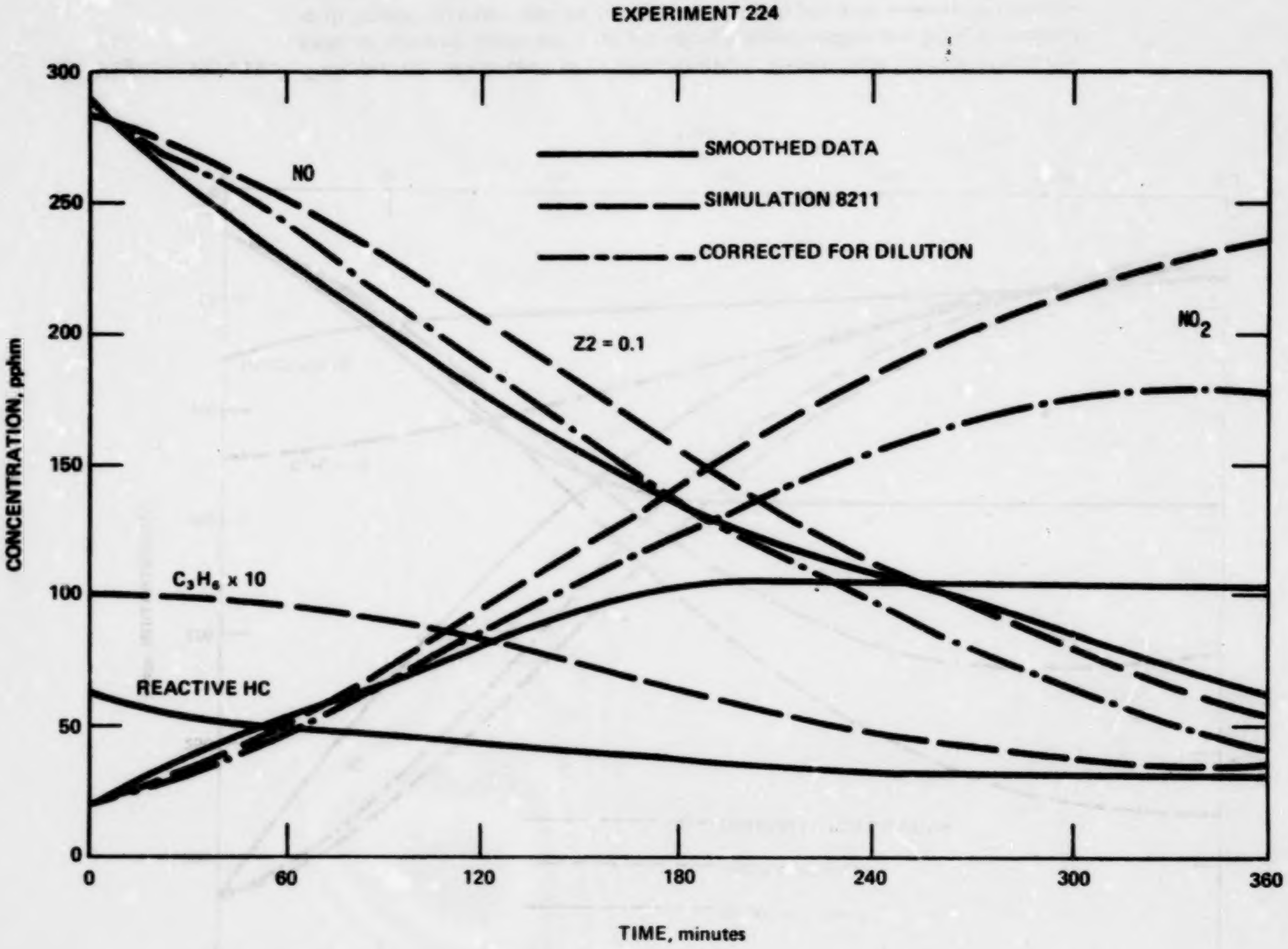

Figure III.20. Time profiles of contaminant concentrations, Experiment 224 (diluted auto exhaust system). Simulation results using revised mechanism M2b, compared with smoothed experimental profiles. Smoothed profiles: —— ; simulation results: — —.

delayed. Apparently, for the most accurate simulation of the first half of experiment 222, a value of about 0.2 for Z2 would be appropriate; however, this would result in increased over-estimation of nitrogen dioxide and under-estimation of ozone at the six-hour mark.

Figure III-18 shows the simulation of experiment 233, using Z2 = 0. As in 222, the simulation predicts faster progress than is observed in the early part of the irradiation, but slower increase of ozone and decrease of NO_2 than is observed in the latter half. The ozone predicted, however, is within 0.25 ppm of the observed value over the last 200 minutes of the test.

Simulations for the auto exhaust experiments in which ozone was negligible are shown in Figures III-19 and III-20. For optimum results under these circumstances, the rate factor for the consumption of dummy hydrocarbons was reduced to half its previous value, and Z2 was taken at 0.1. Figures III-19 and III-20 show, beside the computed simulation curves, other curves for NO and NO_2 corrected by hand calculation to account for dilution at the rate reported for the chamber. Both corrected and uncorrected curves give good approximations to the experimental results in the first part of the test, but the estimated nitrogen dioxide after six hours is higher than that observed.

D. SIMULATION OF TOLUENE-CONTAINING SYSTEMS

The chemical dynamics module of REM is designed for application to photo-oxidation in mixtures containing olefins as the principal reactive hydrocarbon component. However, the contract required us to use it to simulate systems which contained no olefins (the only hydrocarbons present being toluene or toluene and n-butane).

For this purpose we postulated the (chemically absurd) assumption that toluene consists of a mixture of propylene and dummy hydrocarbons, such that the total concentration of these species is the same as the specified total concentration of hydrocarbons in the system to be simulated.

1. The Toluene-Oxides of Nitrogen System

Table III-6 presents salient features of the results of simulations for the toluene-oxides of nitrogen system, compared with the experimental observations. Listed are initial concentrations for each experiment, postulated initial values for the simulation, and both predicted and observed values for NO_2, NO and O_3 at 360 minutes, as well as predicted and observed values of the maximum concentration of NO_2. (Experiments 309, 272 and 305 were not separately simulated because their initial conditions were nearly the same as those in experiments which were simulated, namely, experiments 250, 263 and 300, respectively).

An initial run done to simulate Experiment 250 was based on an assumed equivalence (for reaction rate purposes) of one mole of propylene to five of toluene. Results showed that the simulated course of reaction was substantially too rapid in this case; maximum NO_2 was reached in less than 200 minutes, compared to 300 in the experiment; and although NO_2 at 360 minutes was very close to that measured, the simulated oxidant was twelve times too large and the simulated nitric oxide was six times too small.

A second simulation run was therefore made, assuming one mole of propylene equivalent to twenty-five of toluene. This gave results for ozone and both oxides of nitrogen which were uniformly within 1/4 ppm of the experimental curves (smoothed from EPA data). This assumption was therefore adopted as standard for toluene photo-oxidation, and the remaining toluene experiments were simulated on this basis. Figure III-21 shows the effect of this assumption on nitrogen oxides in Experiment 250.

Rate factors used in these simulations were the same as those used for the auto exhaust experiments in which ozone was produced, experiments 222 and 231; that is, they were the same as those used in all the simulations with the exception of K31, which was taken as 7 $pphm^{-1}$ min^{-1} in these experiments.

Table III-6

Irradiation Chamber Experiments in the Toluene-Oxides of Nitrogen System

Experiment Number	Concentrations, pphm					Resulting Conc'ns (sim/obs)**			
	Initial			Postulated Initial		360 Minutes			Maximum
	NO_2	NO	C_7H_8	C_3H_6	DUMHC	NO_2	NO	O_3	NO_2
250 (a)*	2	123	153	30	123	69/70	2/13	36/3	92/70
(b)				6	147	77/70	12/13	7/3	77/70
309	7	131	166			77/72	12/0	7/10	77/91
263	5	55	171	6.8	164	35/2	2/4	17/31	41/21
272	4	55	150			35/3	2/2	17/31	41/39
259	2	33	164	6.7	157	19/4	1/3	15/26	24/17
271	4	31	120	4.8	115	20/4	2/3	10/18	22/21
258	4	32	288	12.0	276	16/4	1/2	36/24	27/26
277	3	30	320	14.4	306	14/4	1/3	33/18	25/21
300	3	128	322	14.4	308	19/4	1/3	15/26	98/89
305	8	124	314			19/3	1/5	15/39	98/91

* Run 250 was simulated twice (see text). Simulation (b) is based on a propylene equivalence of 1 mole to 25 moles of toluene, as are all the other simulations tabulated, except Simulation (a), which was based on 1 to 5.

** Runs 309, 272 and 305 were not separately simulated; they are compared with simulations for 250, 263 and 300, respectively.

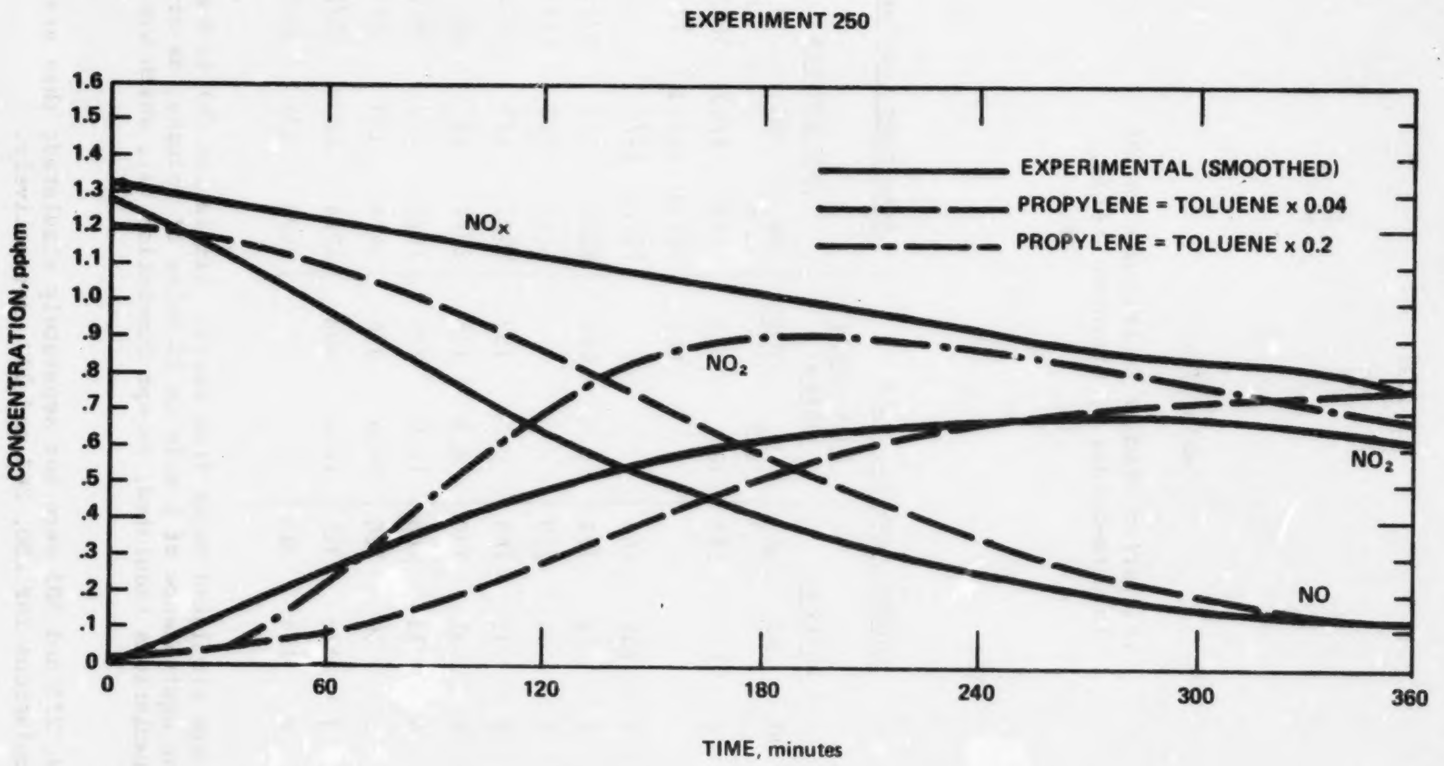

Figure III.21. Time profiles of contaminant concentrations, Experiment 250 (toluene and oxides of nitrogen system). Simulation results using revised mechanism M2c, for two choices of toluene-propylene equivalence ratio, compared with smoothed experimental profiles. Smoothed profiles: ——; simulation results; — —.

2. The Toluene-Butane-Oxides of Nitrogen System

Since the experimental data indicated that a mixture of toluene with n-butane was more reactive in the photo-oxidation system than was toluene alone, our chemical dynamics model required a representation of the additional component, n-butane, in terms of the surrogate hydrocarbons, propylene and DUMHC. For this purpose we postulated the new, chemically absurd assumption that n-butane consists of a mixture of propylene and dummy hydrocarbons, such that the total concentration of these species is the same as the specific total concentration of hydrocarbons in the system under study.

Since n-butane is known to be substantially less reactive than toluene, we assumed that one mole of propylene would be equivalent to a hundred moles of n-butane.

Table III-7 shows the comparison of the simulation results, calculated on this basis, against the experimental observations at 360 minutes. (Parameters of the simulation were the same as for toluene alone). Experiments 270 and 280 were not separately simulated, inasmuch as their initial concentrations closely resembled Experiments 253 and 257, respectively.

3. Discussion of Results with Toluene-Containing Systems

The accuracy of simulation represented by Tables III-6 and III-7, in the face of the rather elementary stage of development of the reaction mechanism used in our chemical dynamics module, is extraordinary. Predicted ozone values were within a factor of two of those observed (at 360 minutes) in fourteen cases out of sixteen. Predicted nitric oxide values were within 2 parts per hundred million of the observed in thirteen cases out of sixteen.

Although concentrations of nitrogen dioxide at 360 minutes were usually overestimated in the simulation, the maximum concentration of nitrogen dioxide during the run as predicted by the simulation was within a factor of two of that observed in every case, and was within a factor of 1.5 in fifteen cases out of sixteen.

Table III-7

Irradiation Chamber Experiments in the Toluene-Butane-Oxides of Nitrogen System

	Concentrations, pphm						Resulting Conc'ns (sim/obs)*			
Exp't No.	Initial				Postulated Initial		360 Minutes			Maximum
	NO_2	NO	C_7H_8	C_4H_{10}	C_3H_6	DUMHC	NO_2	NO	O_3	NO_2
251	11	111	160	302	9.4	453	48/36	1/3	51/44	94/89
260	10	110	142	273	8.4	407	46/42	1/3	49/32	84/66
253	11	50	143	342	9.2	454	24/5	1/2	46/55	47/54
270	3	57	163	278			24/2	1/3	46/62	47/43
257	7	27	129	297	8.1	439	14/13	1/1	34/52	25/28
280	3	30	165	305			14/4	1/1	34/40	25/24

* Runs 270 and 280 were not separately simulated; they are compared with simulations for 253 and 257, respectively.

It is interesting to note that these results, indicating a substantial predictive capability especially in the qualitative sense, were achieved with only a single set of rate factors and with uniform assumptions as to the reactivity of the hydrocarbons involved, and that the rate factors were substantially the same set that also served for simulation of the auto exhaust experiments and the propylene-ethane system. This degree of success, obtained in spite of strictures forbidding the application of advanced understanding of the chemical systems involved, must augur well for the improvement to be expected when such strictures are eventually lifted.

E. SIMULATION OF PHOTO-OXIDATION PRODUCTS IN THE IRRADIATION EXPERIMENTS

Data for the products of photo-oxidation were rather fragmentary, being confined to occasional determinations on formaldehyde, acetaldehyde, peroxyacetyl nitrate, and methyl nitrate. Observed concentrations of methyl nitrate were never larger than 0.01 ppm, so this product will not be further discussed. Table III-8 compares estimated with observed concentrations for the other compounds mentioned.

Observed concentrations of peroxyacetyl nitrate (PAN) were in some cases of the order of magnitude of 0.2 ppm, especially in experiments 325 and 329 of the propylene-ethane system, and 222 and 233 of the auto exhaust series. It may be noted that the higher concentrations of PAN seem to be well correlated with high levels of oxidant, as expected on chemical grounds. Simulated values of PAN ranged from 0.02 to 0.56 ppm, and were more often overestimated than underestimated.

Observed concentrations of the aldehydes ranged up to about 0.50 ppm for each. Simulated values ranged up to about 0.2 for formaldehyde and 0.4 for acetaldehyde. For both of these compounds, the estimates seemed predominantly lower than the observed values.

F. SUMMARY AND CONCLUSIONS

Tables III-2, III-5, III-6 and III-7 present the results of the simulations of the irradiation chamber experiments in terms of the comparison

Table III-8

Comparison of Estimated vs. Observed Concentrations for Formaldehyde, Acetaldehyde, and Peroxyacetyl Nitrate (after 6 hours irradiation)

Experiment		Concentrations, pphm (estimated/observed)		
		Formaldehyde	Acetaldehyde	P.A.N.
Propylene-ethane	329	10/40	22/1	23/11
	325	18/--	41/55	3/17
	318	19/20	30/27	9/0
	336*	19/33	30/31	9/1
	321	6/17	10/13	2/0
	324*	6/20	10/46	2/--
Auto exhaust	222	15/42	17/22	36/14
	233	17/50	20/18	56/19
	224	6/39	6/16	12/--
	231	4/20	4/11	6/0
Toluene-butane	251	7/--	6/34	14/10
	260	7/--	6/23	12/4
	253	5/11	7/32	7/8
	270*	5/--	7/24	7/4
	257	3/--	6/25	3/7
	280*	3/14	6/22	3/2

* Estimates for experiments 336, 324, 270, and 280 are from simulations for experiments 318, 321, 253 and 257, respectively.

of concentrations estimated with concentrations observed, using the best simulation achieved in each system. Table III-1 shows the extent of modification to the parameter set which was required to achieve this degree of simulation.

A review of these results points to the following conclusions:

1. Under most of the conditions represented by these experiments, the maximum levels of nitrogen dioxide and of ozone can be predicted within experimental error using the mechanism given here (M2), with correction for rate of dilution in the chamber (module M2c).

2. The principal deficiencies in this mechanism are indicated by serious overestimation, in certain circumstances, of the ozone concentration after six hours of irradiation, and simultaneous underestimation of the time required for nitrogen dioxide to reach a maximum and decline from it. This is seen especially when initial nitric oxide levels are very high.

3. The mechanism should be susceptible of marked improvement with relatively minor changes, by systematic exploration of the effects of plausible additional reactions.

Chapter IV

SIMULATION OF PHOTOCHEMICAL AIR POLLUTION EPISODES

A. INTRODUCTION

The most direct and demonstrative testing of the atmospheric simulation model, under the current contract, involved the use of weather data and contaminant data from six reasonably typical episodes of photochemical air pollution as observed in Los Angeles in the summer and fall of 1969. Data furnished by the Environmental Protection Agency for this purpose included hourly average values of wind direction, wind speed, temperature and relative humidity at each of twenty-five meteorological stations in the area of the Los Angeles Basin. Radiosonde measurements of the vertical temperature profile at the Los Angeles International Airport for each of the days chosen were obtained from the Los Angeles County Air Pollution Control District.

These data, together with information regarding the location and elevation of the various stations, were sufficient to permit the calculation of air parcel trajectories with associated temperature, humidity, and mixing depth, according to the principles and methods described in Chapter II. Since the objective of the evaluation was to simulate air quality at places where measurements existed, the locations of various air monitoring stations were taken as terminal points for trajectories and their starting points (as well as a series of points of the intervening locus) were estimated with the reverse trajectory routine (cf. Ch. II).

Initial values of the concentrations of contaminants in air parcels, at the starting points thus determined, were estimated by interpolation from data for the Los Angeles air monitoring network, also furnished by EPA. These data consisted of hourly average values for various contaminants, including carbon monoxide, oxides of nitrogen, oxidants, and sulfur dioxide, for a network of ten to twelve stations.

For estimating the concentrations of contaminants expected in the air parcels upon arrival at their specified terminal points, the amounts acquired while en route are needed. They are approximated by interpolation of emission rates from reference values, specified as a function of location by the emission inventory grid maps, and modified as a function of time of day in accord with an assumed curve of diurnal variation.

The atmospheric simulation model is especially designed for the estimation of chemically reactive contaminants and secondary contaminants which are products of chemical reactions. For such contaminants, ordinary air quality models (based on the assumption of Gaussian dispersion) are not adequate. The PES model, however, is equally applicable to reactive and non-reactive contaminants. Carbon monoxide concentrations seem to be little affected by atmospheric chemical reaction on the time scale involved in photochemical smog. It is useful, therefore, to evaluate the performance of the model in estimating carbon monoxide concentrations, so that the complications which can be introduced by deficiencies in the chemical reaction system can be avoided.

The discussion below, therefore, is addressed first to the simulation of carbon monoxide levels, after which the results for reactive contaminants and reaction products are evaluated. Pertinent data for each trajectory run are tabulated in Tables A-1 and A-2, Appendix A, and corresponding trajectories are shown on the maps in Figures A-1 through A-6.

B. CARBON MONOXIDE SIMULATION

To facilitate a broader evaluation of the reliability of the atmospheric simulation with respect to non-reactive contaminants, the numerical integration routine (DIFSUB) was applied for carbon monoxide as the sole contaminant, and the kinetics routine (DIFFUN) was modified with an option to bypass the chemistry.

The model was then run for six days specified by EPA: September 11, 29 and 30, October 29 and 30, and November 4. For each of four receptor locations (corresponding to the air monitoring stations for Downtown Los Angeles, Whittier, Azusa and Burbank), three six-hour trajectories were computed for each day; these trajectories were arranged to arrive at the stations at hours 0930, 1130 and 1330. Initial time for these trajectories was ordinarily 0700. Thus, travel times for the simulated air parcels before reaching the specified receptor locations were, respectively, 2.5, 4.5 and 6.5 hours.

Of the 72 trajectories thus planned, 67 were successfully completed. This included all trajectories to the Los Angeles and Whittier receptor locations, sixteen to Azusa, and thirteen to Burbank. Two of the scheduled trajectories to Azusa for November 4 could not be used because their points of origin were outside the limits of the simulated territory. Two trajectories to Burbank on September 11 and all three on November 4 failed in computation, apparently as a result of blanks in the data base. A set of three trajectories to the Pasadena receptor location for November 4 was computed and substituted for the Azusa trajectories of that date for purposes of evaluation, since Pasadena is the most northeasterly station other than Azusa.

A graphic comparison of the results of these calculations against hourly average values obtained from the air monitoring records is shown in Figures IV-1 to IV-6. For the period 0800 to 1400 PST each day, six hourly average values of carbon monoxide concentration were on record for each station. Estimated values for these same receptor points were available for hours 0930, 1130, and 1330; these are compared with the averages for hours beginning at 0900, 1100 and 1300 respectively. For hours beginning at 0800, 1000 and 1200, calculated

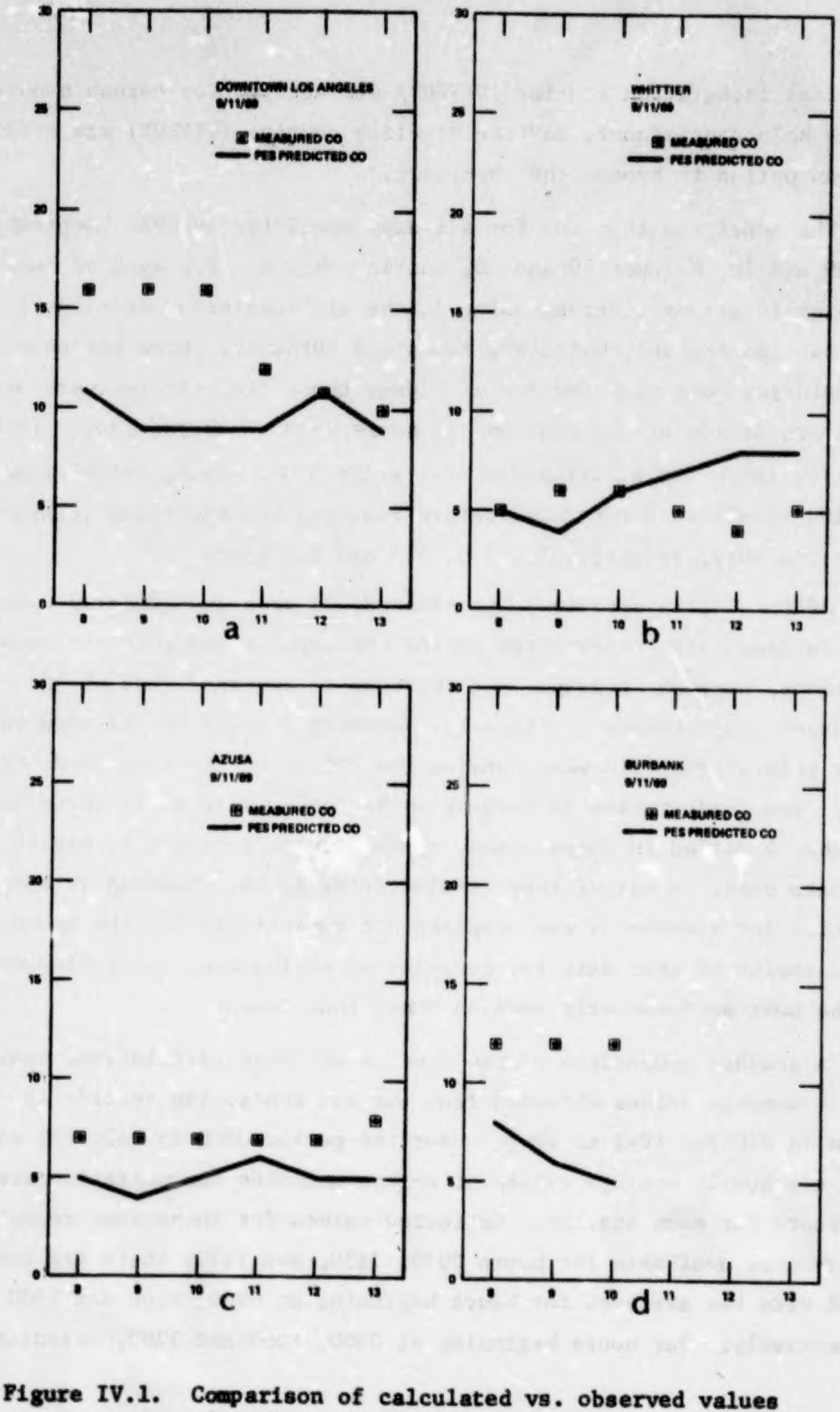

Figure IV.1. Comparison of calculated vs. observed values of carbon monoxide at air monitoring stations on September 11, 1969.

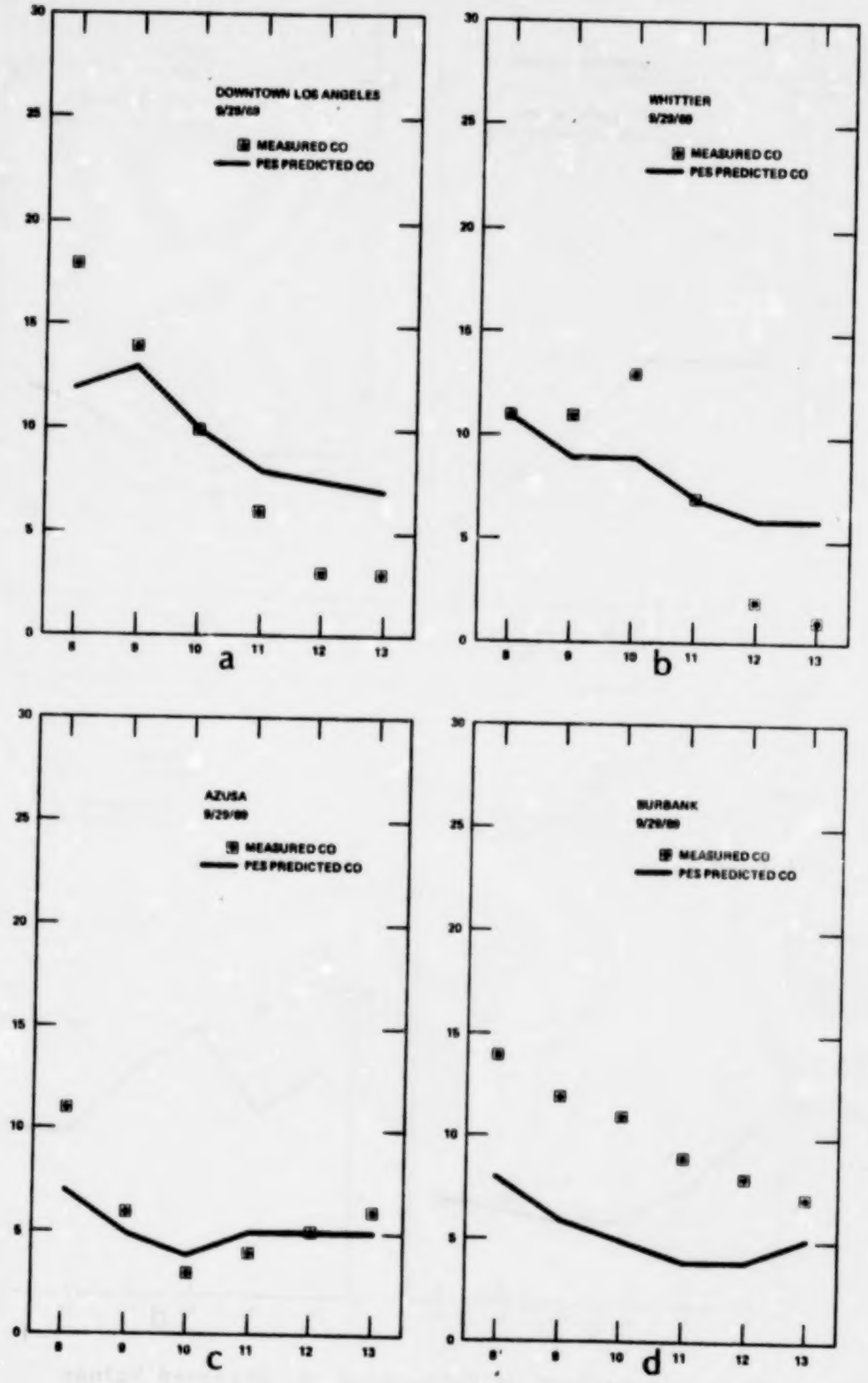

Figure IV.2. Comparison of Calculated vs. Observed Values of Carbon Monoxide at Air Monitoring Stations on September 29, 1969.

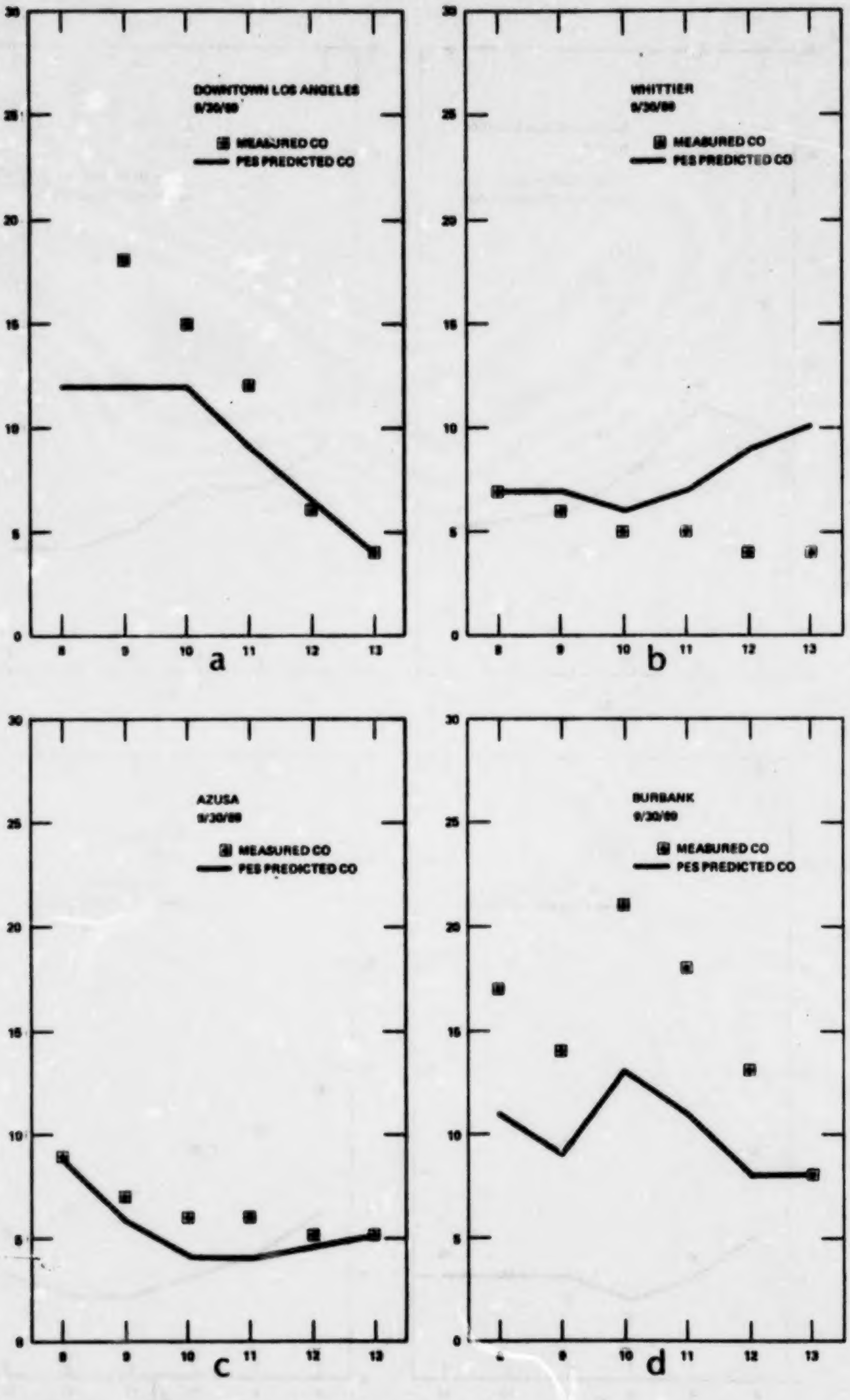

Figure IV.3. Comparison of Calculated vs. Observed Values of Carbon Monoxide at Air Monitoring Stations on September 30, 1969.

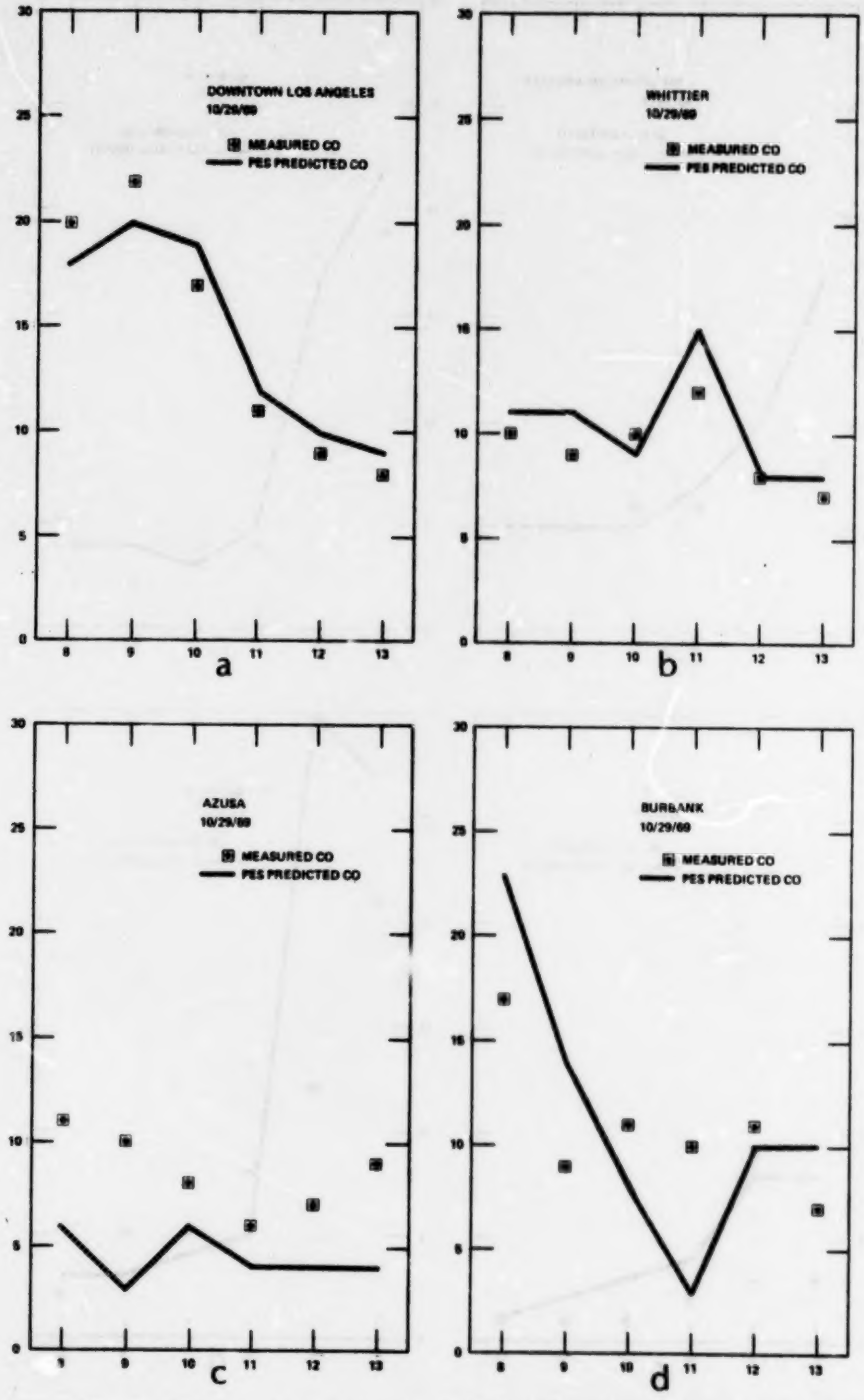

Figure IV.4. Comparison of Calculated vs. Observed Values of Carbon Monoxide at Air Monitoring Stations on October 29, 1969.

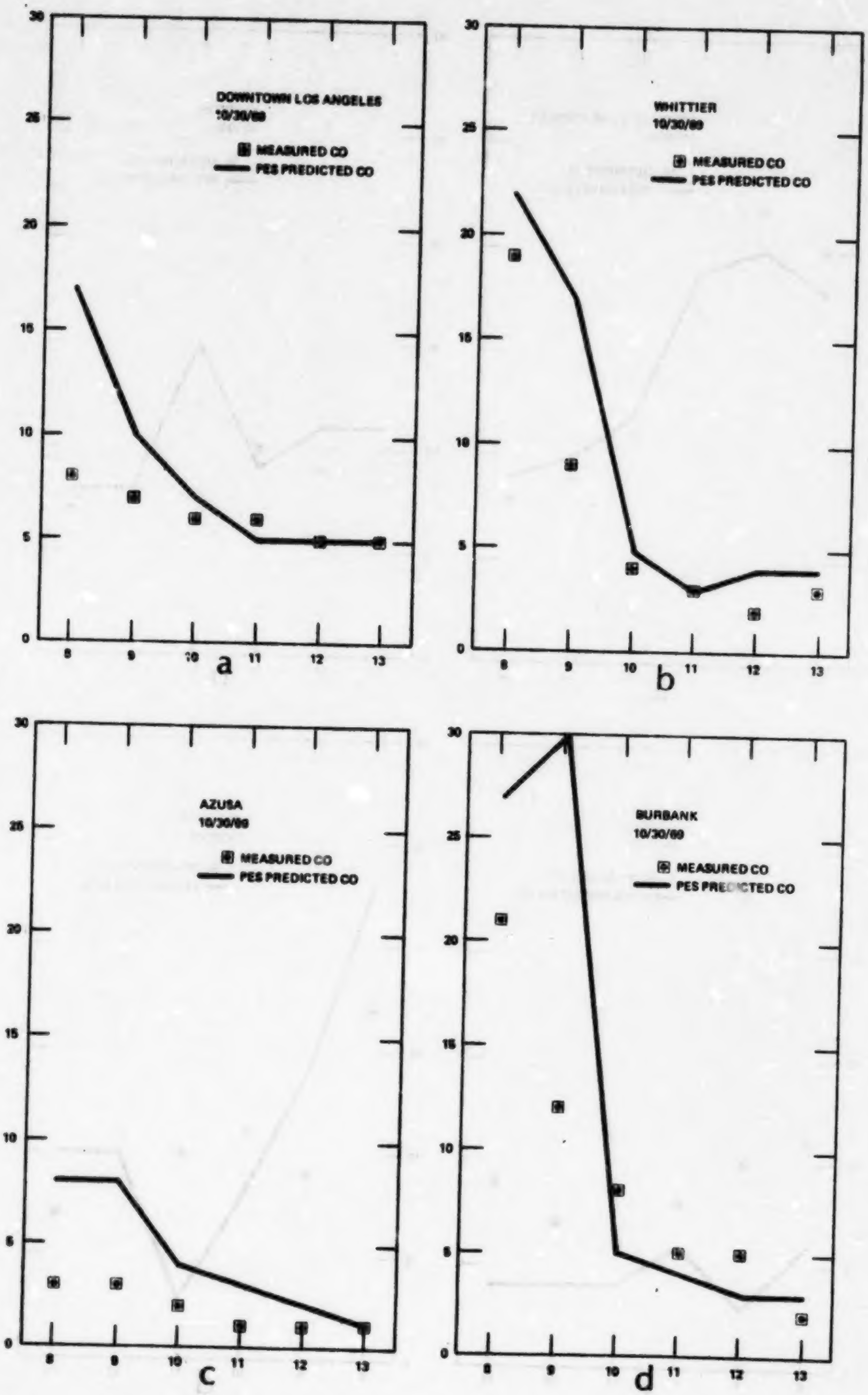

Figure IV.5. Comparison of Calculated vs. Observed Values of Carbon Monoxide at Air Monitoring Stations on October 30, 1969.

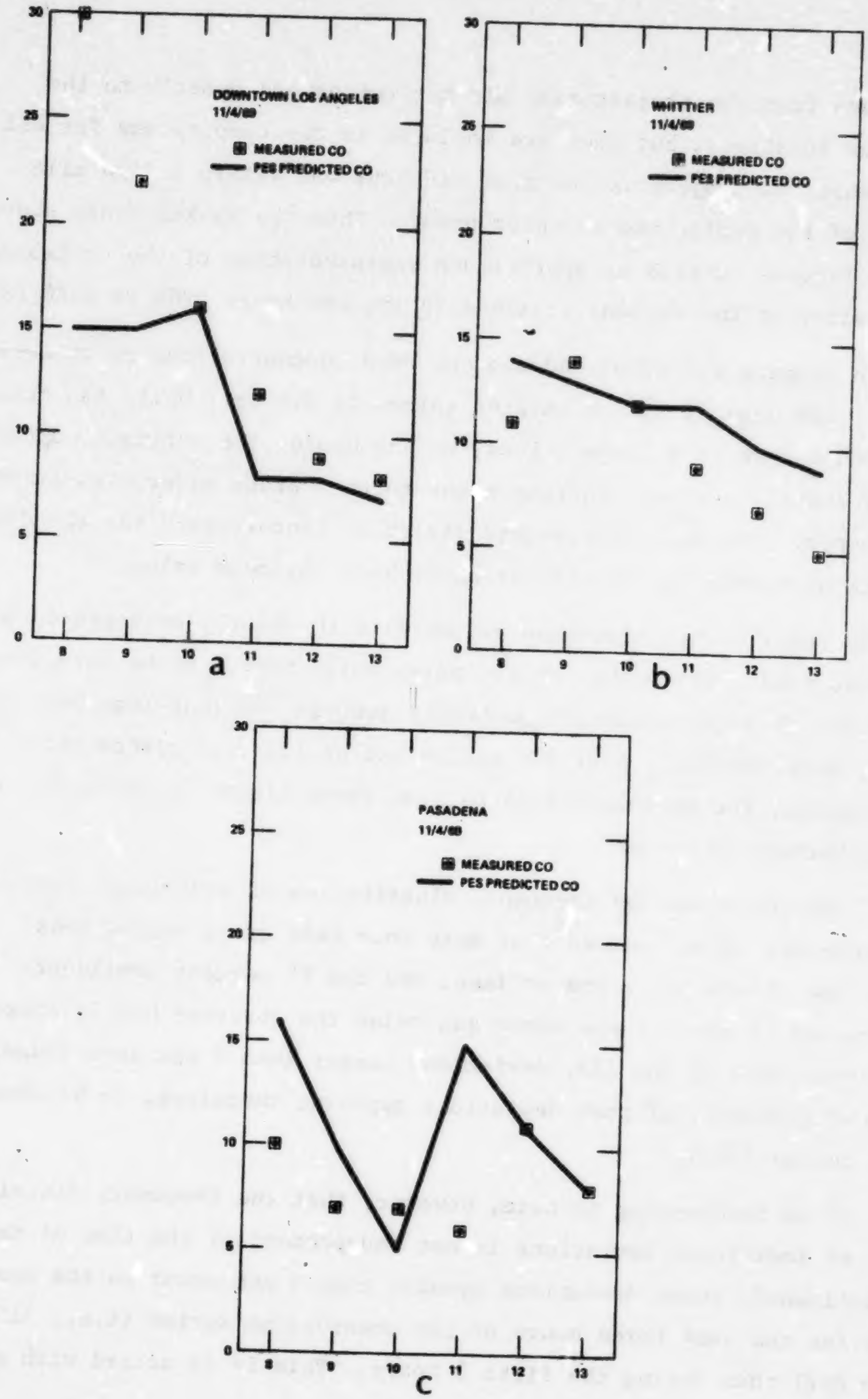

Figure IV.6. Comparison of Calculated vs. Observed Values of Carbon Monoxide at Air Monitoring Stations on November 4, 1969.

CO values from the trajectories did not correspond exactly to the receptor locations, but they are included in the comparisons for all cases when the trajectory locus at mid-hour was within a five mile radius of the designated receptor point. Thus the broken lines shown in the figures furnish an approximate representation of the estimated air quality at the various stations during the hours 0800 to 1400 PST.

To compare the simulated and observed concentrations on an overall basis: the mean of all calculated values is 8.6 ppm, while the mean of observed values is 9.2 ppm. Thus, on the whole, the estimates appear low by about 7 percent, corresponding to an average undercalculation of 0.6 ppm. The root mean square deviation (uncorrected for the difference of means) is 4.5 ppm, or about half the mean value.

To compare the calculated values with the hourly averages on a relative basis, the number of estimates which proved to be more than twice the observed value of the hourly average, or less than half that value, were counted. Over the entire set of 135 comparisons shown in the Figures, the estimates fell outside these limits in 19 cases, or approximately 15 percent.

Examination of the frequency distribution of individual deviations (by absolute value) showed that more than half are 2 ppm or less; about two thirds are 3 ppm or less, and the 95 percent confidence limits are at about 7 ppm above and below the observed hourly average. In three cases of the 135, deviations larger than 9 ppm were found; the rate of incidence of such deviations appears, therefore, to be less than one in forty.

It is interesting to note, however, that the frequency distribution of individual deviations is not independent of the time of day. Significantly fewer deviations greater than 3 ppm occur on the comparisons for the last three hours of the observation period (i.e., 1100 to 1400 PST) than during the first 3 hours. This is in accord with expectations (assuming that the probable error of the simulation estimates is generally related to the magnitude of the concentration being simulated), since carbon monoxide levels usually decline as the hours pass after 0900.

A separate calculation using only the estimates for 0930, 1130 and 1330, when the trajectory locations were very near the receptor locations, showed that the average undercalculation for these cases was less than 0.1 ppm. The root mean square deviation however, was reduced only slightly, to 4.4 ppm; therefore, the complete set of comparisons was retained for further evaluation and review.

From Figures IV-1 ff. it is evident that there were substantial differences in the levels of carbon monoxide at the various monitoring stations. In fact, the overall average of measured values for the six days ranged from 6.3 ppm to 12.3 ppm, as shown in Table IV-1, while the average of estimated values ranged from 5.8 to 10.5 ppm. The average estimated for the Burbank location was low by 2.1 ppm, (23%), while that for Whittier was high by 1.6 ppm (22%). The fraction outside limits of one half to twice the hourly average ranged from 4 of 36 (11%) for Los Angeles and Whittier to 5 of 27 (19%) for Burbank.

The root mean square deviation ranged from a low of 2.9 ppm (Whittier) to a high of 6.0 ppm (Burbank). It appeared to be more or less parallel to the mean observed concentrations, leading to a relatively uniform coefficient of variation, ranging from about 0.40 to 0.53.

Since it would be expected that the reliability of simulation might be different for various days, the data were examined also from this point of view with the results shown in Table IV-2. The carbon monoxide level averaged over all stations for each day ranged from 5.9 ppm (October 30) to 11.3 ppm (November 4), while the average of estimated values ranged from 6.8 ppm (September 11) to 11.3 ppm (November 4). Carbon monoxide levels were overestimated for all stations on October 30,

Table IV-1
Comparison of Estimated Mid-Hour Concentrations to Observed Hourly Average Concentrations for Carbon Monoxide, for Six Smog Days at Different Receptor Locations

	LA	Wh	Az[a]	Bu[b]	All
Estimated ave., ppm	10.5	8.9	5.6	9.2	8.6
Observed ave., ppm	12.3	7.3	6.3	11.3	9.2
Deviation, ave., ppm	-1.8	1.6	-0.5	-2.1	-0.6
Deviation, r.m.s., ppm	5.5	2.9	3.2	6.0	4.5
Deviation, % of obs.	52	40	51	53	4.9

[a] One trajectory for Pasadena included as a substitute for one Azusa trajectory, November 4.

[b] Only 0930 trajectory available for Burbank on September 11; none available November 4.

Table IV-2

Comparisons of Estimated Mid-Hour Concentrations to Observed Hourly Average Concentrations for Carbon Monoxide, for Four Receptor Locations on Different Smog Days

	9/11[a]	9/29	9/30	10/29	10/30	11/4[b]
Estimated ave., ppm	6.8	8.4	8.1	8.9	8.4	11.3
Observed ave., ppm	8.8	9.0	10.3	10.0	5.9	11.3
Deviation, ave., ppm	-2.0	-0.6	-2.2	-1.1	+2.5	0.0
Deviation, r.m.s., ppm	3.8	4.0	5.5	2.9	5.0	5.1
Deviation, % of obs.	43	44	53	29	87	45

[a] Only 0930 trajectory available for Burbank, 9/11.

[b] No trajectory available for Burbank; Pasadena substituted for Azusa trajectory, 11/4.

by an average 2.5 ppm (43%) for September 30, they were underestimated by an average 2.3 ppm (22%). The fraction of estimates outside a factor of two of the observed hourly average ranged from one in 21 or 5% (September 11) to 7 in 24 or 29% (September 29).

For various days, the root mean square deviation ranged from 2.9 ppm (October 29) to 5.5 ppm (September 30). The coefficient of variation was 0.55 or less for all days except October 30, on which it reached 0.87. (October 30 was the day having the lowest observed carbon monoxide levels.)

C. COMPLETE ATMOSPHERIC SIMULATIONS

In accordance with contract requirements, atmospheric simulation runs were performed for each of the six episode days specified by EPA, for four receptor locations. For each receptor a 390 minute trajectory was taken, arriving at the receptor at 1330 PST. In addition, for October 29 only, two additional trajectories to each receptor location were computed, with arrival times 0930 and 1130 PST and travel times 150 and 270 minutes, respectively.

Concentrations of nitrogen dioxide, nitric oxide, ozone and carbon monoxide were calculated following each simulated 30-minute period of travel for each of these thirty-two hypothetical air parcels. Initial concentrations were estimated for the initial locations of the parcels (at 0700 PST) by spatial interpolation of the concentrations observed at the various air monitoring stations. A minimum value of 50 meters was imposed, to override the calculated value of mixing depth wherever the calculated value might be less than that figure.

The calculated concentrations for mid-hour trajectory locations which were within a five-mile radius of the receptor location are tabluated, with the associated observed hourly average values for comparison in Table A-2 . Air monitoring stations chosen for these calculations were those at Downtown Los Angeles, Whittier, Azusa and Pomona, with the Pasadena location as an alternative to Azusa on September 11 and as an alternative to Pomona on September 29 and November 4.

1. Simulation by Trajectories for 1330 PST Arrival

For evaluating success in simulation of photochemical air pollution, the 1300 PST information is especially relevant, inasmuch as this is the modal hour for occurrence of maximum daily oxidant readings; it represents, in a sense, the most likely peak hour for this kind of smog.

Table IV-3 summarizes the information for four contaminants, obtained by comparing the estimated 1230 and 1330 PST concentrations against the hourly averages for 1200 to 1300 and 1300 to 1400 PST, respectively.

Data for carbon monoxide form essentially a subset of the more extensive data discussed in the previous section. The estimates used in this comparison were generated by the standard (DIFFUN) routine, with complete chemical kinetics included; however, inspection confirmed that the values predicted were substantially identical with those previously obtained, in which the chemistry was bypassed. The results for this subset, as shown in Table IV-3, confirm that the 1330 PST trajectories yield carbon monoxide estimates with characteristics reasonably similar to those of the whole set. It may be noted that the carbon monoxide concentrations as observed for these hours are, on the average, smaller than those found for the whole set (5.9 ppm, as compared with 9.2). At the same time, the predictions for the subset have a correspondingly reduced r.m.s. deviation (2.5 ppm vs. 5.5), and there is no bias toward either overestimation or underestimation evident in these data.

Nitrogen dioxide, on the other hand, is appreciably overestimated, as shown in the table; the average estimate is about 45% higher than the average value observed, and of 37 individual comparisons, 30 showed

Table IV-3

Comparison of Estimated Mid-Hour Concentrations to Observed Hourly Average Concentrations for Carbon Monoxide, Nitrogen Dioxide, Nitric Oxide and Ozone, for 1330 PST Trajectories[a]

	CO	NO_2	NO	O_3
Estimated ave., ppm	5.9	0.145	0.013	0.138
Observed ave., ppm	5.9	.099	0.014	.173
Deviation, ave., ppm	0.0	.046	0.001	-.035
Deviation, r.m.s., ppm	2.5	.084	0.008	.089
Deviation, % of obs.	42	85	57	51

[a] Estimates for 1230 PST are included, where within 5 miles of receptor station.

overestimates. The r.m.s. deviation, accordingly, was 85 percent of the mean observed value; however, if translated to equal means, the r.m.s. deviation would be reduced to .07 ppm or less.

For nitric oxide, again there was no appreciable bias in the estimation. However, most nitric oxide observations at these hours were so small (0.01 ppm or less) that the comparison really shows only that the estimated values were of the appropriate order of magnitude.

Ozone is somewhat underestimated by this program, in contrast to nitrogen dioxide. Thus the average estimate was 0.138 ppm, about 20 percent less than the average value observed. The r.m.s. deviation was about half as large as the observed average. Thus, it appears from these comparisons that ozone is predicted somewhat more accurately than nitrogen dioxide, but less accurately than carbon monoxide.

2. Extended Simulation of a Single Episode

The degree to which the model can simulate the progress of a single episode of photochemical smog, in relation to the changes of concentrations with time of day, was further investigated, using the episode of October 29 for the comparison.

Predicted mid-hour concentrations for carbon monoxide, nitrogen dioxide, nitric oxide, and ozone are graphically compared with the corresponding hourly averages as observed at the air monitoring stations (located at Los Angeles, Whittier, Azusa and Pomona) in Figures IV-7 to IV-10. (Data for comparison of oxides of nitrogen for Downtown Los Angeles were incomplete; the only values available were for 0800 to 0900 PST: nitrogen dioxide 20 pphm and nitric oxide 24 pphm.)

A review of these Figures confirms that the model yields an appropriate indication of the general trend of contaminant concentration with time; for both carbon monoxide and ozone, for all four receptor locations. For nitrogen dioxide, the trend indicated by the model is similar to that observed for Whittier, but rather dissimilar for Azusa

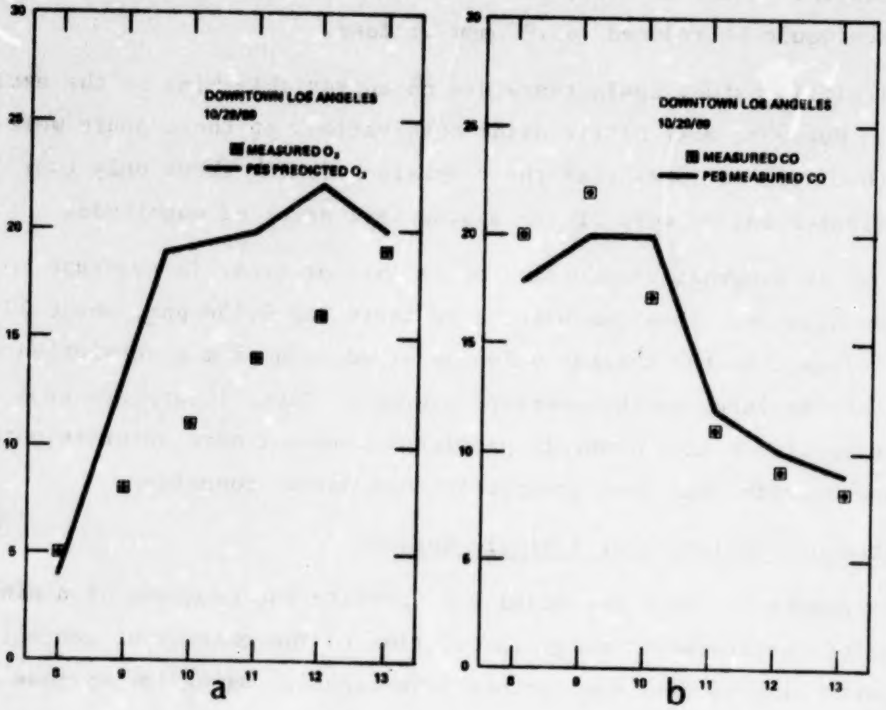

Figure IV.7. **Comparison of Calculated vs. Observed Values of Total Oxidant and Carbon Monoxide at Downtown Los Angeles on October 29, 1969.**

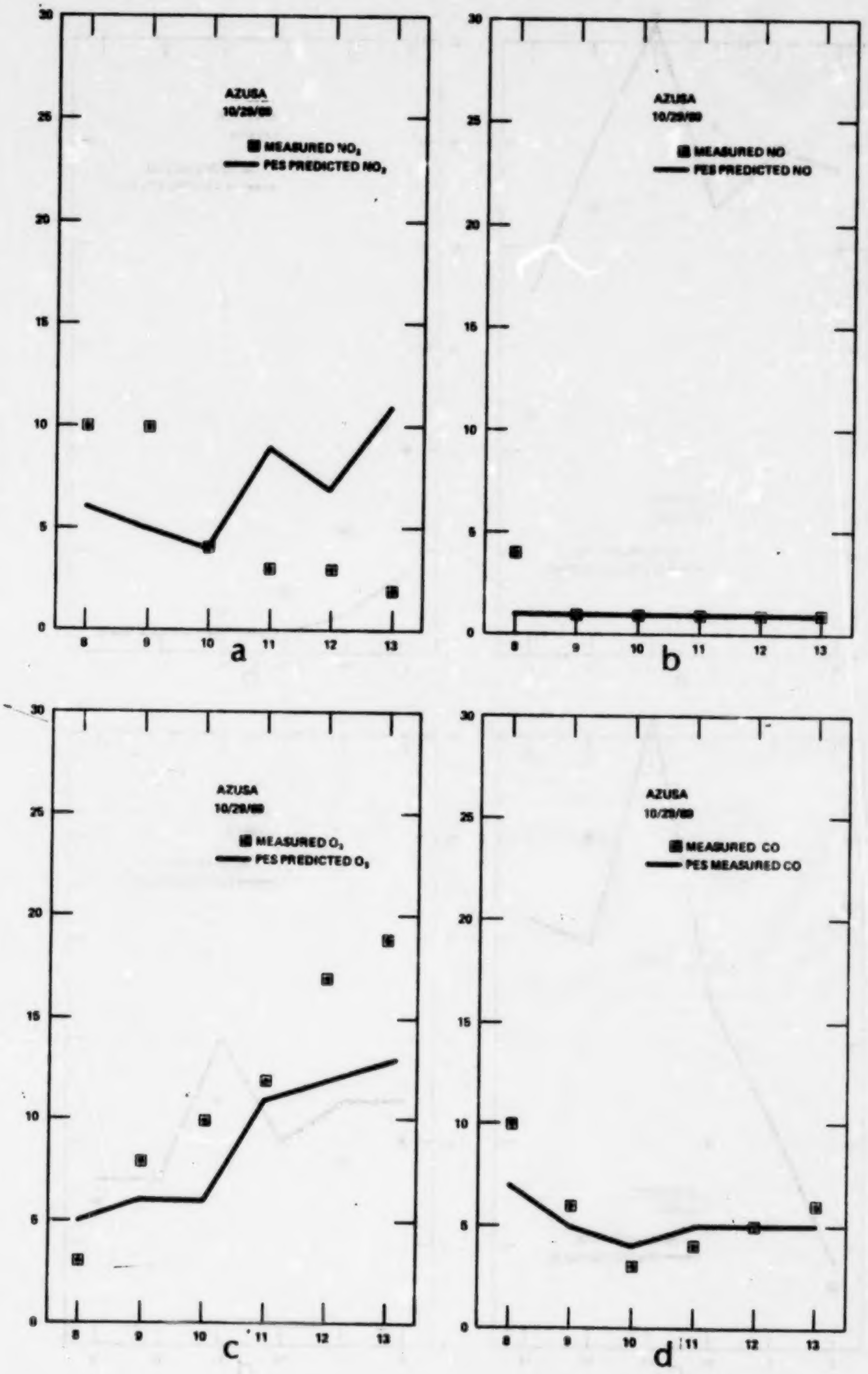

Figure IV.8. Comparison of Calculated vs. Observed Values of Nitrogen Dioxide, Nitric Oxide, Total Oxidant and Carbon Monoxide at Azusa on October 29, 1969.

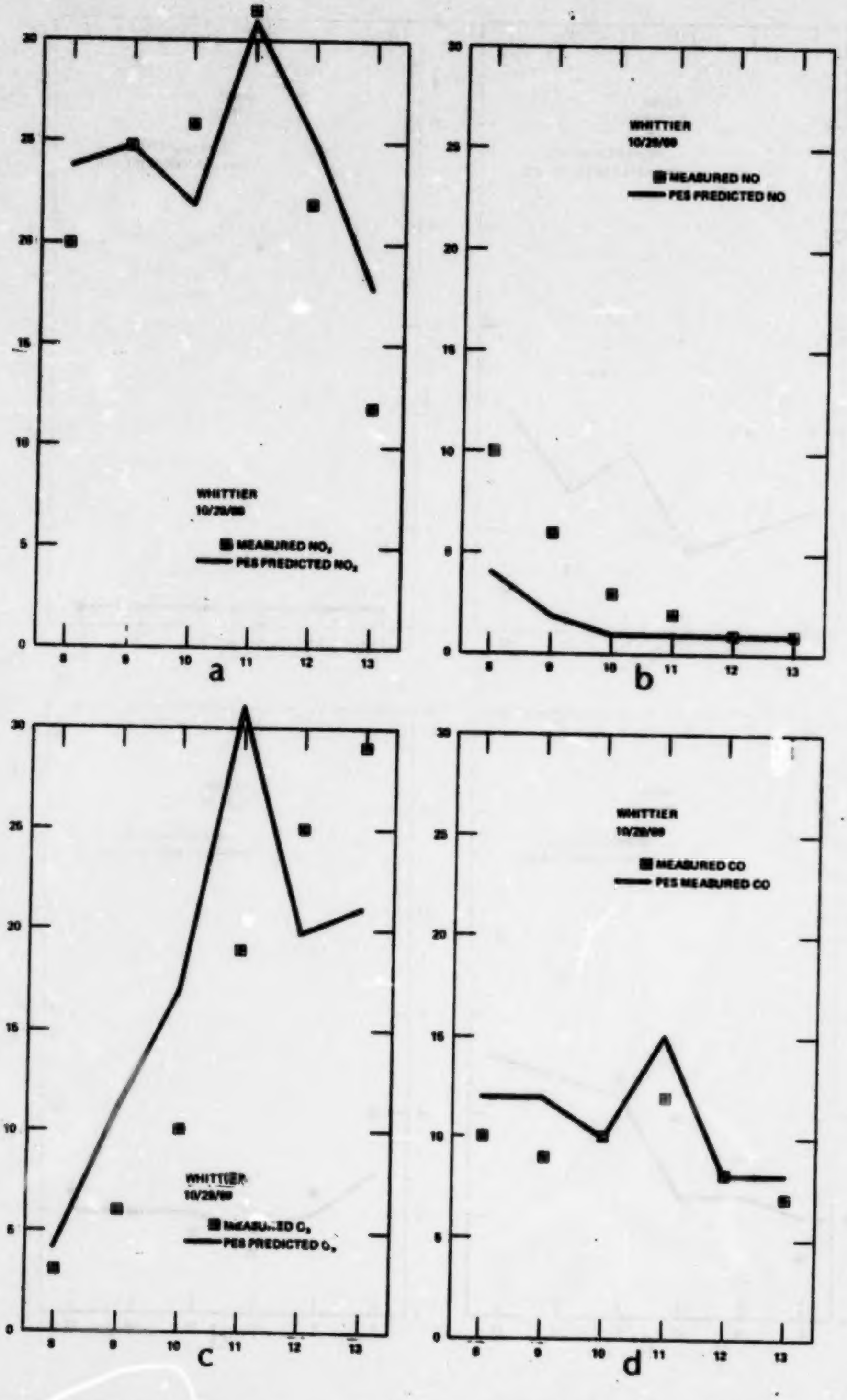

Figure IV.9. Comparison of Calculated vs. Observed Values of Nitrogen Dioxide, Nitric Oxide, Total Oxidant and Carbon Monoxide at Whittier on October 29, 1969.

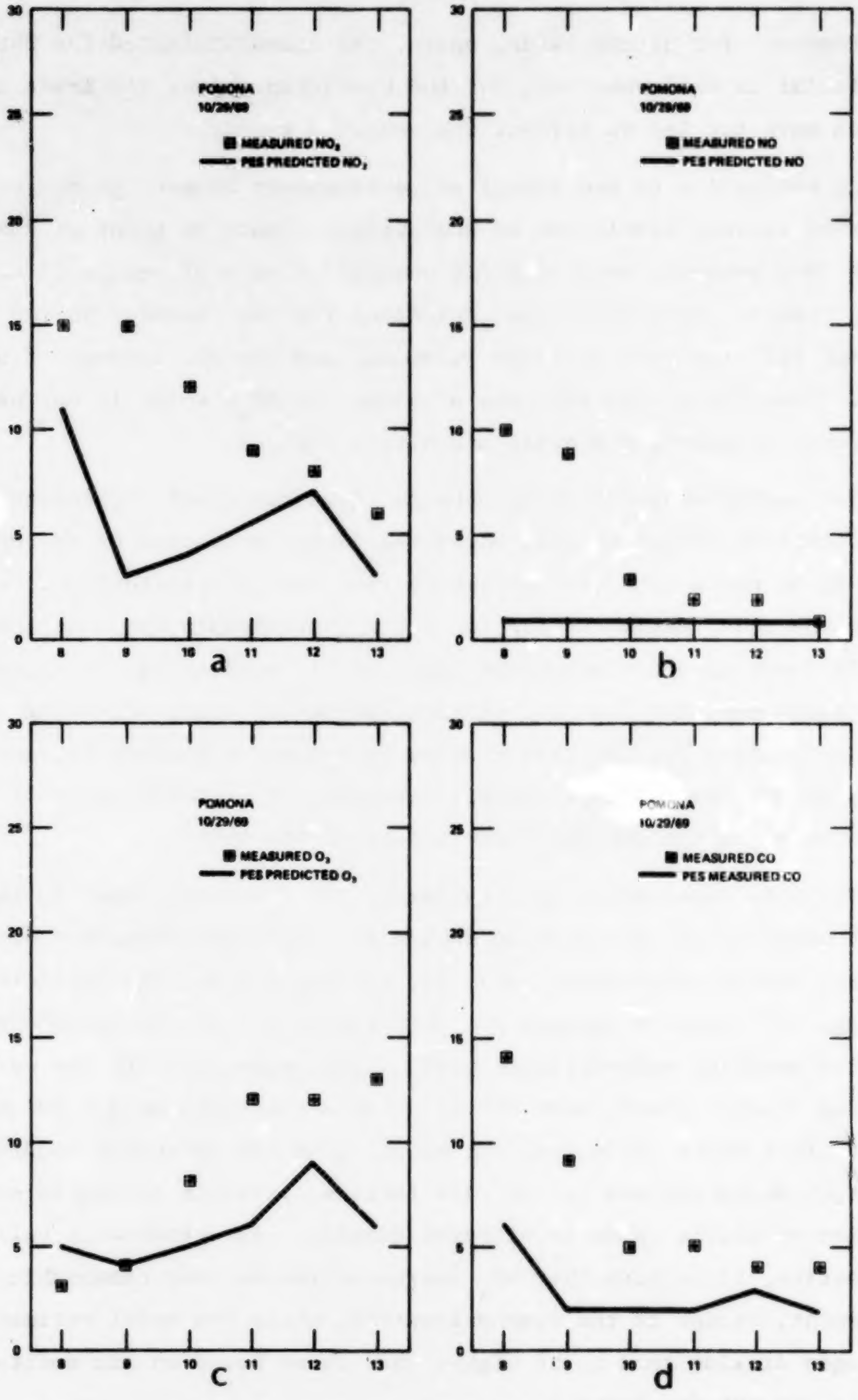

Figure IV.10. Comparison of Calculated vs. Observed Values of Nitrogen Dioxide, Nitric Oxide, Total Oxidant and Carbon Monoxide at Pomona on October 29, 1969.

and Pomona. For nitric oxide, again, the trend indicated for Whittier is similar to that observed, but the predicted values for Azusa and Pomona were too low to reflect the observed trends.

An evaluation of the quantitative agreement between predicted and observed episode levels can be appropriately made in terms of dosage. Table IV-4 presents predicted and observed values of dosage (i.e., integrated concentration times duration) for the six-hour period 0800 to 1400 PST, for each receptor location, and for the average of all four. (The Table also includes a column for NO_x, which is defined as the total of nitrogen dioxide and nitric oxide.)

For carbon monoxide there appears to be reasonable agreement for all locations except Pomona, where the dosage estimated by the model is only 42 percent of that estimated from the air monitoring record. Since the model estimates for the other contaminants are also substantially lower than the estimates based on air monitoring, it appears that there may have been a systematic source of error affecting contaminant values for the trajectories to Pomona on October 29, such as, e.g., an underestimate of traffic emissions or overestimation of ground temperature in the extreme eastern part of the region.

The only other striking discrepancy found in Table IV-4 is the low model estimate of nitric oxide dosage for Whittier. Together with the underestimated single-hour value for Los Angeles and the 3-station average of 7 pphm-hr against 20, this suggests a systematic tendency for the model to underestimate nitric oxide, especially in the earlier morning traffic hours, when nitric oxide concentrations are relatively high. This might imply that the model, with its currently incorporated reaction mechanism and set of rate factors, predicts too rapid conversion of nitric oxide to nitrogen dioxide. In accord with this suggestion, it is seen that NO_x dosage estimates show reasonable agreement, except at the Pomona location, while the model estimates for nitrogen dioxide tend to be higher than those based on air monitoring (again, except for Pomona).

Table IV-4

Comparison of Dosage of Various Contaminants as Estimated from Simulation Model to Dosage Estimated from Air Monitoring Data, Four Locations, Six Hours on October 29, 1969

	CO	NO_2	NO	NO_x	O_3
Station	ppm-hr	pphm-hr	pphm-hr	pphm-hr	pphm-hr
Los Angeles	89/87	(42/20)[a]	(8/24)[a]	(50/44)[a]	98/72
Whittier	67/56	145/137	10/23	155/160	104/92
Azusa	31/34	42/32	6/9	48/41	53/68
Pomona	17/41	31/66	6/27	37/93	35/52
Average	51/55	73/78	7/20	80/98	73/71

[a] These values for the Los Angeles location represent only the hour 0800-0900 PST.

Ozone dosages as estimated from the model calculations are in reasonable agreement with those from air monitoring data for all four locations. They range from about 35 percent higher (at Los Angeles) to about 32 percent lower (at Pomona). This suggests that whatever inaccuracies exist in the estimation of nitrogen dioxide and nitric oxide in the model, these inaccuracies are not reflected proportionally in the prediction of oxidant (ozone) levels.

3. General Accuracy of Atmospheric Simulations

Figures IV-11, IV-12 and IV-13 present scatterplots for the comparison of calculated and observed levels for carbon monoxide, nitrogen dioxide and ozone (or oxidant) respectively, combining data from all the atmospheric simulations discussed above.

a. Carbon Monoxide

With respect to carbon monoxide, the relation of calculated values to observed hourly averages is not much different from the relation found from comparisons with 67 trajectories in which only carbon monoxide was estimated, as discussed in Section B, above. In this more restricted set of data, the average observed carbon monoxide level was 7.2 ppm, while the average estimated was 7.0 ppm, for an average underestimate of 3 percent.

Figure IV-11 shows that, of sixty-one data pairs, only ten (or 16 percent) gave ratios (calculated/observed) greater than 2 or less than 0.5. It is interesting to note, also, that eight of these were attributable to the Pomona location, which yielded anomalously low estimates for all contaminants (v.s., Section C). Thirty-seven, or sixty percent of the sixty-one data pairs, showed deviations of 2 ppm or less.

The correlation coefficient between calculated and observed values is 0.82, accounting for nearly 70 percent of the variance in these

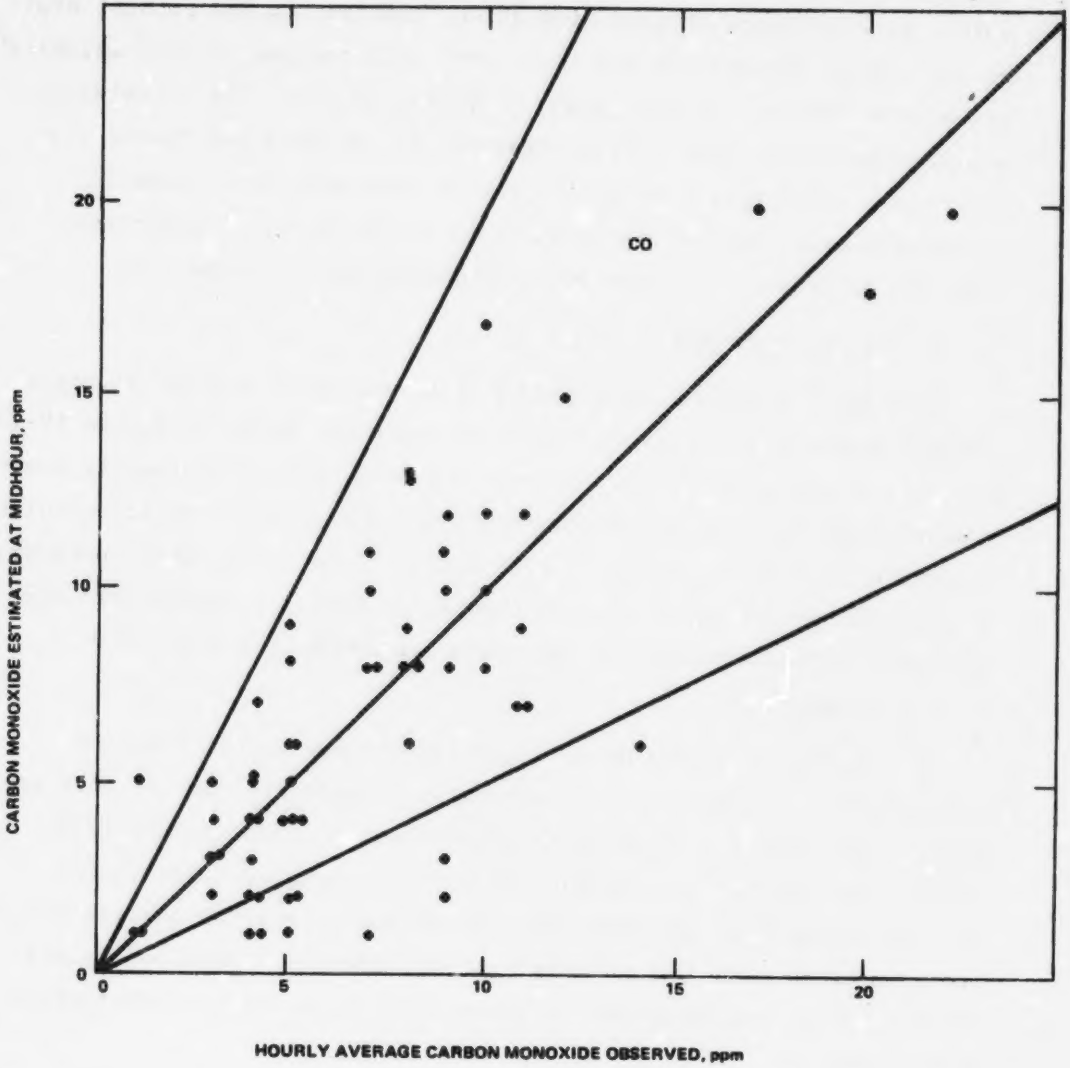

Figure IV.11. Scatter Plot of Calculated vs. Observed Carbon Monoxide for the Atmospheric Simulations.

data sets, and corresponding to a value of 11 for Student's t. These values give evidence of good simulation, considering the present state of the art of air quality modeling, even with the use of well established procedures such as Gaussian plume diffusion models. The correlation would certainly be even further improved if the data for Pomona trajectories, which appear to be subject to some sort of systematic underestimation, were to be adjusted by an appropriate correction; however, no attempt has been made to develop such a correction.

b. Nitrogen Dioxide

Data for a total of 56 comparisons of estimated midhour nitrogen dioxide levels with observed hourly averages are shown in Figure IV-12. For nitrogen dioxide, the scatter of the data pairs is evidently somewhat greater than for carbon monoxide, and the coefficient of correlation is smaller: 0.66, as compared with 0.82. (This coefficient, however, corresponds to a t-value of more than 6, so that its statistical significance is unquestionable; the criterion value of t for $p = 0.1\%$ is only about 3.5).

The average estimate of nitrogen dioxide was higher than the corresponding average of observations by 25 percent; this is substantially less than the 45 percent overestimation found for the 1330 trajectories only (v.s., Section C-1). This apparent improvement results partly from the fact that the estimates for the earlier hours are relatively more accurate, and partly from the inclusion of data for the Pomona trajectories, in which there were several substantial underestimates.

In Figure IV-12, the broken lines indicate upper and lower criterion levels such that points falling between them have ratios of estimated to observed levels between 0.5 and 2, or have differences of 5 pphm or less (a reasonable allowance for experimental error for this contaminant). Six points fall below the lower criterion line, all of these corresponding to Pomona trajectory estimates. Eleven points

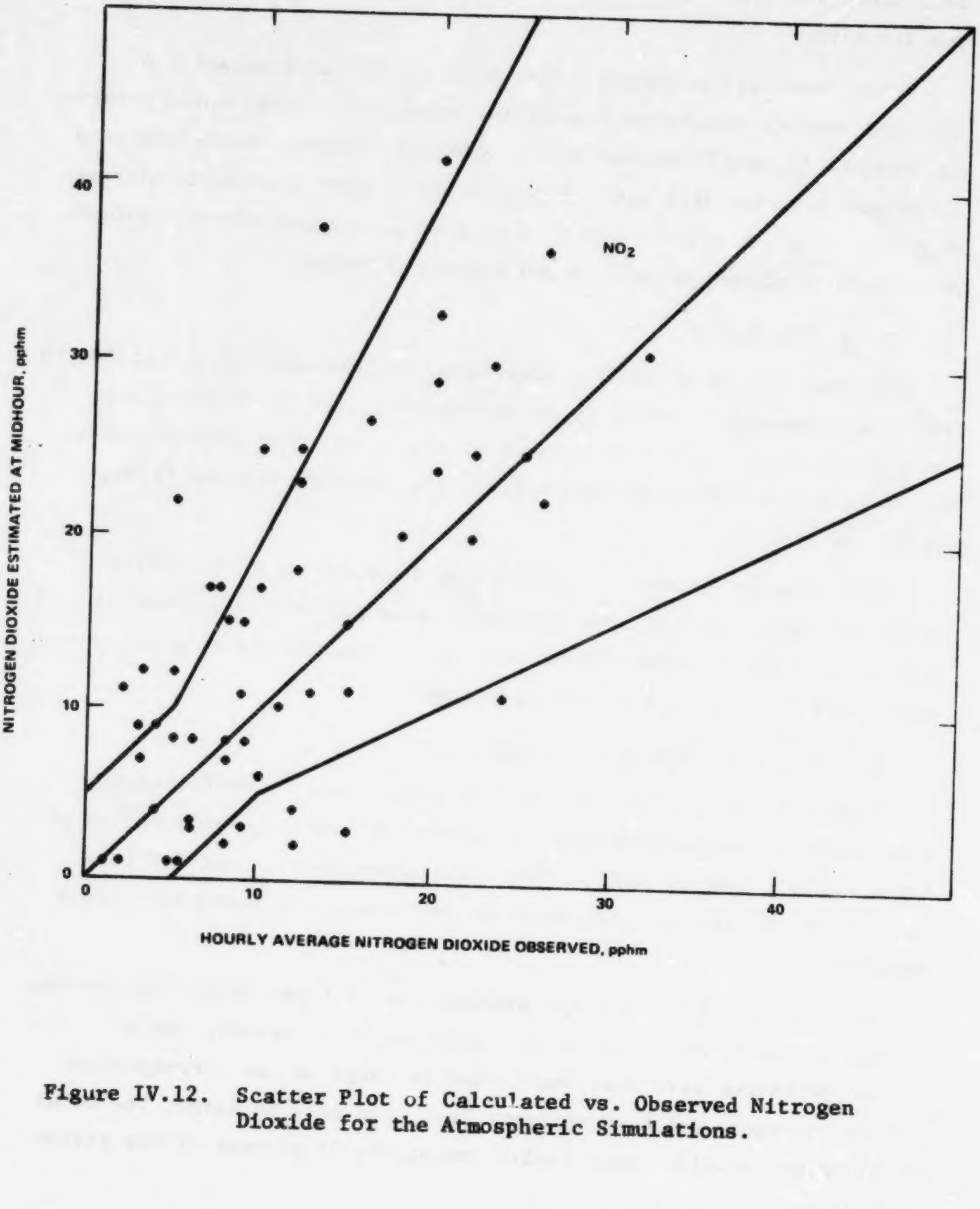

Figure IV.12. Scatter Plot of Calculated vs. Observed Nitrogen Dioxide for the Atmospheric Simulations.

fall above the upper criterion line, and these are not confined to any one location.

These observations suggest that accuracy in the simulation of nitrogen dioxide concentrations by the atmospheric model would perhaps be improved by modifications in the chemical dynamics module designed to reduce the simulated rate of conversion of nitric oxide to nitrogen dioxide, or to increase the simulated rate of consumption of nitrogen dioxide to produce nitric acid and organic nitrates.

c. Nitric Oxide

Observed levels of nitric oxide were, for the most part, too low to be of any consequence relative to air quality. Of 56 observations, only five were greater than 5 pphm; of these, all were underestimated by the model calculations (comparisons are shown in Figures IV-8b, IV-9b and IV-10b).

This relation between estimated and observed values for nitric oxide is consistent with the hypothesis that the chemical dynamics module, as used in these simulations, overestimates the rate of conversion of nitric oxide to nitrogen dioxide.

d. Ozone (vs. Measured Oxidant)

Figure IV-13 presents data for 61 comparisons of estimated mid-hour ozone concentrations with corresponding hourly average values of total oxidant concentration. The correlation coefficient for this collection of data is 0.83, which is very near that found for carbon monoxide,

The average observed total oxidant was 14.1 ppm, while the average of the estimated ozone values was 11.7, about 17 percent smaller. Six of the estimates were more than twice as large as the corresponding hourly averages, while eleven were less than half as large; the total of 17 points outside these limits amounts to 28 percent of the entire collection.

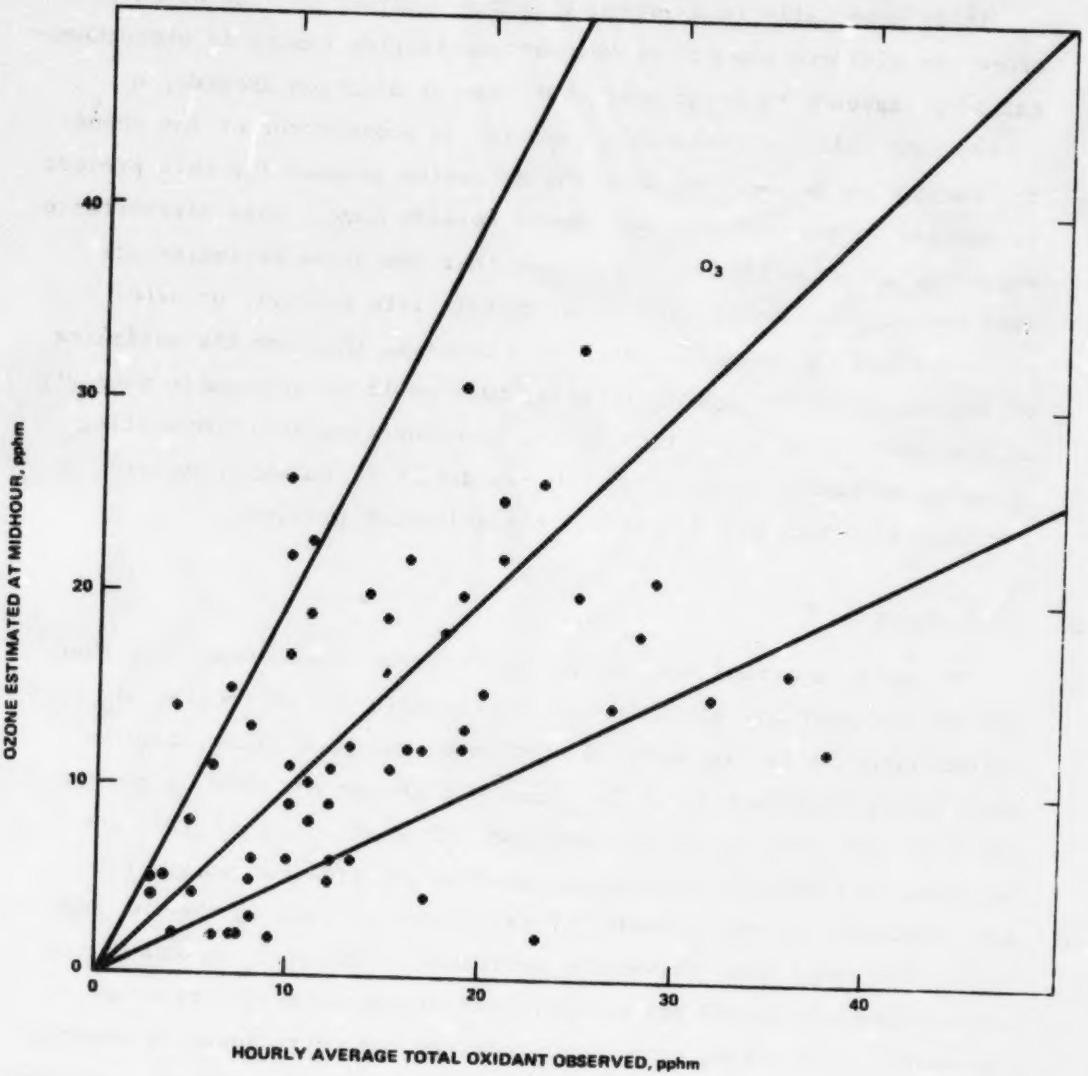

Figure IV.13. Scatter Plot of Calculated vs. Observed Total Oxidant for the Atmospheric Simulations

It is especially interesting that the accuracy of simulation of ozone, an ultimate product of the photo-oxidation system in photochemical smog, appears to be greater than that of nitrogen dioxide, a contaminant which is reasonably regarded as a precursor of the ozone. At least, such is the case when the mechanism assumed for this project is applied to the data for the chosen episode days. This circumstance suggests, although it does not prove, that the ozone estimates are less sensitive to uncertainties in certain rate factors, or other parameters of the chemical reaction mechanism, than are the estimates of the oxides of nitrogen. If true, this would be a valuable property of the atmospheric simulation model, in connection with forecasting of ozone emergency levels, or with evaluation of emission control strategy for abatement of oxidant air pollution problems.

D. CONCLUSIONS

The most important conclusion justified by these results is that REM can successfully simulate observed behavior of photochemical contaminants in the vicinity of stationary receptor sites, despite the Lagrangian structure of the model. Although the same conclusion has been indicated by earlier studies, the evaluation reported here has been considerably more extensive than the previous work. For data representing six episodes of photochemical smog in the Los Angeles Basin, the model gave reasonable estimates of the major contaminants over a six-hour period for each of four widely separated receptor locations. Comparison with hourly average concentrations, as recorded at air monitoring stations of the Los Angeles County network, confirmed the magnitude of the concentrations calculated as instantaneous mid-hour values, using the model.

Nevertheless, the evaluation indicated that agreement between the model estimates and the air monitoring observations might, in certain particulars, be improved by further attention to details of the postulated distribution of contaminant emissions, by the incorporation of more complete information regarding topography and the variation of vertical temperature profiles; and by optimization of the chemical reaction mechanism, and the associated rate parameters, to be incorporated in the chemical dynamics module of REM.

More detailed, specific conclusions are the following:

1. Simulation of carbon monoxide concentrations in the atmosphere by REM is no less accurate, on the whole, than by existing air quality models which do not account for effects of chemical reactions. For most of the conditions simulated by REM with the complete chemistry module, carbon monoxide estimates showed a bias of less than 20 percent. On a total of 61 direct comparisons, the correlation coefficient was 0.82. On a total of 150 comparisons with estimates obtained by REM with a special option for carbon monoxide alone, the correlation coefficient was 0.70, and biases for various days and receptor locations were mainly less than 25 percent. The average bias for the whole body of data was a slight underestimation.

2. Simulation of ozone levels in the atmosphere gives values which are eminently reasonable when compared with the recorded data for total oxidant concentration. Relative to recorded total oxidant, the ozone values were, on the average, low by less than 20 percent. On 61 direct comparisons, the coefficient of correlation was 0.82.

3. Simulation of nitrogen dioxide levels was adequate to reflect major trends in the observed concentrations as a function of time, but was somewhat less accurate than simulation of carbon monoxide and ozone. Estimates of nitrogen dioxide were high by 25 percent on the average, with the degree of overestimation apparently increasing for the later hours. The coefficient of correlation between mid-hour estimates and recorded hourly averages, for 56 comparisons, was 0.66.

4. Observed concentrations of nitric oxide during the period of interest in these smog episodes were, for the most part, too low for

useful simulation. Of five observations which were larger than 0.05 ppm, the corresponding model estimates were all less than 0.05 ppm. It therefore appears likely that the model, with its presently incorporated chemistry, tends to underestimate nitric oxide by overestimating the rate of its oxidation to nitrogen dioxide.

APPENDIX

RESULTS OF REM SIMULATIONS

Table A-1

Carbon Monoxide Simulations

Trajectory Run Number	Termination Point	Start Time	Starting Value (PPM)	End Time	Other Points Within 5 Mi. of Station	Calculated/ Observed (PPM)
September 11, 1969						
101	Downtown L.A.	0700	12		0830	11/16
				0930		9/16
					1030	7/16
102	Downtown L.A.	0700	9		1030	9/16
				1130		9/12
					1230	11/11
103	Downtown L.A.	0930	9		1230	9/11
				1330		9/10
104	Whittier	0700	5		0830	5/5
				0930		4/6
					1030	4/6
105	Whittier	0700	7		1030	6/6
				1130		7/5
106	Whittier	0700	8		1230	8/4
				1330		8/5*
107	Azusa	0700	8		0830	5/7*
				0930		4/7
					1030	3/7
108	Azusa	0700	10		1030	5/7
				1130		6/7
					1230	4/7
109	Azusa	0700	5		1230	5/7
				1330		5/8
110	Burbank	0700	12		0830	8/12
				0930		6/12
					1030	5/12

---

*Missing data; value interpolated from other hourly observations at monitoring station.

Table A-1

Carbon Monoxide Simulations (cont'd)

Trajectory Run Number	Termination Point	Start Time	Starting Value (PPM)	End Time	Other Points Within 5 Mi. of Station	Calculated/ Observed (PPM)
			September 29, 1969			
111	Downtown L.A.	0700	15		0830	12/18
				0930		13/14*
					1030	10/10*
112	Downtown L.A.	0700	15		1030	9/10*
				1130		8/6
113	Downtown L.A.	0930	14	1330		7/3
114	Whittier	0700	14		0830	11/11
				0930		9/11
					1030	6/13
115	Whittier	0700	15		1030	9/13
				1130		7/7*
116	Whittier	0700	9		1230	6/2
				1330		6/1
117	Azusa	0700	10		0830	6/11
				0930		3/10
					1030	2/8
118	Azusa	0700	14		1030	6/8
				1130		4/6
119	Azusa	0700	16	1330		4/9
120	Burbank	0700	18		0830	23/17
				0930		14/9
					1030	8/11

---

*Missing data; value interpolated from other hourly observations at monitoring station.

Table A-1

Carbon Monoxide Simulations (cont'd)

Trajectory Run Number	Termination Point	Start Time	Starting Value (PPM)	End Time	Other Points Within 5 Mi. of Station	Calculated/ Observed (PPM)
			September 29, 1969 (cont'd)			
121	Burbank	0700	16		1030	6/11
				1130		3/10
122	Burbank	0700	17		1230	10/11
				1330		10/7
			September 30, 1969			
123	Downtown L.A.	0700	20		0830	12/32
				0930		12/18
					1030	12/15*
124	Downtown L.A.	0700	18	1130		9/12
125	Downtown L.A.	0700	17	1330		4/4
126	Whittier	0700	12		0830	7/7
				0930		7/6
					1030	6/5*
127	Whittier	0700	17		1030	8/5*
				1130		7/5*
128	Whittier	0830	18		1230	9/4
				1330		10/4
129	Azusa	0700	12		0830	9/9*
				0930		6/7
					1030	4/6
130	Azusa	0700	14		1030	4/6
				1130		4/6

---

*Missing data; value interpolated from other hourly observations at monitoring station.

Table A-1

Carbon Monoxide Simulations (cont'd)

Trajectory Run Number	Termination Point	Start Time	Starting Value (PPM)	End Time	Other Points Within 5 Mi. of Station	Calculated/ Observed (PPM)
			September 30, 1969 (cont'd)			
131	Azusa	0700	16	1330		5/5
132	Burbank	0700	22		0830	11/17
				0930		9/14
133	Burbank	0700	20		1030	13/21
				1130		11/18
134	Burbank	0700	14		1230	8/13
				1330		8/8
			October 29, 1969			
135	Downtown L.A.	0700	17		0830	18/20
				0930		20/22
					1030	19/17
136	Downtown L.A.	0700	10		1030	12/17
				1130		12/11
					1230	11/9
137	Downtown L.A.	0700	10		1230	10/9
				1330		9/8
138	Whittier	0700	14		0830	11/10
				0930		11/9
					1030	9/10
139	Whittier	0700	21		1030	17/10
				1130		15/12
					1230	13/8
140	Whittier	0700	11		1230	8/8
				1330		8/7

Table A-1

Carbon Monoxide Simulations (cont'd)

Trajectory Run Number	Termination Point	Start Time	Starting Value (PPM)	End Time	Other Points Within 5 Mi. of Station	Calculated/ Observed (PPM)
			October 29, 1969 (cont'd)			
141	Azusa	0700	10		0830	7/11
				0930		5/6
					1030	4/3
142	Azusa	0700	11		1030	6/3
				1130		5/4*
					1230	4/5
143	Azusa	0700	12		1230	5/5
				1330		5/6
144	Burbank	0700	14		0830	8/14
				0930		6/12
					1030	5/11
145	Burbank	0700	14		1030	4/11
				1130		4/9
					1230	4/8
146	Burbank	0830	14		1230	4/8
				1330		5/7
			October 30, 1969			
147	Downtown L.A.	0700	16		0830	17/8
				0930		10/7*
					1030	7/6
148	Downtown L.A.	0700	16		1030	5/6
				1130		5/6
					1230	5/5
149	Downtown L.A.	0700	16		1230	6/5
				1330		5/5

---

*Missing data; value interpolated from other hourly observations at monitoring station.

Table A-1

Carbon Monoxide Simulations (cont'd)

Trajectory Run Number	Termination Point	Start Time	Starting Value (PPM)	End Time	Other Points Within 5 Mi. of Station	Calculated/ Observed (PPM)
October 30, 1969 (cont'd)						
150	Whittier	0700	18		0830	22/19
				0930		17/9
					1030	9/4
151	Whittier	0700	9		1030	5/4
				1130		3/3
152	Whittier	0700	15		1230	4/2
				1330		4/3
153	Azusa	0700	8		0830	8/3
				0930		8/3
					1030	4/2
154	Azusa	0700	8		1030	4/2
				1130		3/1
					1230	2/1
155	Azusa	0700	7		1230	2/1
				1330		1/1
156	Burbank	0700	18		0830	27/21
				0930		30/12
					1030	12/8
157	Burbank	0700	17		1030	5/8
				1130		4/5
					1230	3/5
158	Burbank	0700	17		1230	3/5
				1330		3/2

Table A-1

Carbon Monoxide Simulations (cont'd)

Trajectory Run Number	Termination Point	Start Time	Starting Value (PPM)	End Time	Other Points Within 5 Mi. of Station	Calculated/ Observed (PPM)
			November 4, 1969			
159	Downtown L.A.	0700	15		0830	15/30
				0930		15/22
					1030	16/16
160	Downtown L.A.	0700	11		1030	9/16
				1130		8/12*
					1230	8/9
161	Downtown L.A.	0700	12		1230	7/9
				1330		7/8*
162	Whittier	0700	14		0830	14/11
				0930		13/14
					1030	12/12
163	Whittier	0700	13		1030	12/12
				1130		12/9
164	Whittier	0700	12		1230	10/7
				1330		9/5
165	Pasadena	0700	16		0830	16/10
				0930		10/7
					1030	5/7
166	Pasadena	0700	23		1030	19/7
				1130		15/6
					1230	11/11
167	Pasadena	0700	10		1230	9/11
				1330		8/8

---

*Missing data; value interpolated from other hourly observations at monitoring station.

Table A-2

Photochemical Pollutant Simulation Trajectories

Trajectory Run Number	Termination Point	Start Time	Starting Values				End Time	Other Points Within 5 Mi. of Station	Calculated/Observed			
			PPHM			PPM			PPHM	PPHM	PPHM	PPM
			NO_2	NO	O_3	CO			NO_2	NO	O_3	CO
			September 11, 1969									
1	Downtown L.A.	0700	12	14	2	14	1330	1230	17/7* 22/5	1/2* 2/1	15/7 10/11	7/11 8/10
2	Whittier	0700	12	15	1	8	1330	1230	30/23 33/20*	2/2 2/1*	14/4 18/18	7/4 8/5*
3	Pomona	0700	11	9	11	6	1330		3/6*	1/1*	2/23	1/7
4	Pasadena	0700	9	13	2	11	1330	1230	29/20* 38/13	1/3* 2/2	18/28 17/36	11/7 13/8
			September 29, 1969									
5	Downtown L.A.	0700	11	27	2	14	1330		8/6*	5/3*	2/7	3/3
6	Whittier	0700	10	21	2	9	1330		17/10	1/1	12/19	5/1
7	Azusa	0700	15	31	2	16	1330		8/5*	1/1*	12/38	3/9
8	Pasadena	0700	9	28	2	15	1330	1230	15/9* 12/5	1/1* 1/1	15/32 15/20	6/- 5/-

*Missing data; value interpolated from other hourly observations at monitoring station.

-Missing data; no interpolation possible.

Table A-2

Photochemical Pollutant Simulation Trajectories (cont'd)

Trajectory Run Number	Termination Point	Start Time	Starting Values				End Time	Other Points Within 5 Mi. of Station	Calculated/Observed			
			PPHM			PPM			PPHM	PPHM	PPHM	PPM
			NO_2	NO	O_3	CO			NO_2	NO	O_3	CO
						September 30, 1969						
9	Downtown L.A.	0700	9	36	2	17	1330		15/8*	4/5*	4/17	5/4
10	Whittier	0700	10	38	2	18	1330		11/24*	1/1*	8/5	4/4
11	Azusa	0700	11	37	2	16	1330		12/6*	1/1*	14/27	4/5
12	Pomona	0700	11	36	2	17	1330		11/13*	1/1*	16/15	4/5
						October 29, 1969						
13	Downtown L.A.	0700	14	27	3	17		0830	42/20	8/24	4/5	18/20
							0930		50/-	3/-	13/8	20/22
								1030	48/-	2/-	23/11	20/17
14	Downtown L.A.	0700	16	15	2	10		1030	35/-	2/-	19/11	12/17
							1130		32/-	1/-	20/14	12/11
								1230	29/-	1/-	22/16	11/9
15	Downtown L.A.	0700	16	14	2	10		1230	26/-	1/-	22/16	10/9
							1330		24/-	1/-	20/19	9/8
16	Whittier	0700	13	16	2	14		0830	24/20	4/10	4/3	12/10
							0930		25/25	2/6	11/6	12/9
								1030	22/26	1/3	17/10	10/10

[*] Missing data; value interpolated from other hourly observations at monitoring station.

[-] Missing data; no interpolation possible.

Table A-2

Photochemical Pollutant Simulation Trajectories (cont'd)

Trajectory Run Number	Termination Point	Start Time	Starting Values PPHM			PPM	End Time	Other Points Within 5 Mi. of Station	Calculated/Observed PPHM	PPHM	PPHM	PPM
			NO_2	NO	O_3	CO			NO_2	NO	O_3	CO
							October 29, 1969 (cont'd)					
17	Whittier	0700	14	33	3	21		1030	37/26	1/3	26/10	17/10
							1130		31/32	1/2	31/19	15/12
								1230	25/22*	1/1*	33/25	13/8
18	Whittier	0700	14	17	2	11		1230	20/22*	1/1*	20/25	8/8
							1330		18/12	1/1	21/29	8/7
19	Azusa	0700	8	3	1	10		0830	6/10	1/4	5/3	7/11
							0930		5/10	1/1	6/8	5/6
								1030	4/4	1/1	6/10	4/3
20	Azusa	0700	10	7	2	11		1030	9/4	1/1	9/10	5/3
							1130		9/3	1/1	11/12	5/4*
								1230	7/3*	1/1*	12/17	4/5
21	Azusa	0700	13	10	3	12		1230	12/3*	1/1*	12/17	5/5
							1330		11/2*	1/1*	13/19	5/6
22	Pomona	0700	13	6	2	10		0830	11/15	1/10	5/3	6/14
							0930		3/15	1/9	4/4	2/9*
								1030	2/12	1/3	3/8*	1/5

*Missing data; value interpolated from other hourly observations at monitoring station.

Table A-2

Photochemical Pollutant Simulation Trajectories (cont'd)

Trajectory Run Number	Termination Point	Start Time	Starting Values				End Time	Other Points Within 5 Mi. of Station	Calculated/Observed			
			PPHM NO_2	PPHM NO	PPHM O_3	PPM CO			PPHM NO_2	PPHM NO	PPHM O_3	PPM CO
October 29, 1969 (cont'd)												
23	Pomona	0700	10	5	1	10		1030	4/12	1/3	5/8*	2/5
							1130		3/9	1/2	6/12	2/5
								1230	2/8*	1/2*	5/12	2/4
24	Pomona	0700	8	4	1	10		1230	7/8*	1/2*	9/12	3/4
							1330		3/6*	1/1*	6/13	2/4
October 30, 1969												
25	Downtown L.A.	0700	7	42	1	16		1230	11/9	1/1	12/13	4/5
							1330		10/11*	1/1*	11/15	4/5
26	Whittier	0700	9	20	2	15		1230	8/9*	1/2*	11/10	3/2
							1330		8/8	1/3	8/10	3/3
27	Azusa	0700	4	16	2	7		1230	1/2*	1/1*	2/7	1/1*
							1330		1/1*	1/1*	2/9	1/1
28	Pomona	0700	5	21	2	8		1230	1/5*	1/3*	2/4	1/4
							1330		1/5*	1/2*	2/6	1/4

---

*Missing data; value interpolated from other hourly observations at monitoring station.

Table A-2

Photochemical Pollutant Simulation Trajectories (cont'd)

Trajectory Run Number	Termination Point	Start Time	Starting Values PPHM			Starting Values PPM	End Time	Other Points Within 5 Mi. of Station		Calculated/Observed		
			NO_2	NO	O_3	CO			PPHM NO_2	PPHM NO	PPHM O_3	PPM CO
				November 4, 1969								
29	Downtown L.A.	0700	12	24	2	12		1230	20/18	1/1*	22/10	10/9
							1330		15/15	1/1	12/16	6/8*
30	Whittier	0700	12	25	2	16		1230	27/16*	1/1*	22/10	10/7
							1330		25/10	1/1	23/11	9/5
31	Azusa	0700	12	27	2	14	1330		17/7*	1/2*	26/23	8/7
32	Pasadena	0700	11	28	2	10		1230	25/12*	1/1*	22/21	9/11
							1330		23/12	1/1	25/21	8/8

*Missing data; value interpolated from other hourly observations at monitoring station.

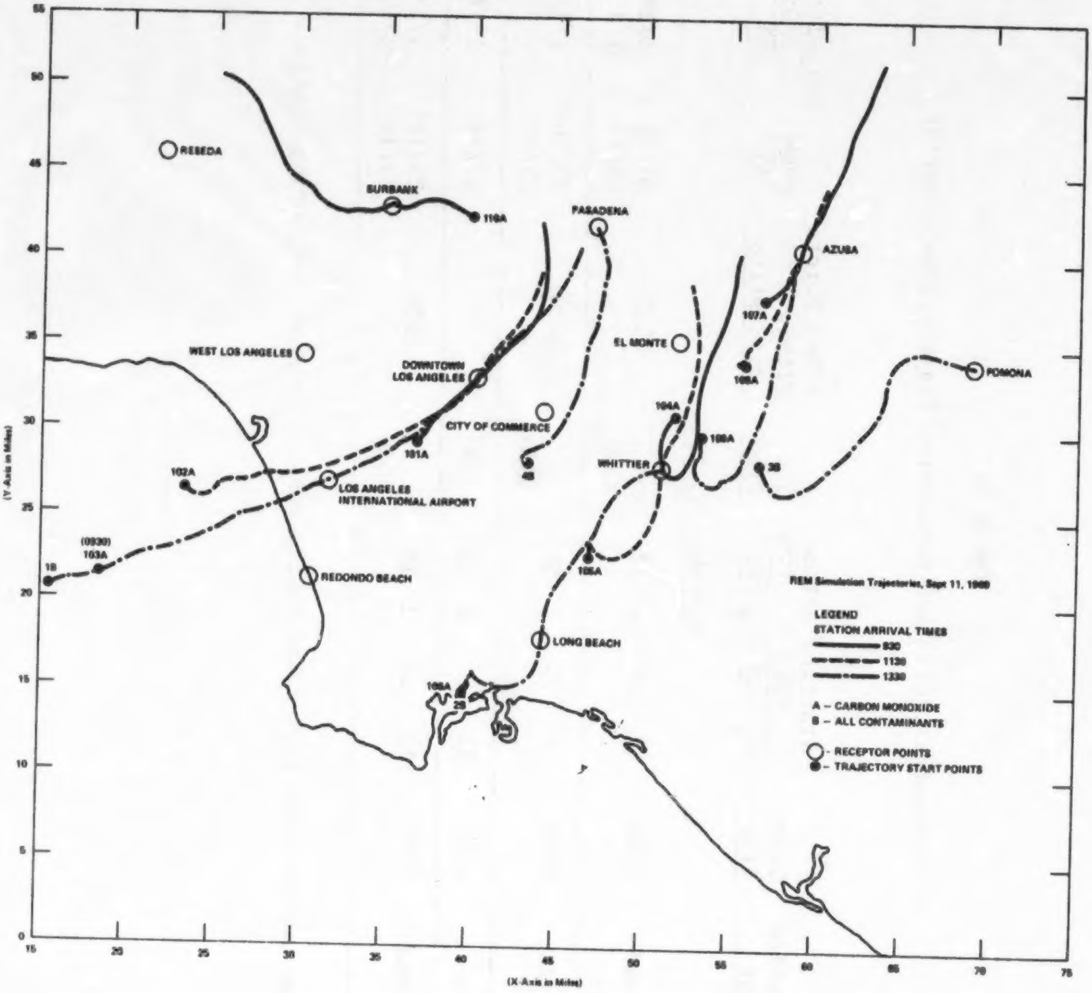
RESEDA
BURBANK
110A
PASADENA
AZUSA
WEST LOS ANGELES
DOWNTOWN LOS ANGELES
EL MONTE
107A
108A
POMONA
104A
CITY OF COMMERCE
109A
101A
102A
WHITTIER
4B
3B
LOS ANGELES INTERNATIONAL AIRPORT
(0930)
103A
1B
105A
REDONDO BEACH
LONG BEACH
106A
2B
REM Simulation Trajectories, Sept 11, 1969
LEGEND
STATION ARRIVAL TIMES
930
1130
1330
A – CARBON MONOXIDE
B – ALL CONTAMINANTS
○ – RECEPTOR POINTS
● – TRAJECTORY START POINTS
55
50
45
40
35
30
25
20
15
10
5
0
(Y-Axis in Miles)
15
20
25
30
35
40
45
50
55
60
65
70
75
(X-Axis in Miles)

Figure A.1
Trajectories for September 11, 1969

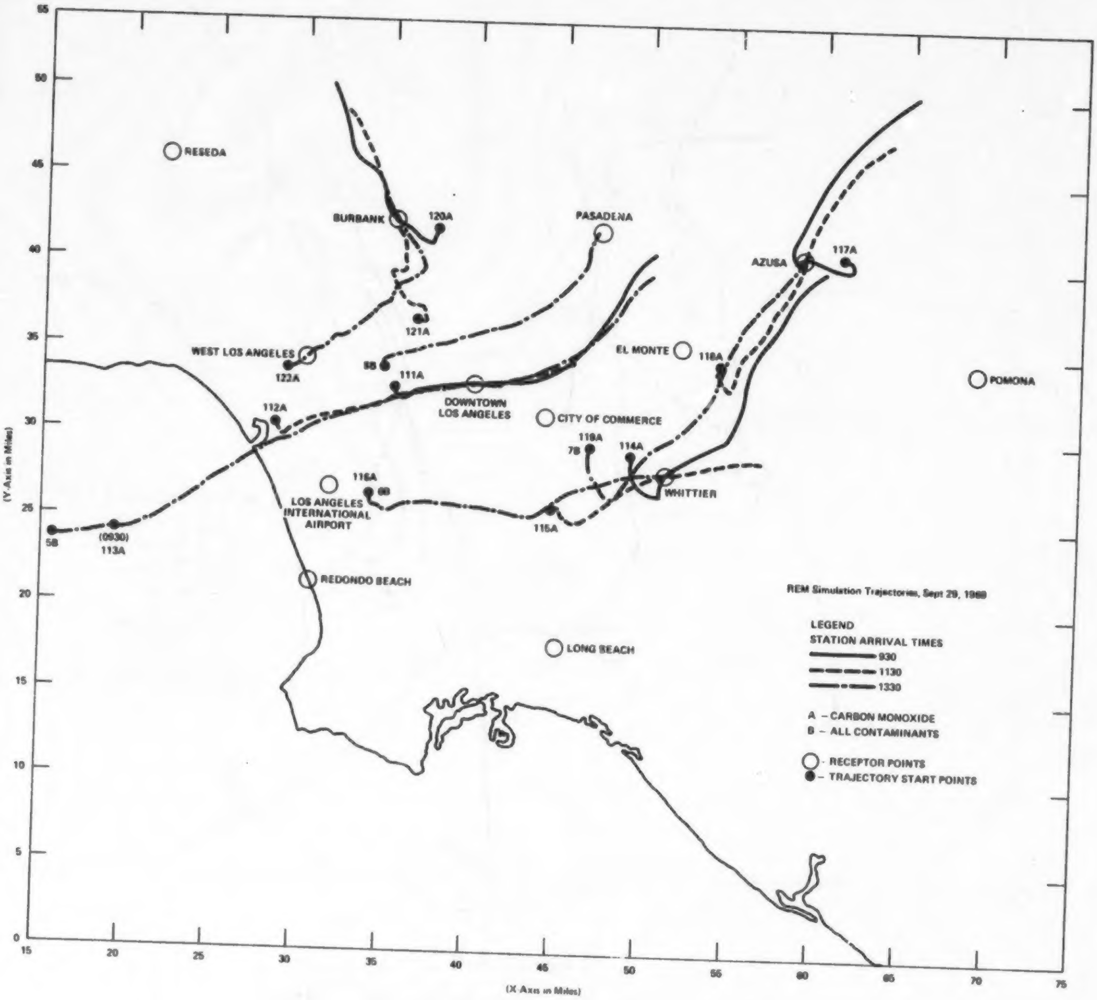
55
50
45
40
35
30
25
20
15
10
5
0
(Y-Axis in Miles)
15
20
25
30
35
40
45
50
55
60
65
70
75
(X Axis in Miles)
RESEDA
BURBANK
120A
PASADENA
AZUSA
117A
121A
WEST LOS ANGELES
122A
9B
111A
EL MONTE
118A
POMONA
DOWNTOWN LOS ANGELES
CITY OF COMMERCE
112A
119A
7B
114A
WHITTIER
116A
6B
LOS ANGELES INTERNATIONAL AIRPORT
115A
5B
(0930)
113A
REDONDO BEACH
LONG BEACH
REM Simulation Trajectories, Sept 29, 1969
LEGEND
STATION ARRIVAL TIMES
930
1130
1330
A – CARBON MONOXIDE
B – ALL CONTAMINANTS
○ - RECEPTOR POINTS
● – TRAJECTORY START POINTS

Figure A.2
Trajectories for September 29, 1969

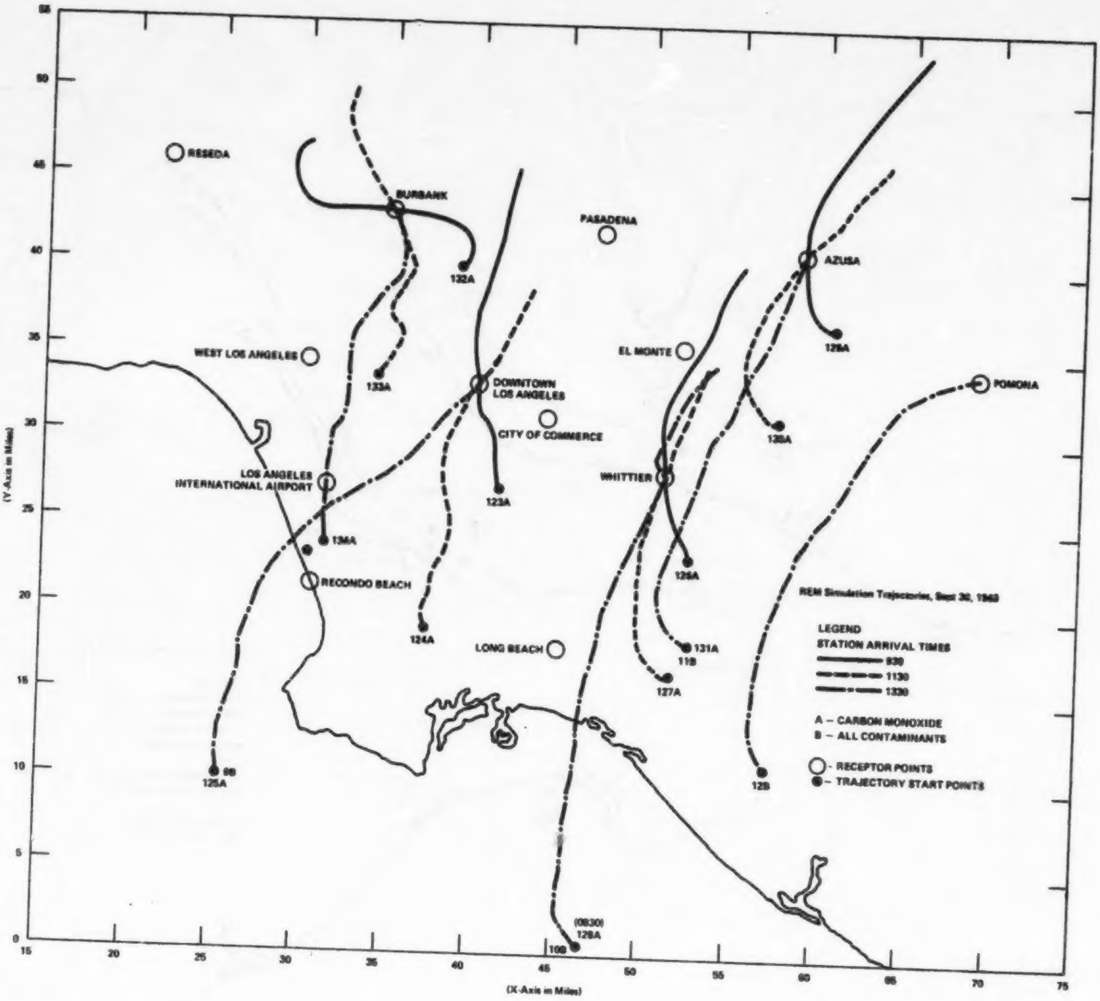
RESEDA
BURBANK
132A
133A
PASADENA
WEST LOS ANGELES
DOWNTOWN LOS ANGELES
CITY OF COMMERCE
LOS ANGELES INTERNATIONAL AIRPORT
134A
123A
RECONDO BEACH
124A
LONG BEACH
EL MONTE
WHITTIER
AZUSA
128A
130A
126A
131A
11B
127A
POMONA
12B
9B
125A
(0830)
129A
10B
REM Simulation Trajectories, Sept 30, 1969
LEGEND
STATION ARRIVAL TIMES
930
1130
1330
A – CARBON MONOXIDE
B – ALL CONTAMINANTS
○ - RECEPTOR POINTS
● - TRAJECTORY START POINTS
(Y-Axis in Miles)
(X-Axis in Miles)
0
5
10
15
20
25
30
35
40
45
50
55
15
20
25
30
35
40
45
50
55
60
65
70
75

Figure A.3

Trajectories for September 30, 1969

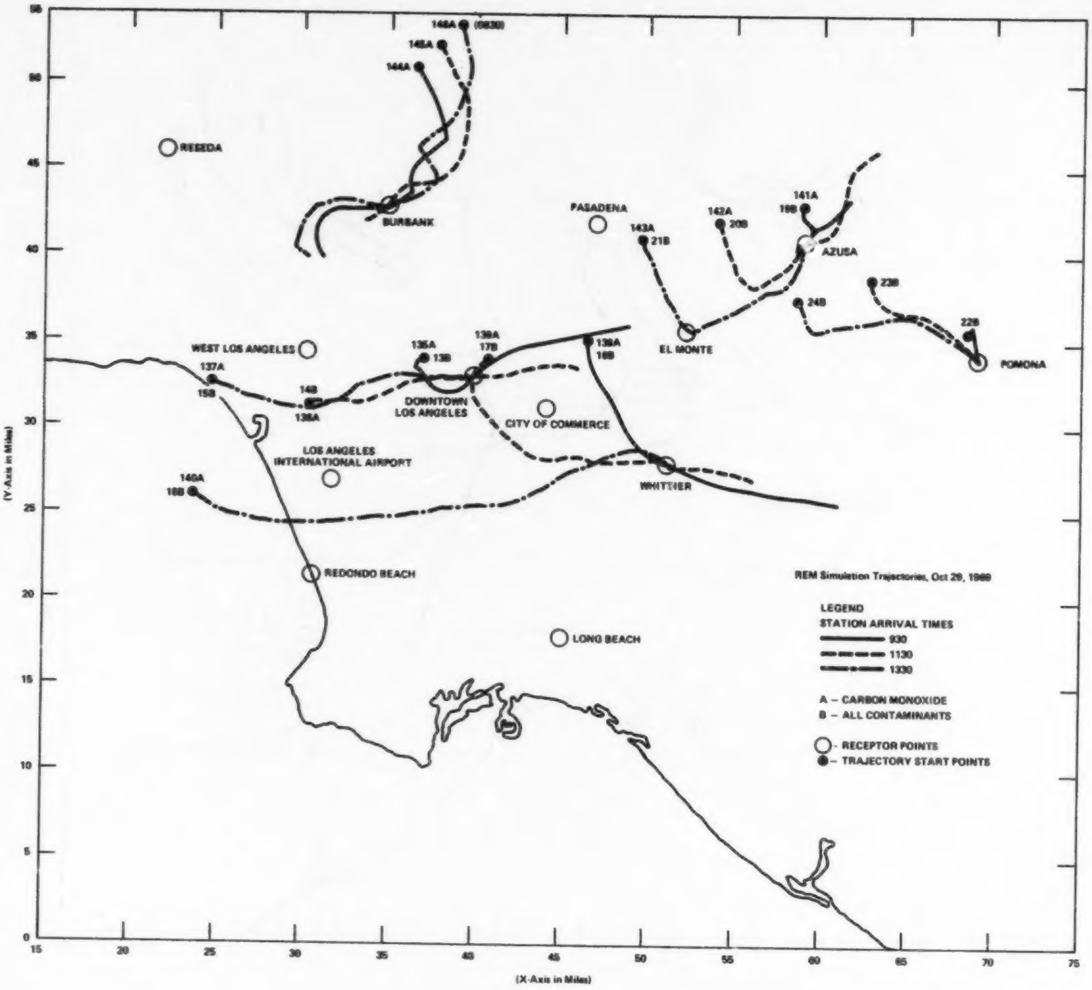
146A (0830)
145A
144A
RESEDA
BURBANK
PASADENA
143A 21B
142A 20B
141A 19B
AZUSA
23B
24B
22B
EL MONTE
POMONA
WEST LOS ANGELES
137A 15B
14B
136A
135A 13B
139A 17B
138A 16B
DOWNTOWN LOS ANGELES
CITY OF COMMERCE
LOS ANGELES INTERNATIONAL AIRPORT
140A 18B
WHITTIER
REDONDO BEACH
LONG BEACH
REM Simulation Trajectories, Oct 29, 1969
LEGEND
STATION ARRIVAL TIMES
930
1130
1330
A – CARBON MONOXIDE
B – ALL CONTAMINANTS
○ – RECEPTOR POINTS
● – TRAJECTORY START POINTS
(Y-Axis in Miles)
(X-Axis in Miles)
0
5
10
15
20
25
30
35
40
45
50
55
15
20
25
30
35
40
45
50
55
60
65
70
75

Figure A.4

Trajectories for October 29, 1969

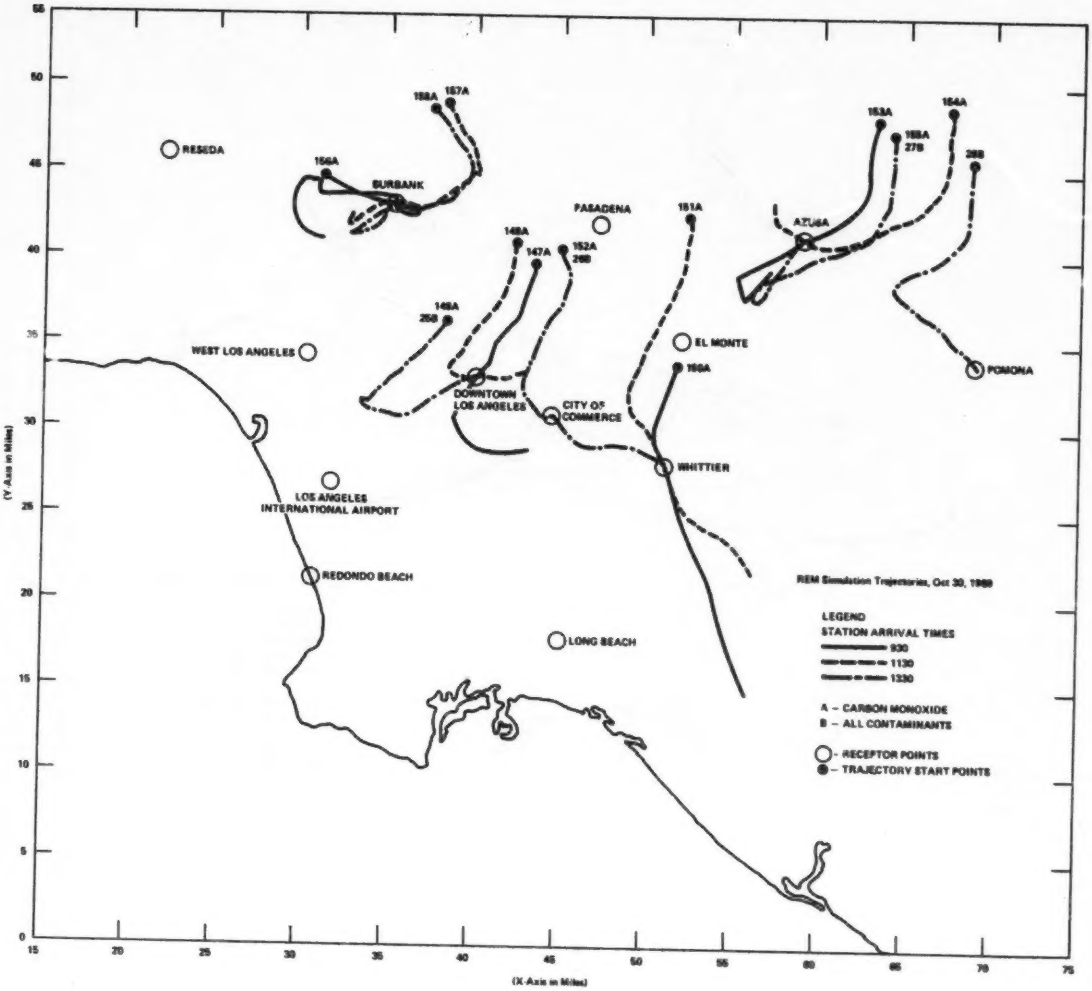
158A
157A
RESEDA
156A
BURBANK
PASADENA
151A
153A
155A
27B
154A
28B
AZUSA
148A
147A
152A
26B
149A
25B
WEST LOS ANGELES
EL MONTE
150A
POMONA
DOWNTOWN
LOS ANGELES
CITY OF
COMMERCE
WHITTIER
LOS ANGELES
INTERNATIONAL AIRPORT
REDONDO BEACH
LONG BEACH
REM Simulation Trajectories, Oct 30, 1969
LEGEND
STATION ARRIVAL TIMES
930
1130
1330
A – CARBON MONOXIDE
B – ALL CONTAMINANTS
○ – RECEPTOR POINTS
● – TRAJECTORY START POINTS
(Y-Axis in Miles)
(X-Axis in Miles)
0
5
10
15
20
25
30
35
40
45
50
55
60
65
70
75

Figure A.5

Trajectories for October 30, 1969

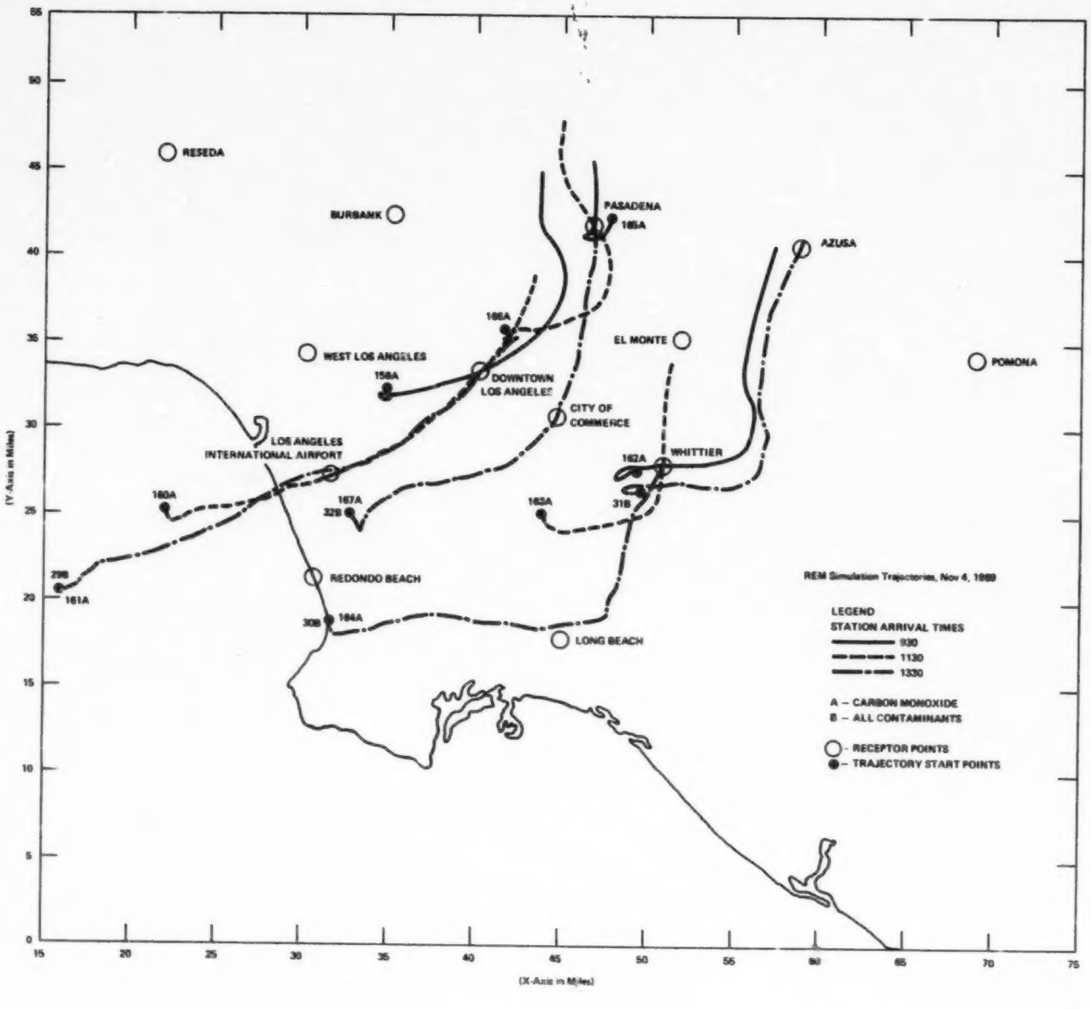
RESEDA
BURBANK
PASADENA
165A
AZUSA
166A
EL MONTE
POMONA
WEST LOS ANGELES
158A
DOWNTOWN LOS ANGELES
CITY OF COMMERCE
LOS ANGELES INTERNATIONAL AIRPORT
WHITTIER
162A
160A
167A
32B
163A
31B
29B
161A
REDONDO BEACH
30B
164A
LONG BEACH
REM Simulation Trajectories, Nov 4, 1969
LEGEND
STATION ARRIVAL TIMES
930
1130
1330
A – CARBON MONOXIDE
B – ALL CONTAMINANTS
○ – RECEPTOR POINTS
● – TRAJECTORY START POINTS
(Y-Axis in Miles)
(X-Axis in Miles)
0
5
10
15
20
25
30
35
40
45
50
55
15
20
25
30
35
40
45
50
55
60
65
70
75

Figure A.6
Trajectories for November 4, 1969